ABSTRACT

CRIMI, CHRISTOPHER SCOTT. Analysis of Patellar Height of the Cranial Cruciate Ligament Deficient Canine Stifle Following Three Tibial Osteotomy Procedures. (Under the direction of Dr. Ola Harrysson and Dr. Denis Marcellin-Little.)

The cranial cruciate ligament (CCL) plays a significant role in providing functional stability to the canine stifle joint and has been the topic of an increasing amount of attention in the veterinary community. The objective of this study was to evaluate the effects of CCL deficiency and common procedures for treatment of a ruptured CCL on patellar location within the trochlear groove. Five identical and anatomically accurate physical models of the left hind limb of a healthy dog were constructed using a combination of rapid-prototyping technologies and casting techniques. One model remained the intact control, one simulated a CCL deficient stifle and each of the remaining models underwent one of the three tibial osteotomy procedures to be examined: the Tibial Plateau Leveling Osteotomy (TPLO), Tibial Tuberosity Advancement (TTA), and the Triple Tibial Osteotomy (TTO). Physical testing via a custom testing apparatus was carried out for five stifle positions (75º, 96º, 113º, 130º, 148º) representing the normal range of motion of a large-breed dog. Confirmation of a cranial translation following transection of the CCL was in good agreement with literature. Cranial cruciate transection also caused a slight proximal shift of the patella with respect to the trochlear groove. The results of the models further suggest that both the TPLO and TTO procedures result in a more proximally located patella with respect to the trochlear groove, while the TTA results in a more distally located patella.

Analysis of Patellar Height of the Cranial Cruciate Ligament Deficient Canine Stifle Following Three Tibial Osteotomy Procedures

by
Christopher Scott Crimi

A thesis submitted to the Graduate Faculty of
North Carolina State University
in partial fulfillment of the
requirements of the Degree of
Master of Science

Industrial Engineering

Raleigh, North Carolina

2008

APPROVED BY:

Dr. Harvey A. West II	Dr. Andre P. Mazzoleni
Dr. Ola L. A. Harrysson Chair of Advisory Committee	Dr. Denis J. Marcellin-Little Co-Chair of Advisory Committee

BIOGRAPHY

Christopher Scott Crimi was born on July 10th, 1982 in Leominster, Massachusetts. After attaining a BS in Industrial and Systems Engineering from the University of Florida, he moved to Raleigh to pursue a Master of Science degree from North Carolina State University. After graduation from NCSU, he is looking forward to a job in the medical manufacturing field.

ACKNOWLEDGEMENTS

My gratitude goes out to all those who contributed their time and knowledge to this project. Many thanks to Dr. Anke Langenbach, Dr. Tibor Lazar, and Dr. Denis Marcellin-Little for performing the surgeries and donating implants used in this study.

Thank you to my parents and siblings, for taking such interest in my work, and always being proud of me. This work would not have been realized without my wife and colleague, Christina. Thank you for your love and for picking me up when I needed it most.

TABLE OF CONTENTS

LIST OF FIGURES

LIST OF TABLES

1. DATA PROCESSING AND MODEL DESIGN

1.1 INTRODUCTION

The stifle joint is one of the most complex and extensively examined joints in the dog. Injury to one of its components becomes a multifaceted problem requiring a thorough understanding of not only joint biomechanics but functional anatomy as well. Among the most influential of the stifle ligaments, the cranial cruciate ligament (CCL) plays an especially significant role in providing functional stability to the canine stifle joint. Several research experiments have concluded that the CCL is the primary component opposing cranial tibial thrust and aids in limiting tibial internal rotation and hyperextension of the stifle [25,27,33,121]. CCL rupture remains one of the most common orthopedic conditions in dogs and this debilitating disease can lead to serious complications such as osteoarthritis, meniscal injury, and severe rear limb lameness [8,46,55].

Patella alta has been considered a significant cause of recurrent dislocation of the patella [50,56,62,82]. However, there is an apparent lack of both experimental and clinical information regarding patellar luxation and patella alta diagnosis in the canine and no studies to date have evaluated patellar location resulting from a loaded cranial cruciate deficient stifle. Many researchers have used modeling as a tool to analyze the mechanical characteristics of the patellofemoral joint but most of these have been limited to 2D representation [53]. With the advent of advanced medical imaging techniques, such as

Computed Tomography, a more thorough knowledge of both normal and afflicted stifle anatomy is possible. Rapid prototyping technology has also become influential in the area of biomodeling. It is being used today as a means for surgical planning, custom prosthesis design, and reconstructive surgery. It has also been influential in experimental environments. However, very few fully three-dimensional prototyped models of canine limbs exist. The issue of altered stifle biomechanics following CCL rupture, particularly the resulting patellar location within the trochlear groove, is of clinical importance and in need of further research as it pertains to the canine stifle.

The objective of this study was to develop anatomically accurate three-dimensional physical models using a combination of rapid prototyping technologies and casting techniques in order to investigate the stifle joint mechanics of both a normal healthy canine limb and that of a CCL deficient stifle. The models were used to compare the patellar position within the trochlear groove and determine the effects of ligament rupture on patellar height and patellofemoral stability. To this date, no such information exists.

Cranial cruciate rupture remains one of the most widely diagnosed and threatening conditions to stifle stability and rear limb function. By means of in vitro and in vivo experiments as well as mathematical and computer models, many researchers have focused their efforts on understanding the stifle joint mechanics and the changes and behaviors associated with cranial cruciate ligament rupture. Despite the frequent research attention it receives, much of what is used to evaluate canine stifle joint biomechanics still comes from human analysis due to a scarcity of species-specific knowledge. Furthermore, no known studies have sought to describe the effects of CCL rupture on patellar position. Due to the differences in both geometry and joint motion, data for patellar movement in humans should not be extended directly to the dog and more species specific analysis should be done. Understanding consequences of ligament rupture will aid in future efforts to develop new methods of treatment.

1.2 BACKGROUND INFORMATION

1.2.1 Cranial Cruciate Ligament Rupture

The canine stifle joint is a complex, synovial joint allowing motion in three planes. Due to its complexity and the cooperation of all of the ligaments, muscle groups, cartilage and bony structures, treatment of injury to any of its components becomes an involved, complicated task. The cruciate ligaments are particularly important to joint function, acting as constraints of craniocaudal motion. The cranial cruciate ligament prevents cranial displacement of the tibia and limits excessive internal tibial rotation. It also aids in preventing hyperextension of the joint [8]. The caudal cruciate ligament prevents caudal tibial translation and also helps to limit tibial internal rotation.

There is a high prevalence of CCL insufficiency among dogs. The economic impact of treating dogs with CCL insufficiency in the US was projected at just over $1 billion in 2003 [58]. Diagnosis of complete CCL rupture is made by detection of joint laxity, seen as craniocaudal instability after applying a cranially directed load on the proximal tibia. Other methods have also been developed to test for ligament insufficiency. Cruciate ligament injury can be related to their function and possibly caused by excessive loads during extreme conditions or actions. Complete rupture of the CCL has been shown to cause progression of degenerative joint disease, meniscal injury, joint instability and is one of the largest sources of chronic rear limb lameness in dogs.

1.2.2 Patella Alta and Patella Baja (Infera)

The location of the patella within the trochlear groove plays an important role in canine stifle joint stability [34,50,56,62,82]. A patella that is displaced too proximally, known as patella alta, loses the buttressing effect of the trochlear groove and will be more prone to luxation [34,56,62]. Conversely, studies have shown that a patella located too distally, known as patella baja (infera), is associated with chondromalacia, a degenerative condition afflicting the articular cartilage of the caudal surface of the patella [62]. The issue of patellar location has historically been focused on human subjects; however, extrapolating the findings to dogs must be done with caution because of the species-specific anatomy. Due to the fact that the canine stifle is the most frequently afflicted joint of the dog, the issue of patellar location with respect to the trochlear groove is of clinical importance and in need of further research.

1.2.3 Rapid Prototyping

Rapid Prototyping (RP) technology is a group of methods used to quickly fabricate a physical model from three-dimensional computer aided design (CAD) data. This process creates a physical model that almost exactly corresponds to the virtual model depending on the method of RP used. Machines implementing an additive fabrication technique read the data from the CAD drawing and lay down successive layers of whatever medium is used for that machine (i.e. liquid, powder or sheet material). The 3D model is then built up layer by layer. The construction of a model with contemporary methods can vary in total time, depending on the method and model complexity.

Stereolithography (SLA®) is commonly thought of as the first RP technique (3D Systems, Valencia, CA, USA). The company 3D Systems was founded in 1986. Since then, a number of different RP techniques have become available including Selective Laser Sintering (SLS®), Laminated Object Manufacturing (LOM™), Fused Deposition Modeling (FDM™), Solid Ground Curing (SGC), and Ink Jet printing techniques.

.

Rapid Prototyping has also been referred to as solid free-form manufacturing and has been used in several industries, such as medical applications, for visualization purposes. In addition, RP models can be used for testing, to create male models for tooling, to create silicone rubber molds and investment casts, or can they can be the final part. Rapid Prototyping decreases development time by allowing corrections to a product to be made early in the process.

The medical field has been impacted in a very positive way from rapid prototyping technologies. RP methods are used to design and develop medical devices and instrumentation. The largest benefit of RP in this task is the customizable nature of the method. A custom bone plate, hearing-aid, replacement teeth, etc. can be made effectively and efficiently with RP. Another area benefiting from rapid prototyping is the field of prosthetics and implantation. This advanced technology makes it possible to manufacture a custom prosthesis that will fit a patient precisely.

Rapid prototyping is also used by medical professionals for pre-surgical planning and visualization purposes. Complex operations such as craniofacial surgeries can be practiced ahead of time with the use of a physical RP model. Models are frequently present in the operating room and used as templates and guides for surgery.

1.3 REVIEW OF LITERATURE AND RESEARCH

Advancements in medical technology and computer software have helped researchers make significant strides in modeling and predicting joint behavior. What has long been difficult to visualize is becoming tangible and thus more comprehensible. This section presents a brief overview of the research and literature related to stifle joint mechanics as well as the data processing and model design aspects of this thesis. The literature on this subject is expansive so a concentrated selection of significant work was chosen to provide a clear understanding of imaging techniques, useful technological tools, related anatomical issues and advancements in computer and physical modeling.

1.3.1 Anatomy of the Stifle Joint

The canine stifle joint has been the focus of much orthopedic interest in the veterinary community, the biomechanics of which has been the subject of many recent investigations. Determining how the different components of the stifle are loaded during various activities is important for the understanding of normal joint function as well as gaining insight into the mechanisms responsible for common injuries such as cranial cruciate ligament rupture [105]. To properly correct an injury to any component of the stifle joint by returning normal stifle motion and minimizing further degeneration, an understanding of the normal anatomy of the entire stifle is essential [27].

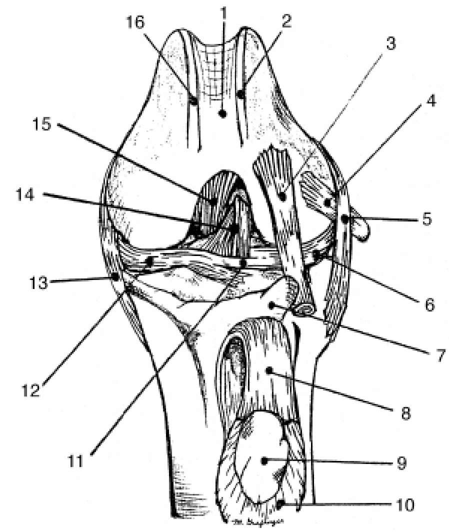

Fig. 1. Cranial view of the left stifle showing associated ligaments and structures. 1, femoral trochlea; 2, lateral ridge of femoral trochlea; 3, tendon of long digital extensor; 4, tendon of popliteus; 5, lateral collateral ligament; 6, lateral meniscus; 7, tibial tuberosity; 8, patellar ligament; 9, patella; 10, parapatellar fibrocartilage; 11, intermeniscal ligament; 12, medial meniscus; 13, medial collateral ligament; 14, cranial cruciate ligament; 15, caudal cruciate ligament; 16, medial ridge of the trochlea.

Figure 1.3.1: The components of the canine stifle [Carpenter, Cooper 27]. Used with permission from the publisher.

The following sections outline some of the most prominent work regarding the biomechanics and function of the stifle joint as well as its reaction to one of the most frequently occurring orthopedic conditions: cranial cruciate ligament rupture.

1.3.1.1 The Stifle Ligaments, Muscles and Patellar Tendon

There are four primary ligaments critical to stifle joint stability [25,27]. These are the cranial cruciate, caudal cruciate, medial collateral, and lateral collateral ligaments. The combined forces of the two main muscles groups (quadriceps and gastrocnemius) are also responsible for joint articulation and stability during weight bearing. The biomechanical properties of the stifle ligaments are crucial to their function and thus the focus for many experimental studies. Through a 3-dimensional mathematical model, Shahar and Banks-Sills described the variation in forces in the various ligaments of the intact stifle during the stance phase of a slow walk [105]. They determined that the cranial cruciate ligament is loaded throughout most of the stance phase and reaches a peak at about 40% of this phase. Peak loading for the other ligaments, such as the lateral collateral ligament, were also determined. According to this study, the medial collateral and caudal cruciate ligaments are not loaded at all during the stance phase of a slow walk. In the CCL-transected model the LCL is loaded throughout the stance phase, the caudal is loaded throughout the first 70% of the stance phase and the MCL is not loaded. At the time of this study, there were no in vivo measurements of joint reaction forces or stifle ligament forces to compare their results. The authors stated that many of their assumptions oversimplified the model which may have produced results that do not represent the true physiology of the canine stifle. Later studies confirmed that their estimation of ligament behavior, especially the collateral ligaments, during the stance phase was inaccurate. Vasseur and Arnoczky examined the collateral ligaments in cadaveric canine stifles and determined that the MCL was taut in extension and only partially lax during flexion [120]. Also, the LCL was found to be only engaged (taut) during extension and completely lax when the joint was flexed. Both ligaments were found to play an integral role in the rotational behavior of the joint, working together to prevent varus-valgus angulation in extension and allowing internal tibial rotation during flexion. These conclusions are similar to studies on the collateral ligaments of human knee joints [72,123].

In situ forces and strains have been measured, though inconsistently, for the human knee and very little has been done with respect to canines. Monahan *et al.* measured the strains of all of the canine stifle ligaments *in vivo* by use of mercury strain gages [78]. Each ligament, however, was measured from a different dog due to strain gage attachment issues. Combined with other uncertainties pertaining to gage function and reliability, their results may not be entirely accurate or consistent. Their study also included only varus-valgus loading and did not take into account muscle contraction. Mathematical models, such as that proposed by Blankevoort and Huiskes [19], provide additional insight into the ligament forces and joint mechanics for certain ranges of motion. These models also significantly simplified the complex anatomy of the knee joint but, as the model by Blankevoort and Huiskes showed, can still realistically simulate characteristics of joint biomechanics. For their study, the geometry and function of the menisci was not included which led the authors to believe the resulting ligament forces were overestimated.

Several research studies have been done on the properties of the patellar tendon because it has been used as a graft for replacing ruptured cranial cruciate ligaments in the past. A study by Cabaud *et al.* analyzed the effects of removing a section of the patellar ligament for placement as an artificial CCL [24]. Their study showed the collagen fibers of the tendon to be normal after surgery and that the strength and stiffness in the host tendon actually increased. Burks *et al.* showed contradictory results and a decrease in similar parameters [21]. Linder *et al.* followed a procedure similar to Burks *et al.* and determined that removal of the medial third of the patellar tendon in dogs caused a decrease in stiffness, failure load and modulus as well as a significant difference when compared with control tendons [67]. Shahar and Banks-Sills assumed in their mathematical model that the patellar ligament was inextensible based on the geometric properties of being much stiffer and thicker than the other knee ligaments [105]. Some have disagreed with this assumption, but Johnson *et al.* determined through physical testing and comparison between ratios of ligament to patellar length that this is a reasonable assumption from 75º of flexion to 148º of extension [34]. Their study only included 13 dogs, however, and solely from large-breeds.

Studies on the meniscus and articular cartilage have also been reported. In a study by Jurvelin *et al.*, a variation of Poisson's ratio of the articular cartilage in the canine knee joint was identified [57]. Donahue *et al.* showed that the tibiofemoral contact pressure was highly sensitive to the circumferential, axial and radial modulus of the menisci as well as the horn stiffness [37]. This information may be influential in the accuracy of advanced models of the stifle joint in that an invalid attachment of the menisci may cause contact and joint motion predictions to be erroneous.

1.3.1.2 Joint Motion and Gait Analysis

Kinematics help describe features of normal motion of the dog during activities such as walking. It has also been useful in identifying changes in joint motion and elucidating anomalies in joint composition [40,69]. Several different techniques have been used in research. Feeney *et al.* investigated the variability and reliability in 2-dimensional kinematic analysis of digitized tapes as a possible diagnostic tool in clinical settings [40]. They found that this method offered acceptable intra- and inter-observer repeatability for both the normal gait and sit-to-stand motions. Reliabilities were highest for the lower limb joints (carpal, tarsal and stifle) because of more easily identifiable markers. This study did not provide insight into the neck motion during these activities as potential head movement caused their measurements to be unreliable. They were not able to measure accuracy directly but had good agreement with other studies on the joint motion of the hind limb joints. Dogs with clinical lameness were not assessed so there was no conclusion as to whether this method would be helpful in identifying clinical lameness.

Goniometry is another tool widely used to evaluate joint motion in dogs. This measurement technique was validated in a study by Jaegger, Marcellin-Little and Levine [52]. Measurements using a universal plastic goniometer were not significantly different to radiographic measurements. Sedation was also found to have little influence on the joint position. Only Labrador Retrievers were tested and the authors cautioned against potential invalidity of the results if extrapolated to dog breeds with significantly different structure. A study on the comparison of electrogoniometry and the common universal plastic goniometer (UG) found that the use of an electrogoniometer (EG) results in higher variability as compared to both UG and radiographic measurements for a majority of the joint positions tested [117]. Measurements taken with an EG were significantly different for the carpus (when in flexion) and the elbow (in both flexion and extension) joints. Intra-observer variability was concluded to be of low impact to the variability of the different methods. Only German Shepherds were tested but comparison to measurements obtained for Labrador

Retrievers [52] suggested that significant differences for certain joint measurements existed and might be attributable to differences in joint shape, muscle mass and general biomechanics.

Marsolais *et al*. provided information for joint range of motion and limb motion for dogs during swimming [69]. Significant differences were detected for extension and flexion capabilities of the lower limb joints, such as the hip and stifle, as compared with slow or fast walking and an overall increase in the range of motion during swimming was concluded. The authors extended this study to dogs that had undergone extracapsular stabilization treatment for CCL rupture and found that those dogs also had an increased range of motion during swimming. This, as the authors proposed, suggests that swimming may be beneficial during rehabilitation after surgical treatment.

1.3.1.3 The CCL deficient stifle

Since the first clinical attempts to surgically rectify the cranial cruciate ligament deficient stifle in 1952, this orthopedic condition has received more attention than any other musculoskeletal problem in the dog [8]. The surgical treatment for CCL rupture continues to be a subject of investigation in the veterinary and research communities. The purpose of this section is to review the literature regarding cranial cruciate ligament rupture and its impact on the stifle joint.

In a paper regarding CCL rupture, Hayashi *et al.* report that the cellular changes in the canine ruptured CCL are associated with extensive distruption of the ligamentous matrix.

Progressive mechanical overloading is also apparent and there was no correlation found between these changes and variables such as age, sex, body weight, or duration of lameness [46]. Other studies have suggested, however, that characteristics such as breed, age and existence of conformational abnormalities are risk factors for developing cranial cruciate disease [55].

Slocum and Slocum were the first to describe a more active model of the biomechanics of the canine stifle incorporating not only the ligaments, but also the forces created during weight bearing as well as the musculature of the pelvic limb [110]. This was the first model to recognize the force called cranial tibial thrust. They determined that the magnitude of this thrust is dependent on both the tibial compression during weight bearing as well as the slope of the tibial plateau. This means of describing the biomechanical function of the canine stifle has assisted veterinary surgeons in understanding both intact and CCL deficient stifles. In this paper, Slocum and Slocum also confirmed that hyperextension of the stifle deforms the CCL to the point of injury.

Schwandt *et al.* compared the angles between the patellar ligament and the tibial plateau in canine stifle joints with an intact CCL as well as those suffering from a ruptured CCL. Their study focused only on partial CCL rupture. They found that larger patellar tendon angles exist in stifles with a partially ruptured CCL as compared to those with an intact CCL. They also determined that a greater shear force affects the CCL in stifle joints with partial ruptures [100]. Ralphs and Whitney detected a positive correlation between complete rupture in the

CCL and medial meniscal damage [90]. Lateral meniscal injuries as a result of CCL injury were also evident and may be more commonly associated with CCL injury than previously recognized.

Using computer assisted kinematic gait analysis, DeCamp *et al.* demonstrated that the movement of the coxofemoral, tarsal and femorotibial joints during the normal canine gait are affected by cranial cruciate ligament rupture [35]. Another gait analysis was done by Tashman *et al.* and they confirmed that a cranial tibial translation as well as instability increased immediately after loss of CCL. They confirmed a degradation of these changes with an increase in duration of lameness [114].

1.3.2 Patellar Articulation

Patella alta has been considered a significant cause of recurrent dislocation of the patella [50,56,62,82]. Thus, the issue of patellar location within the trochlear groove is of clinical importance and in need of further research as it pertains to the canine stifle.

1.3.2.1 Vertical Patellar Position

In 1971 Insall and Salvati developed a method for defining patellar position by relating the greatest diagonal length of the patella to the length of the patellar ligament [51]. They found that in human subjects this ratio is approximately 1.0 in the normal knee joint and that a deviation of 0.2 or more represents an abnormal patellar position. The calculation was found to be easy to make and independent of the degree of knee flexion. Miller *et al.*. applied this method to sagittal MR images of the fully extended knee and found it to be a reliable method [75]. Blackburne *et al.* later developed another method for determining patellar height in humans by defining the ratio of the articular patellar length to the height of the distal pole of the patella above the tibial plateau [17]. They claim this method removes the variability resulting from the tibial tubercle not being a standard distance below the tibial plateau. A study by Berg *et al.* compares these two methods and others to determine which is the most reliable and reproducible method of measuring patellar height in humans [16]. They found the method by Blackburn *et al.* to be the most reproducible in a study of 15 patients measured by 3 observers. A similar study by Seil *et al.* also compared several patellar height ratios and recommended the Blackburne-Peel method because of its low inter-observer variability and ability to discriminate between patella alta, baja, and norma [101].

One cause for concern in attempting to extend the aforementioned methods to dogs is that they do not precisely relate the location of the patella to the trochlear groove over a range of angles. Additionally, they were not specifically designed to account for procedures which alter the tibial tubercle as it relates to the tibial plateau in the canine stifle. After using a variation of the Insall-Salvati method to verify that the patellar ligament is inextensible in canines over a passive range of motion, Johnson *et al.* developed a method that relates the proximal and distal aspects of the patella to its location within the trochlear groove (Figure 1.3.2) [34].

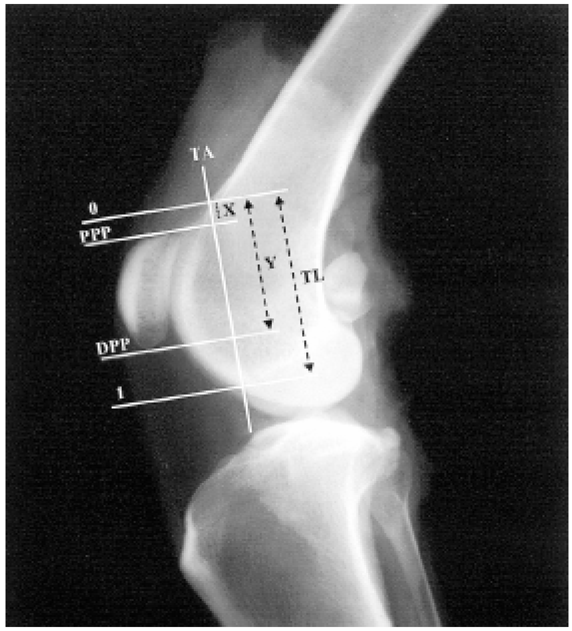

Figure 1.3.2: Diagram for measuring patellar location [Johnson *et al.*, 34]. Used with permission from the publisher.

Although more precise in relating the patellar position within the trochlear groove, this new method was involved and time consuming to perform. Extrapolating data between patients was technically difficult due to the fact that the technique required a precise angle of examination and that the proximal and distal aspects of the trochlear groove may be defined differently between subjects. Their stifle joint angle measurement method was close to the measurement method used in a gait analysis study by both Hottinger *et al*. [48] and Feeney *et al.* [40]. Thus, the extrapolation of kinematic analysis angles to anatomic angles was logical and the comments regarding the 96º to 148° range at a trot also appeared to be logical.

In another paper by Mostafa *et al.*, a similar method for defining patellar height in canines was used. The authors defined a ratio between the greatest length of the patella and the length of the patellar ligament from the most proximal extent of the tibial tuberosity to the distal aspect of the patella [82]. They covered a region of flexion from 43 to 134 degrees and found an association between medial patellar luxation (MPL), patella alta, and an increased length of the patellar ligament. The patellar ligament length in was only constant throughout a relatively limited portion of the range of motion (70 - 110°) with a maximal value occurring at approximately 90°. They provided an equation to allow for correction of the ligament length based on joint angle. For their study, an unconventional method for measuring stifle angles was used, relying on limited measurements of the distal portion of the femur and proximal portion of the tibia, due to the fact that they did not have complete radiographs of the legs. Consequently, the angles in the Johnson *et al.* and Mostafa *et al.* studies are not analogous. Compared with the widely recognized measurement methods stated by Jaegger *et al.* [52], the measurement method by Johnson *et al.* would overestimate the stifle joint angle and Mostafa *et al.* would underestimate these angles. Thus, when Mostafa *et al.* report that the patellar ligament has statistically constant length between 70º and 110°, they may be reporting a range of 80º to 120° if they had used the method by Johnson *et al.*

1.3.2.2 Patella Alta and Patella Baja (Infera)

Most of the research on patella alta and patella baja that exists has been performed on human subjects. According to Lancourt and Cristini, patella alta may be a contributing factor to patellar luxation and chondromalacia [62]. Using the Insall-Salvati (IS) method, they measured patellar position in four separate groups of patients: those with no history or complaints of knee joint pain, those with chondromalacia, those with dislocating patellae, and those with apophysitis of the tibial tubercle. They found a statistically significant difference between the IS ratios of the four groups suggesting a link between patellar position and the aforementioned complications.

Johnson *et al.* relate the ratio of the patellar length to patellar ligament length and define it as 1.71±0.02 (mean ± SEM) in the clinically normal canine stifle of large breed dogs [56]. The authors further define a ratio greater than 1.97 to signify patella alta and a ratio less than 1.45 to signify patella baja. In the case of patella alta, the proximally located patella may lose the buttressing effect of the trochlear groove and thus be more susceptible to dislocation [34,56]. Further research pertaining to canine patellar luxation is needed and no reports have shown the effects of cruciate rupture or repair on patellar position in dogs.

1.3.2.3 Patellofemoral Contact

There have been several studies aimed at evaluating the role and significance of patellofemoral stabilizing components [39,53]. It is believed that any abnormality in factors such as patellar geometry, magnitudes and line of action of the quadriceps muscles, tibial rotation, etc. may lead to anomalies in the patellofemoral contact or patellar movement [53]. Jafari *et al.* [53] investigated the significance of structures such as the trochlear groove and medial and lateral retinacula on the shift and tilt of the patella in humans. Their study was restricted to two dimensions and a system of nonlinear equations based on actual geometry with several assumptions such as a fixed femur. The results indentified that differences in geometry from a normal trochlear groove have an effect on the patellar movement and cause excess tilt and rotation. Likewise, a drastic increase or decrease of quadriceps tension also had a noticeable effect on the patella. For all the combinations of trochlear groove anatomy and quadriceps force, however, no combination resulted in patellar subluxation or dislocation. Their results showed also that the retinacula, especially the medial, play a significant role to patellofemoral stability under tension from the quadriceps muscles. A study by Elias *et al.* concurred that the choice of quadriceps force distribution plays an important role in the patellofemoral biomechanics [39]. Due to the assumptions and simplifications of this research, the results should only be taken as a basic estimation. Patellofemoral articulation is a notable topic and in need of further research, especially in regards to the dog.

1.3.3 Medical Imaging

Modern medical imaging technology is used extensively in both clinical context and scientific research. Machines such as Magnetic Resonance Imagine (MRI), X-ray and Computed Tomography (CT) give physicians more ability to examine and diagnose a patient while giving researchers a better understanding and greater accessibility to the body.

1.3.3.1 CT technology

While several devices exist, such as those mentioned earlier, improved diagnostic capabilities of Computed Tomography (CT) make it one of the most valuable and frequently used research tools in the medical and engineering fields. Computed tomography was first introduced in the 1970's, but has only more recently begun to be used for preventative medicine because of significant improvements to scanning technology. The introduction of helical scanning and, most recently, multi-slice technology has transformed the CT from a transaxial imaging mechanism to a fully three-dimensional technique, capable of yielding high quality images that one can manipulate through computer post-processing [89,98,108]. Moeller *et al.* [77] also promotes the use of the CT as "one of the two modalities that have the greatest practical importance in modern sectional imaging" and, similar to Prokop *et al.*, attributes its importance to the high resolution and quality of the images [89]. It has been said that CT technology may have a hand at revolutionizing other forms of medical imaging such as virtual endoscopy, colonography, angioscopy and cardiac imaging [77,89,108]. This is supported by the continual revisions and updates on related publications and manuals. This prediction and enthusiasm is by and large based on the most modern of CT technology: the multi-slice scanner.

While older models such as helical CT remain in high use worldwide, multi-slice CT is the forerunner in this area of medical imaging technology and has the capability of higher quality images, faster scanning time, more flexibility and comfort for the patient and overall a "more pronounced clinical impact" over helical scanning [95,108]. Multi-slice CT scanners are similar to their predecessors but contain more than one detector ring, with up to 64 rows in the latest generation of scanners [95].

1.3.3.2 Concerns with CT technology

There are those who agree with Silverman [108] and are confident that CT technology will continue to evolve and improve the medical imaging community with possible advancements like appreciably faster scanners and wholly volumetric scanning acquisitions. There are others, however, who believe the future of medical imaging lies elsewhere. An update on the policy implications of the CT scanner mentions that the Federal Government is not contributing significantly any longer to the R&D of CT technology [87].

Radiation dosage associated with high resolution CT scanning continues to be a controversial issue [98]. Since concerns regarding this issue were first raised, back in the 1990s, several surveys and studies have been done to quantify the amount of radiation the patient receives during scanning. Although it has replaced some techniques that use higher radiation exposures, CT is still a relatively high dose modality. According to both Reiser and Kachelriess, radiologists are focused on image quality, which is a function of dose, so CT images are often achieved using high radiation exposure which frequently goes unnoticed by the radiologist [93]. They furthermore state that even after surveys showed that this issue needed to be regarded with higher consideration, little has been done to remedy it. Current levels of radiation are high especially in the pediatric populace.

Rivère says several techniques and protocols are currently being explored that will cut down on radiation dosage without compromising resolution [95]. He shows support of automatic tube current modulation, calling it a “promising approach, already implemented on a number of commercial scanners". Introduced by Naidich *et al*. in 1990, others state that although this method yields adequate images there was a considerable increase in noise [93].

1.3.4 Finite Element Analysis

Developed in 1943 and once limited to expensive mainframe computers owned by industries such as aerospace, defense and nuclear, today Finite Element Analysis is widely used for research, product design and product refinement in almost every industry. Several books are available on the subject which is also a field of specialization for many engineers. The medical and veterinary community has also benefited greatly from this technological tool. There has been much work and research, particularly on human anatomy, that has incorporated the use of FEA in solving structural analysis problems. Fewer studies have been done with respect to canine anatomy. Some of the most useful studies regarding FEA in medical and veterinary modeling are mentioned in the following sections.

1.3.4.1 Modeling in Humans and Canines

Though little research on the canine stifle has directly incorporated finite element analysis, several studies have been done on human anatomy and other regions of the dog using this powerful modeling tool. Since the introduction of finite element based medical research, several researchers have focused on the increased accuracy of three-dimensional solid geometric models from digitized scans. Several others have added the complex nature of soft tissues, articular cartilage and structures like the menisci in the knee [38,65,84,111]. Donahue *et al.* determined, through a geometrically accurate 3D FEA model of the human knee, that the assumption of rigid body motion to the bony structures (i.e. femur and tibia) are valid and only change the results by a small percentage [38]. Also of significance was their discovery that unrealistic rotational constraints beyond that of flexion/extension resulted in large errors for contact variables. These additional constraints had been frequently used in previous studies so this study reported important information for future endeavors. The research was limited in several ways including modeling the ligaments as nonlinear springs, neglecting the effects of the LCL and posterior cruciate ligament and excluding the patellofemoral joint contact. These simplifying assumptions were made because of the limited computational power and technological capabilities at the time of the study. Beillasa, *et al.* studied the general dynamic joint response in the human leg during strenuous activities, such as impact and showed that, although based on several assumptions which should not be used to define subject-specific response, finite element analysis makes it finally possible to illuminate this dynamic state [14]. However, some significant limitations include a lack of the lateral and medial collateral ligaments as well as the fact that the cruciate ligaments were represented by spring elements. Li *et al.* determined in their finite element model of the human knee joint that the inclusion of the meniscus is necessary for more reliable approximation of knee kinematics [64]. Their study, however, contained several limitations in the representation of this component which has since been improved upon by others [124,126].

Barink *et al.* implemented a 3-dimensional dynamic FEA model to simulate patellar movement, ligament behavior, and joint kinematics in a prosthetic human knee joint [11].

The study found a relatively linear relationship between patellar movement and knee flexion, but the model was oversimplified excluding proper nonlinear material properties as well as the proper insertion point of the lateral collateral ligament. Their predictions for varus valgus laxity may also be incorrectly estimated due to the absence of the patellar retinaculum.

Though more limited in its use on the canine stifle, finite element analysis is also being used to determine joint mechanics in dogs. A study by Shahar, Banks-Sills and Eliasy was the first report of results of finite element analyses of a clinical canine hip replacement system [103]. This study demonstrated the differences between two types of hip replacement stems commonly used in clinical veterinary practice (cementless and cemented) and proved that FEA was a useful means of approximating stress, strain and displacements for a complex geometry that would otherwise be difficult to determine. The authors assumed the bones to be linearly elastic, isotropic and homogeneous though they stated that the modulus of cortical bone varies over a large range. This is due to a lack of reliable material properties for canine anatomy. Thus, this study may not have fully and properly described the situation but approximated the circumstances to the best of their knowledge and obtained reasonable and meaningful results. In another study by Shahar, Banks-Sills and Eliasy the stress and strains in an intact canine femur for two loading conditions during mid-stance were investigated [104]. Prior to this study, information on this topic was unavailable. It was found that without the proper affects of surrounding muscle forces, stress and strains on the femur were overstated.

1.3.4.2 FEA of Ligaments

Direct measurement of the stress or strain distribution within the ligaments of the knee is a challenging task. Various techniques including strain gauges [10,47], displacements [68,94], Roentgen stereophotogrammetry [71,119], buckle transducers [13], Hyperelastic Warping [85] and robotic technology [123] have been used to describe the nature of human ligaments such as the ACL. An alternative to in vivo experimental studies is the use of computer methods, particularly the three-dimensional capabilities of FEA. Due to the similarities in material properties and function, research on human knees and ligaments is still valuable to research involving canine limbs. Research pertaining to the study of ligaments in both humans and dogs, with considerably more available for humans, is discussed in this section.

Of the primary ligaments in the knee (or canine stifle), the ACL (CCL in dogs) is by far the most researched. Several of the first studies that used FEA and involved ligaments modeled them as nonlinear springs [11,64]. Advancements in technology and computational power have allowed researchers to model ligaments as 3-dimensional nonlinear entities resulting in models that more accurately mimic these anatomical structures [122]. However, there are still comparatively few full three-dimensional finite element models that have been developed. Pioletti *et al.* developed an FEA model based on a full thermodynamic constitutive law for the ACL, incompressible isotropic hyperelastic formulation, and derived material data from uniaxial tensile tests [86]. The assumption of isotropy was later shown to severely limit the outcome of the model for a compression load directed along the collagen fibers and generate high compressive stresses that disagreed with experimental observations

[66]. An extension of the Pioletti model was seen in work by Daniel who developed a 3D orthotropic viscoelastic FEA model of the ACL [32]. This model included both the transverse isotropy and time-dependent material behavior but offered no information regarding ligament behavior during passive flexion. Limbert *et al.* expanded on a neo-Hookean incompressible isotropic hyperelastic potential constitutive model to include the application of the initial stress field within the ACL at full extension [65]. They determined that the inclusion of a pre-stress improved the prediction of the resultant force within the ACL for a passive knee flexion and supported previous assertions that the ACL in human has no stress-free position.

1.3.5 Summary

The stifle joint is one of the most complex and extensively examined joints in the dog. Due to the intricate relationships between its ligamentous components, muscle groups, articular cartilage and bony structures, injury to one of its constituents becomes a multifaceted problem requiring a thorough understanding of not only joint biomechanics but its functional anatomy as well. However, much of what is used to evaluate the stifle joint in canine models still comes from human analysis due to a scarcity of knowledge specific to canine joint mechanics and material properties. With the advent of advanced medical imaging techniques, such as Computed Tomography, a more thorough knowledge of both normal and afflicted stifle anatomy is possible.

Patella alta has been considered a significant cause of recurrent dislocation of the patella [50,56,62,82]. However, there is an apparent lack of both experimental and clinical information regarding patellar luxation and patella alta diagnosis in the canine. Due to the differences in both geometry and joint motion, data for patellar movement in the human should not be extended directly to the dog and more species specific analysis should be done. Many researchers have used modeling as a tool to analyze the mechanical characteristics of the patellofemoral joint but most of these have been limited to 2D representation [53]. The findings by Jafari *et al.* [53] suggest that the trochlear groove and quadriceps forces are unlikely candidates for dislocation risk factors and further studies on the causes of patellar subluxation are necessary. The issue of patellar location within the trochlear groove is of clinical importance and in need of further research as it pertains to the canine stifle.

A number of experimental studies have been done to describe the forces, strains and failure of stifle ligaments and surrounding components. There are a number of limitations, however, with these experimental methods. A significant alternative to experimental studies is the use of computer models. In particular, the use of finite element analysis is popular as it allows the three-dimensional structure to be analyzed and the stress/strain distribution to be visualized anywhere within the model. Several finite element models have been developed for human anatomy and this method has been equally useful in estimating the mechanical response of canine joint structures that are difficult or impossible to measure by other means. However, there remain very few fully three-dimensional models of the canine knee and several issues that would benefit from the implementation of such technology.

Cranial cruciate rupture remains one of the most widely diagnosed and threatening conditions to stifle stability and rear limb function. By means of in vitro and in vivo experiments as well as mathematical and computer models, many researchers have focused their efforts on understanding the stifle joint mechanics and the changes and behaviors associated with cranial cruciate ligament rupture. Understanding this condition and its effect on joint mechanics will aid in future efforts to develop new methods of treatment.

1.4 STATEMENT OF THE PROBLEM

Rupturing of the cranial cruciate ligament is one of the most common orthopedic conditions in dogs and the most frequent cause of rear limb lameness because of subsequent pain and instability of the stifle joint. It afflicts all ages and breeds of dogs and can lead to other serious problems such as osteoarthritis and meniscal injury. Several surgical procedures are available to treat ligament rupture, the most popular being the tibial osteotomy procedures. While this area of veterinary orthopedics has received an increasing amount of research attention over the past decade, there is still much to discover regarding the effects of these surgical procedures on the function of the canine stifle. In particular, no information currently exists regarding the effects that CCL deficiency and treatment have on patellar location with respect to the trochlear groove. The intention of this thesis is to determine these effects via a 3D physical, rapid-prototyped model of the entire canine rear limb. The results of particular interest are patellar location and evidence of patella alta or patella baja as well as any sign of patellofemoral instability. The results from this study will help provide more data and information concerning canine anatomy, CCL rupture and surgical treatment options.

1.5 MATERIALS AND METHODS

1.5.1 Subject Specifics

The subject used for this study was a Doberman pinscher, age 5.5 at the time the scans were taken. His weight at time of scan was 50kg and his left hind limb had a tibial plateau, measured from mediolateral radiographs using conventional methods [12,41,92], of 28º. The subject was euthanized for reasons unrelated to this project.

1.5.2 CT to 3D Modeling: Pre-processing

Images of the subject's left hind leg were attained using computed tomography. This data was obtained prior to this study for reasons unrelated to the project. Due to proximal tibial deformities in the subject's right hind leg, it was decided that the left hind leg would be used to create all models for this study. The CT scan was chosen based on the following objective criteria: the scan was free from scatter and the patient's left hind leg exhibited good physical condition representative of this type of large-breed dog, and the patient was of median age and weight as compared with other studies of large-breed dogs found in literature [26,52,90,100]. The CT data was imported and manipulated using Mimics 11.11 (Materialise, Leuven, Belgium). The threshold was set in order to highlight the dense bony structures of the leg including the femur, tibia, patella, fibula, and hock as shown in Figure 1.5.1 below. The entire left hind leg was isolated just below the acetabulum and each of the aforementioned bony structures was separated into a different mask and verified for geometric accuracy.

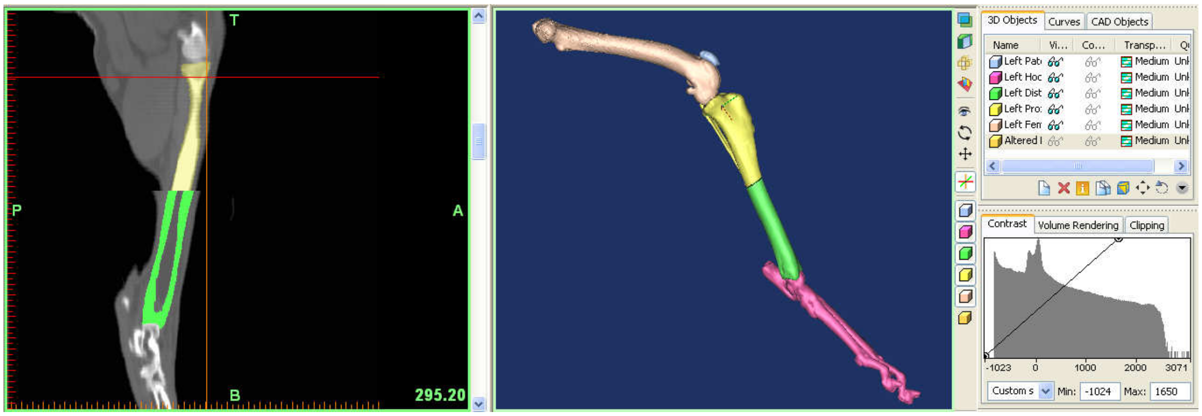

Figure 1.5.1: Isolation of bony structures in Mimics 11.11 [Materialise, Leuven, Belgium].

The files were refined in Magics 12.01 (Materialise, Leuven, Belgium) before being ready to create the physical models. Specifics on the other processing operations done in Magics are highlighted in the following section.

1.5.3 Geometric Markers

In order to facilitate post-processing of the physical models and assist in alignment of components during assembly, geometric markers were added to the tibia, femur, and patella. On the tibia, two markers were inserted at 50% and the distal 75% of the tibial shaft length, in accordance to other similar studies [83]. The shaft length was measured from the intercondylar eminence to the lateral malleolar of the talus and a line connecting these two points defined the diaphyseal tibial axis (DTA) or tibial long axis [83]. The marker placed at the 50% location was a cylinder of diameter 5mm and protruded 2mm medially from the cortex of the bone. The other DTA marker protruded 25mm both medially and laterally to aid in fixturing during several post-processing operations. This is shown in Figure 1.5.2. Markers were also added to the cranial and caudal aspects of the medial tibial condyle, as shown in Figure 1.5.3. These were used to determine the Tibial Plateau Slope (TPS) which is a line tangential to the linear portion of the medial tibial condyle and can be found by connecting these two points [41,83,92]. The tibial plateau angle of 28° was measured using conventional methods as the angle between this tangential line and a line perpendicular to the tibial long axis [52].

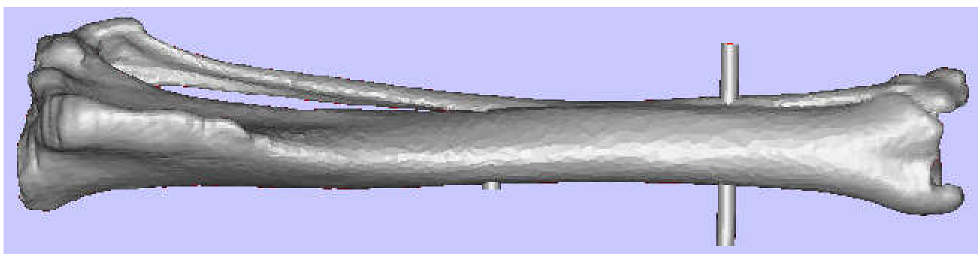

Figure 1.5.2: Tibial markers at 50% and 75% of shaft length along the tibial long axis.

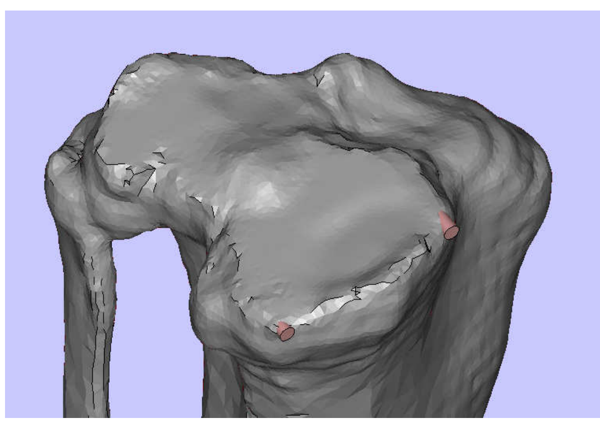

Figure 1.5.3: Markers at the cranial and caudal aspects of the medial tibial condyle, defining the tibial plateau.

The proximal tibial axis (PTA) is determined by a line joining the cranio-caudal midpoint at the distal aspect of the tibial crest and the cranial aspect of the medial tibial condyle. A marker at the distal aspect of the tibial crest also aids in determining the DTA. These markers can be seen in Figures 1.5.4 (a-b) below.

(a)

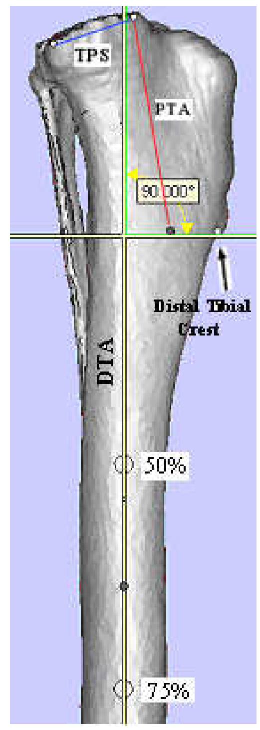

(b)

Figure 1.5.4: Proximal tibial markers (a) tibial crest marker (b) all tibial markers and measured axes (TPS, PTA, DTA).

Geometric markers were added to the femur for the same reason. To establish the femoral long axis, two markers were positioned according to literature as a line joining the lateral femoral epicondyle and the greater trochanter [52]. The total length of the femur, measured from the greater trochanter to the lateral epicondyle, was approximately 250mm. To help with post-processing, additional markers were placed at 33% of that length (82.5mm from the proximal end) and 66% (165mm from the proximal end). This is shown in Figure 1.5.5.

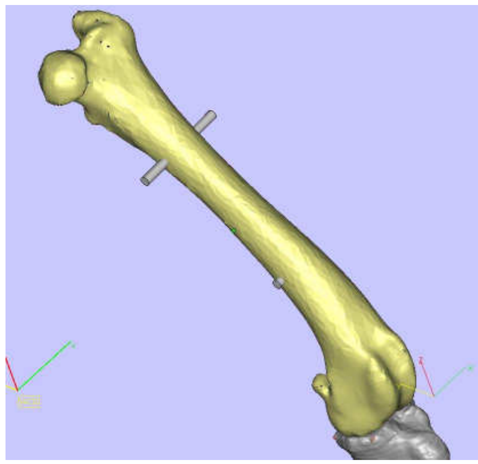

Figure 1.5.5: Markers at 33% and 66% of femoral shaft length along femoral long axis.

Geometric markers were also placed on the patella, one at the most distal aspect and one at the most proximal aspect as shown in Figure 1.5.6. These markers were used to identify displacement and rotation undergone by the patella at the different angles of interest for this project [34, 56, 82].

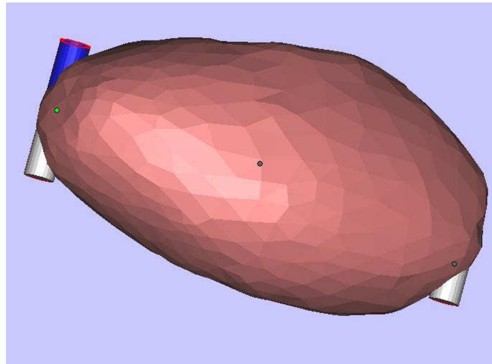

Figure 1.5.6: Patella markers and proximal and distal ends.

1.5.4 Constructing the Proximal Interphalangeal Joint

The angle between the metatarsals and phalanges was chosen to be fixed at 110º for all stifle angles of this project. Since there is no literature defining the angle of the metatarsal-phalangeal joints at our specific angles of interest, this was chosen based on literature as an acceptable position for corresponding stifle angles around and during the stance phase of the gait [48]. In order to manually set this angle, the hock was separated at the proximal interphalangeal joints. This was achieved by creating semicircular cuts at each joint using a boolean operation as shown below in Figure 1.5.7.

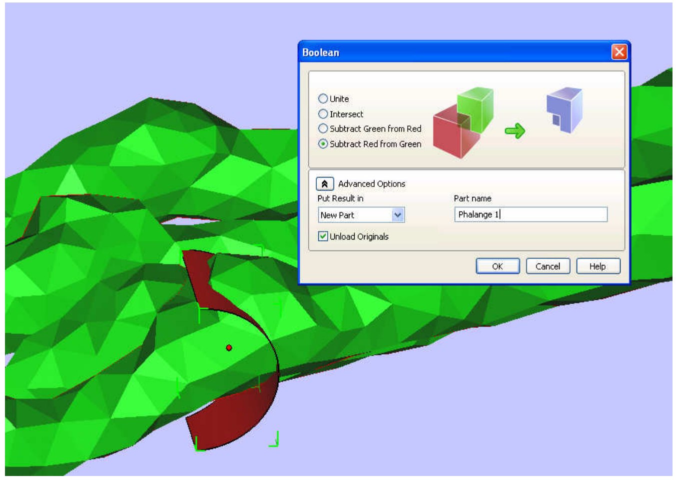

Figure 1.5.7: Boolean operation to separate phalanges at metatarsal-phalangeal joints.

After making each of the four cuts, the subsequent shells were separated into individual parts using the "Shells to Parts" function within the Fix Wizard. In order to facilitate articulation and alignment in the physical model, hinges were incorporated into the computer model utilizing 2mm thick semi-circles and rectangles in conjunction with several Boolean operations shown in Figures 1.5.8 and 1.5.9. The resulting connection allows the phalanges to be positioned at 110º, which is shown illustratively in Figure 1.5.10.

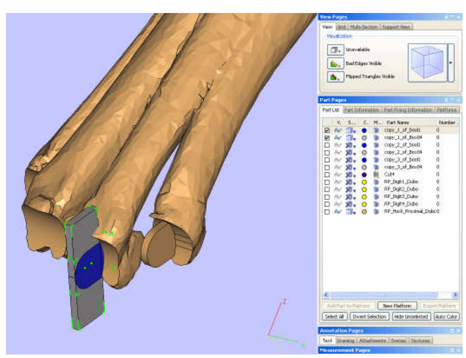

Figure 1.5.8: Boolean operation used to create joint movement of the phalanges.

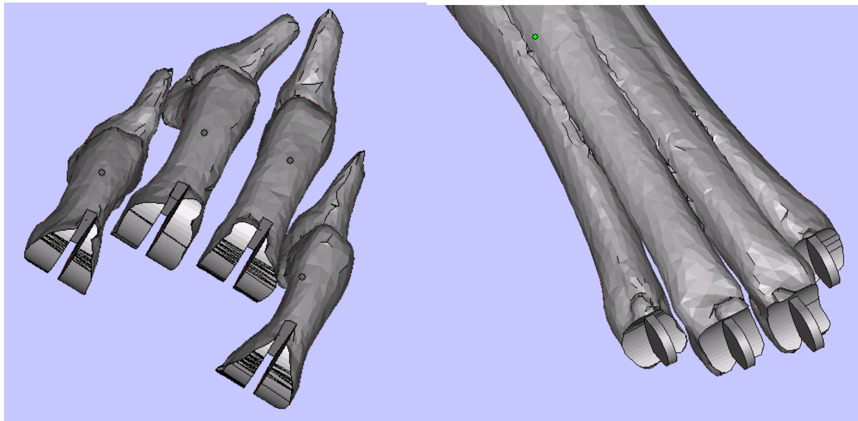

Figure 1.5.9: Resulting articular surfaces of the distal metatarsals and proximal phalanges.

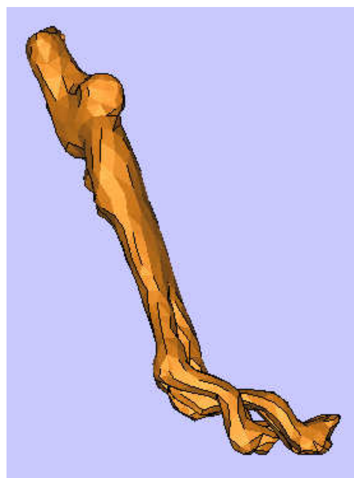

Figure 1.5.10: Illustration of angled proximal interphalangeal joint to 110º.

1.5.5 Modeling the Meniscus

In the dog, the lateral and medial menisci deepen the tibial articular surface and provide better accommodation of the femoral condyles on the tibial plateau. They help increase the stability of the stifle, act as shock absorbers to protect the articular surfaces of the tibia and femur, and aid in lubrication of the joint [27]. Injury to the meniscus is attributed to progression of degenerative joint disease [25,27,90]. It was not the intent or focus of this project to model the exact likeness or response of the menisci but it was necessary to replicate the alignment and offset between the femur and tibia in order to have an accurate model of the canine stifle. Using Magics, the lateral and medial menisci were created as one component through a series of boolean operations. Part of the boolean process and the resulting meniscus are shown below in Figure 1.5.11 (a-b).

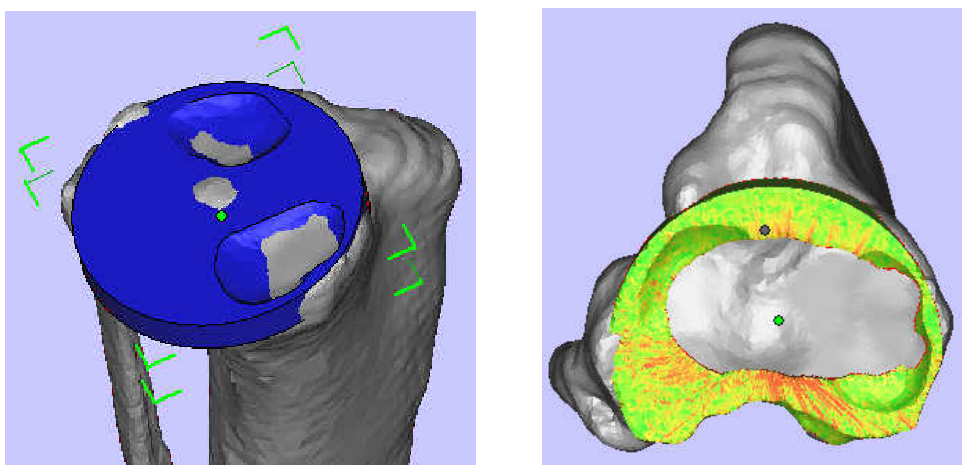

(a) (b)

Figure 1.5.11: Meniscus created using boolean operations in Magics. (a) first boolean operation (b) further removal of interior

After performing the boolean operations, the “Shrink Wrap” function in Magics was used to thicken the general shape of the structure and make it more anatomically realistic. This was followed by performing a boolean operation with the femur in each of the angles of interest resulting in the final version of the meniscus shown below in Figure 1.5.12 (a-b).

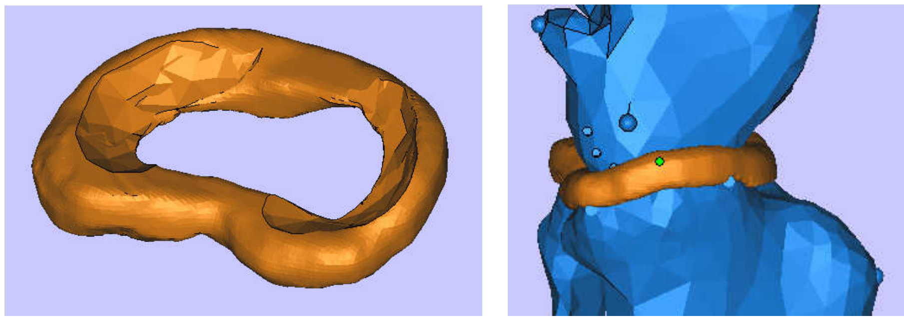

(a) (b)

Figure 1.5.12: Final model-ready meniscus. (a) top view of meniscus (b) meniscal boundary between articulating surfaces of tibia and femur

1.5.6 Ligament and Muscle Origin and Insertion Points

In order to assure that the ligaments and muscles of interest would be placed in the same position on each physical model, divots representing the origins and insertions were created in the computer model so that the rapid prototyped master pattern would have them as well. Anatomical models and preserved specimens like the ones in Figure 1.5.13 (a-b) were used to determine insertion points and soft tissue geometry.

(a) (b)

Figure 1.5.13: Anatomical models used to determine origin and insertions of ligaments. (a) dog leg model with painted attachment points (b) cadaver dog leg used to reproduce ligaments.

Fifteen origin and insertion points in total were marked pertaining to the 5 ligaments (cruciates, collaterals, and patellar) and 2 muscles (gastrocnemius and quadriceps) being modeled. These points were marked on the model by using 3mm diameter spheres, indented into the bone and subtracted from it to make small divots. Diagrams of the origin and insertion points along with a color coded key are shown below in Figure 1.5.14 (a-d). The only points not shown are the insertion of the gastrocnemius muscle, located at the proximal ridge of the calcaneous, and the origin of the quadriceps, located more proximally on the femoral shaft.

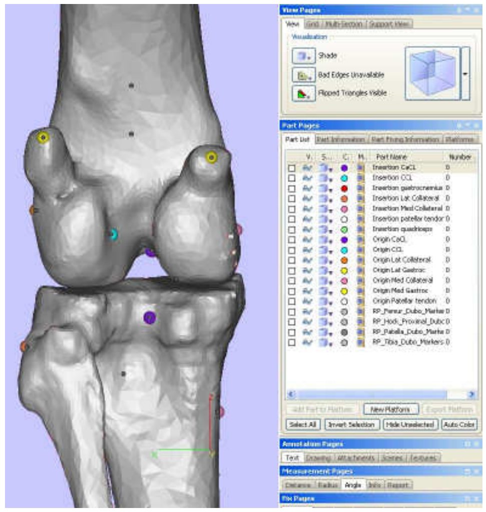

(a) (b)

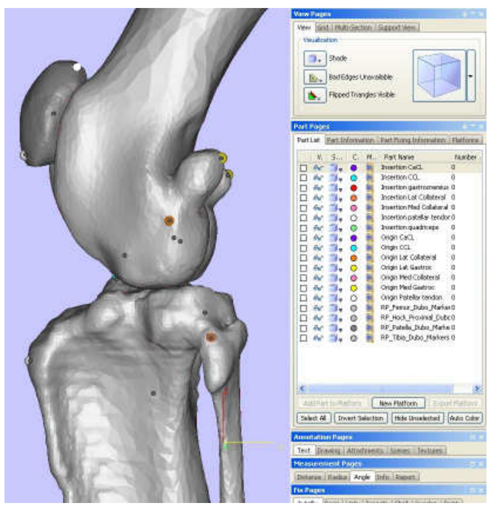

(c) (d)

Figure 1.5.14: Origin and insertion point for stifle ligaments. (a) caudal view (b) cranial view (c) lateral view (d) medial view

1.5.7 Hip Joint Considerations

The testing fixture was designed to constrain the femoral head so that load is applied along the mechanical axis of the leg (Figure 1.5.15). A hole for attachment purposes was implemented in the pre-processing step so that all models would be identically fastened to the testing fixture. Figure 1.5.16 shows the resulting hole through the femoral head.

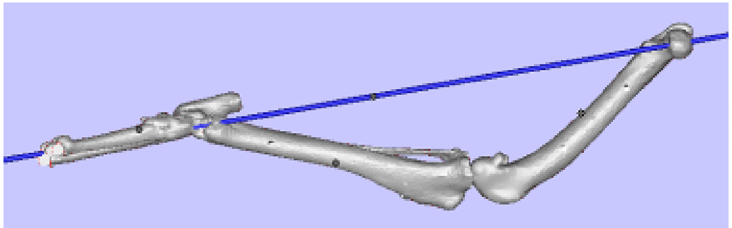

Figure 1.5.15: Mechanical axis of rear leg used to create hole through femoral head.

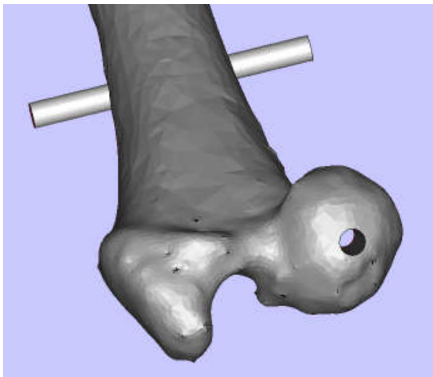

Figure 1.5.16: Femoral head hole to allow attachment to the testing fixture.

1.5.8 Measuring Patellar Location

In order to accurately position the patella in each testing orientation (stifle angles of 75°, 96°, 113°, 130°, 148°), the measurement of patellar ligament length (L) to patellar length (P) was first compared with literature and validated as a satisfactory starting position. The measurement of L:P was obtained using two separate methods [34,82] and each was found to be well within the ranges reported in the respective paper. According to Johnson *et al*. [34], the patellar ligament was measured from the caudal aspect of the ligament insertion point to the distal end of the patella, as shown in Figure 1.5.17a. This resulted in an L:P of 1.62, compared with a mean ± SD of 1.68±0.18 stated in the literature. A slightly different definition of patellar ligament was used in the paper by Mostafa *et al.* (shown in Figure 1.5.17b). Here, the ligament was measured from the cranial aspect of the area of insertion on the patella to the cranial insertion located on the tibial tuberosity. This measurement resulted in an L:P of 1.99 which was only 0.021 less than the mean value reported for that study and well within the SD of 0.2. Thus, it was concluded that the scans used for this study and original position of the patella were adequate.

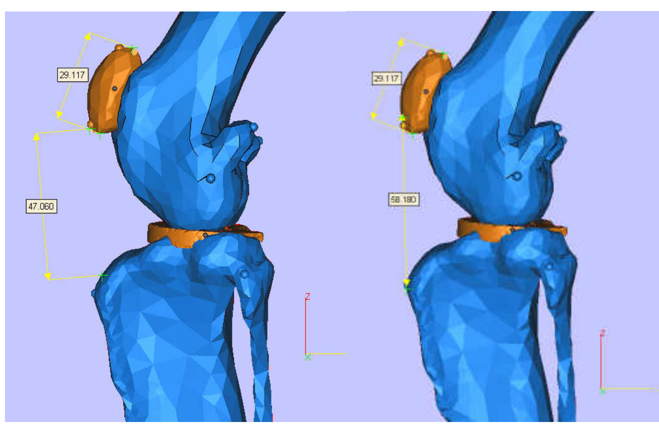

(a) (b)

Figure 1.5.17: Patellar and patellar ligament lengths via two different measurement methods. (a) Lengths according to Johnson *et al.* [34] (b) Lengths according to Mostafa *et al.* [82]

The stifle angles used for this study are within the reported ranges for which the patellar ligament can be assumed inextensible [34]. Therefore, the original length of the patellar ligament could be used to position the patella in all subsequent orientations throughout the proposed range of motion.

1.5.9 Measuring the Stifle Angles

Five separate stifle angles were tested during this study to provide data over an entire range of motion. According to literature regarding typical flexion and extension angles during walking and trotting phases of large-breed dogs [34,48] the following angles were used for this study: 75°, 96°, 113°, 130°, 148°.

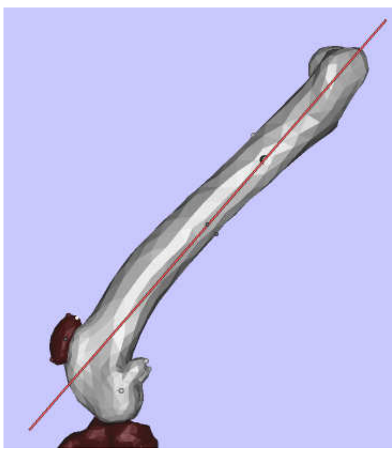

Figure 1.5.18: A line representing the femoral long axis.

The stifle angle was defined according to literature as the angle between the tibial shaft and the longitudinal axis of the femur [52]. The femoral long axis was defined as a line that extends from the greater trochanter to the lateral femoral epicondyle. The axis created, shown in Figure 1.5.18, was used to determine the stifle angle on all subsequent models. The original stifle angle was measured to be 128.13°, as shown in Figure 1.5.19. Using the patellar ligament length specifications previously stated, the orientations for all stifle angles were constructed and are shown below in Figure 1.5.20 (a-e).

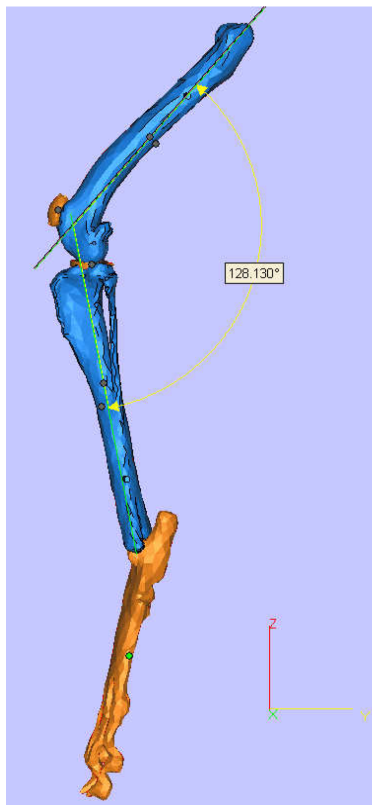

Figure 1.5.19: Lateral view showing the original stifle angle from CT data.

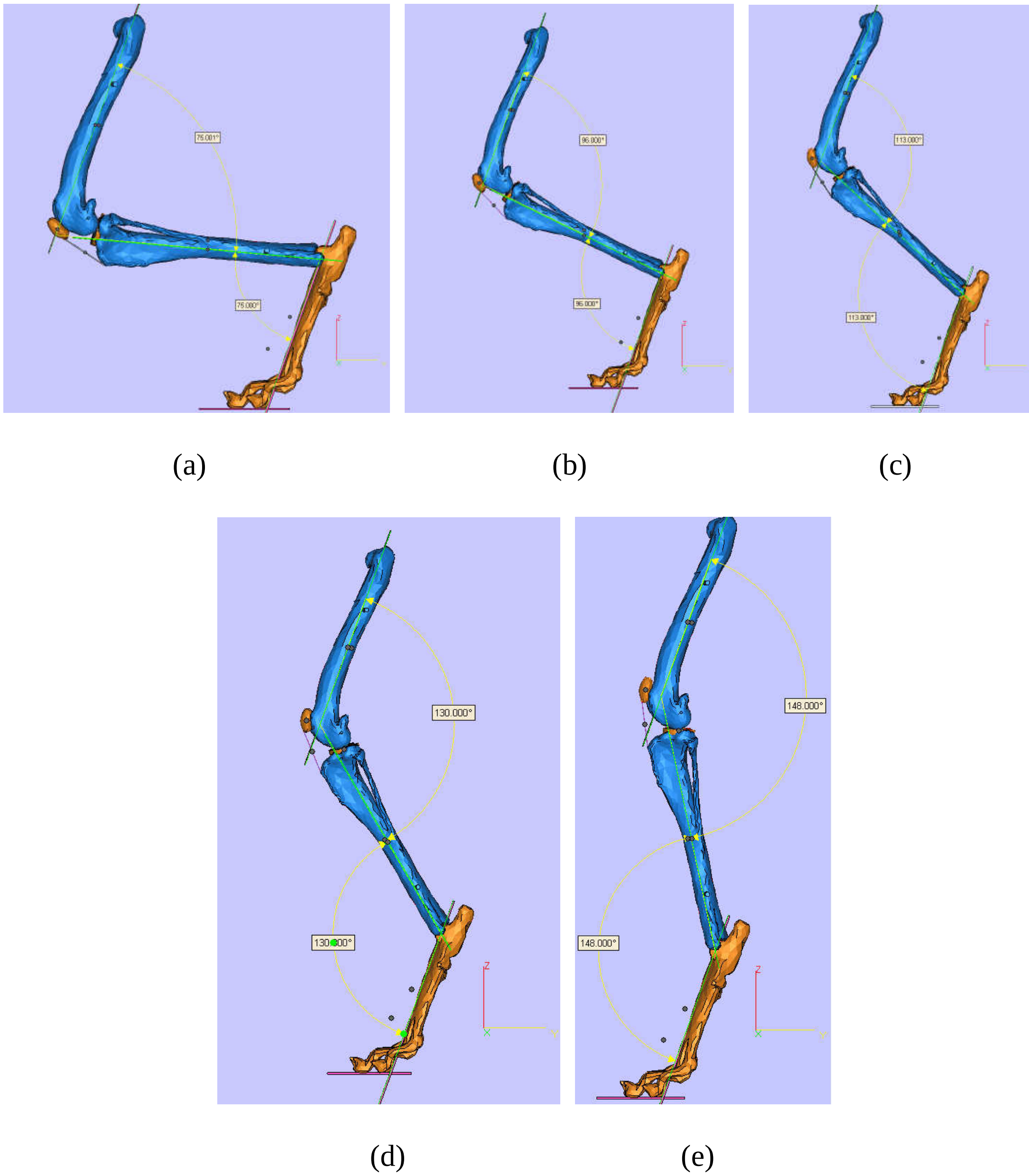

Figure 1.5.20: Stifle angle orientations for RP models. (a) stifle angle of 75° (b) stifle angle of 96° (c) stifle angle of 113° (d) stifle angle of 130° (e) stifle angle of 148°

1.5.10 Rapid Prototyping Utilization

The 3D, anatomically correct models for this project were created using a combination of rapid prototyping, silicone molding, and casting techniques. An initial prototype of the leg assembly was first created on an SLA® 190 (3D Systems Corporation, Rock Hill, SC) and was valuable in brain storming and ascertaining necessary design modifications before constructing the final product. Due to size limitations of the build platform, the files for each component were segmented in Magics and positioned in 3D Lightyear 1.1 (3D Systems Corporation, Rock Hill, SC) as shown in Figure 1.5.21 to obtain the necessary build files. These quickcast models, shown in Figure 1.5.22, aided immensely in visualizing the articulation of the various components of the leg as well as designing the testing fixture.

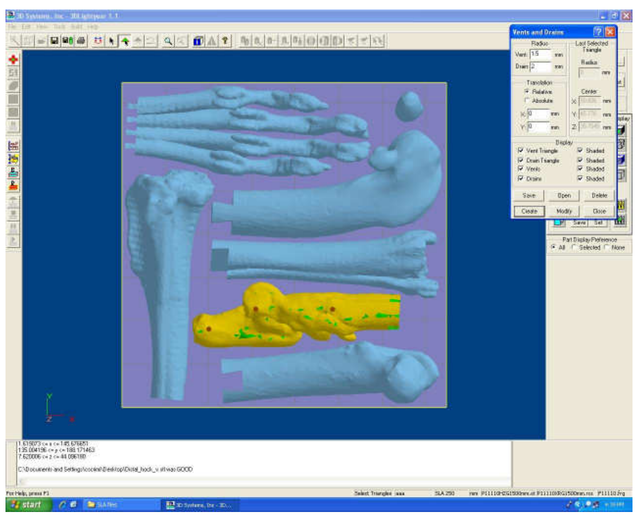

Figure 1.5.21: Build platform positioning of sectioned components [3D Lightyear 1.1, 3D Systems Corporation].

Figure 1.5.22: Quickcast models made from SLA® used for fixture design and visualization.

After implementing ligament origin and insertion points as well as several additional features used for alignment purposes, a final design for the model was ready to be built. The Dimension FDM™ (Stratasys, Inc., Eden Prairie, MN, USA) was utilized for this build due to machine availability. The individual components of the model were positioned on the build platform as shown in the screenshot from Magics 12.01 (Materialise, Leuven, Belgium) in Figure 1.5.23 below.

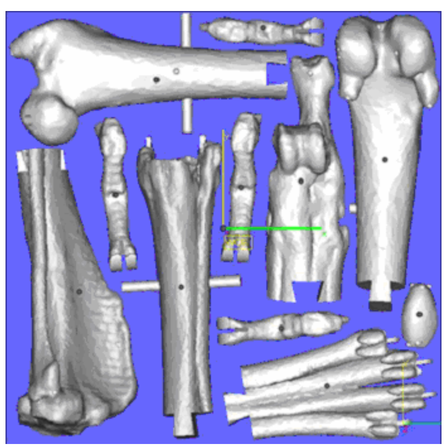

Figure 1.5.23: Final build arrangement on Dimension FDM™ (Stratasys, Inc.).

1.5.11 Silicone Mold Procedure

Wax was used to reattach the separated FDM™ parts (i.e. the femur, tibia, and hock). The joints were sanded flush to remove any excess wax and the surfaces were prepared for casting. The casting molds were created using Mold Max™ 30 silicone rubber (Smooth-On, Inc., Easton, Pennsylvania, USA). Figure 1.5.24 below shows the suspension of the FDM™ parts in the container for mold creation.

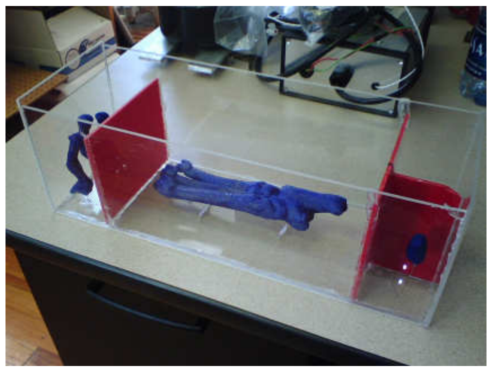

Figure 1.5.24: Suspension of phalanges, proximal hock and patella for silicone mold creation.

After the molds were fully cured and vents and drains were cut, the models were cast out of a composite consisting of EP5340 two-part epoxy (Eager Polymers, Chicago, IL, USA), bone meal (ScottsMiracle-Gro, Marysville, OH, USA) and glass fibers mixed to a specific ratio as used in previous research [43]. This ratio of ingredients has been shown to simulate the mechanical properties of real bone to a degree that will be more than sufficient for the purposes of this research due to the fact that the leg models will not be undergoing extensive loading. For the same reasons, a medullary cavity and cancellous bone were neglected from this study. The composite has a pot life of 20 minutes, during the first 5 minutes of which the mixture was thoroughly stirred to ensure a homogenous distribution of bone meal throughout the composite. Figure 1.5.25 shows a mold with glass fibers set in place. A 50ml syringe was used to inject the composite into the molds shown in Figure 1.5.26a below. It should be noted that no glass fibers were used in the patella due to this component's small size.

Figure 1.5.25: Tibial mold with glass fibers randomly oriented along shaft.

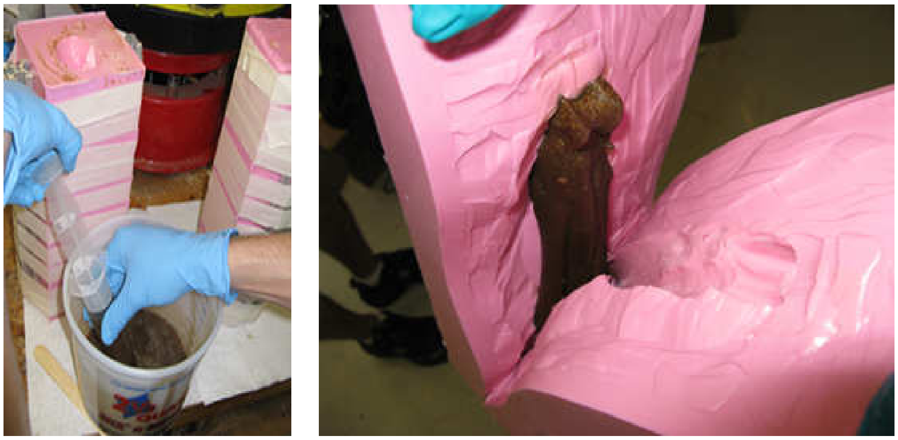

(a) (b)

Figure 1.5.26: The bone casting process. (a) injection of epoxy composite in silicone molds (b) removal of a successfully cast hock

1.5.11.1 Casting the Meniscus

The aforementioned computer generated model of the meniscus was prepared in 3D Lightyear 1.1 (3D Systems Corporation, Rock Hill, SC) and printed on the 3D Systems SLA® 190 to be cast similar to the bone components (Figures 1.5.27 and 1.5.28). Due to the intricacy of the geometry, three copies were produced simultaneously. Several available materials were tested for use as the meniscus. Since it is beyond the scope of this project to develop a material that mimics the actual anisotropic mechanical properties of the canine meniscus, it was decided that the Mold Max™ 30 silicone rubber (Smooth-On, Inc., Easton, Pennsylvania, USA) would be used because of its durability and stiffness characteristics.

Figure 1.5.27: Three copies of RP menisci built on the SLA® 190 [3D Systems Corp.].

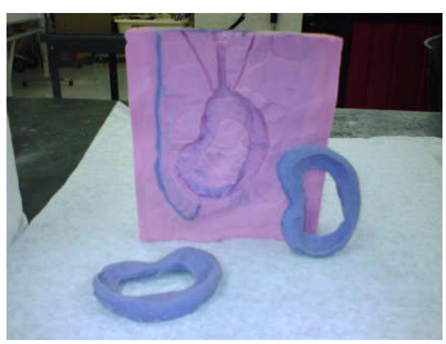

Figure 1.5.28: Silicone mold and castings for the model menisci.

After casting the bone components of the model, several post-processing steps remained to be performed. Geometric markers were filled with acrylic paint for identification and viewing purposes and to help make accurate and repeatable assemblies of the leg models. As can be seen from the example of the cast femurs in Figure 1.5.29 below, each component type was produced as six identical castings.

Figure 1.5.29: Six identical femur castings with easily identifiable geometric markers.

1.5.12 Tibia Drilling Jig

In order to attach the hock to the tibia, a more rigid connection had to be developed after the bone models were cast. Initially, half a hinge joint had been placed distally on the tibia computer model; however, this feature proved to be too delicate to securely fasten the hock to the tibia. To counter this problem, a combined fixture and jig was developed (Figure 1.5.30) for drilling two holes distally in each tibia in the exact same locations on each model.

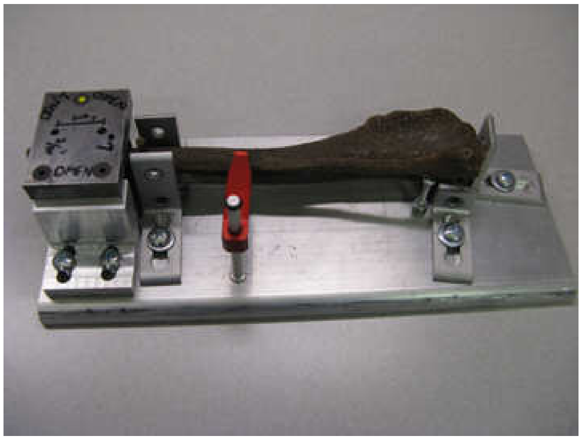

Figure 1.5.30: Fixture for securing tibia in order to drill holes for tarsal attachment brackets.

The bone models are seated snugly in the fixture shown above in Figure 1.5.30. The jig is bolted over the distal tibia providing guide holes for the #7 and 3/16" twist drills. Figure 1.5.31 shows the results including some of the associated hardware used to connect the tibias to the hock.

Figure 1.5.31: Tibiae with identically drilled holes at distal end for tarsal joint attachment.

A single hock was created to be used with all leg models in order to reduce the associated variability that is caused by the amount of manual machining work performed on the part. In order to facilitate easy swapping of the hock between leg models, two connecting rods were CNC (computer numerically controlled) machined from a 3/8" plate of 6061 T6 aluminum. These plates slide over the ¼-20 bolt and 3/16" dowel pin in the distal tibia as well as the ¼" dowel pin placed through the hock as shown in Figure 1.5.32 (a-b). They are held in place by a hand-tightened nut on each side.

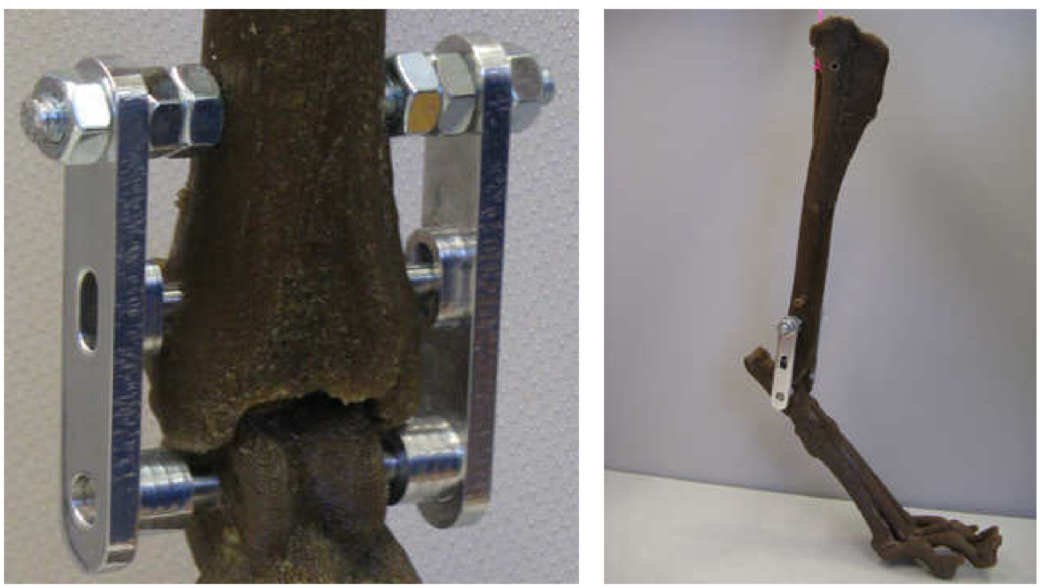

(a) (b)

Figure 1.5.32: Tarsal joint attachment hardware. (a) CNC machined brackets (b) attachment of tibia and hock at the tarsal joint

1.5.13 Drilling femoral head hole

To drill the ¼” hole through the femoral heads in the exact same position, the bones were pinned on the .2” hole that were cast into the femoral heads as shown in Figure 1.5.33a. The bones were then flipped and pinned on the resulting ¼” hole and drilled from the opposite side (Figure 1.5.33b). A 0.2510” ream in a hand chuck was used to complete the operation.

(a)

(b)

Figure 1.5.33: Drilling of the femoral head hole. (a) pinning of the pre-cast hole (b) drilling the thru hole to be used for fixture attachment

1.5.14 Attaching the Ligaments

Several methods for attaching the ligaments to the bones were explored. Some of these included tying strings to screws, embedding eye hooks in the models, and gluing the ligament material directly into the bone. It was decided that custom set screws would serve the purpose best by allowing the ligaments to be seated flush against the bones as they are in reality, and allow for the ligaments to be easily removed and replaced in case they were damaged during the subsequent surgeries. In order to use the set screws, holes were drilled and tapped into the models using the divots representing the origins and insertion points as starting locations for a hand drill. Size 10-32 set screws were notched using a Dremel and cutting disc and a similar notch was cut into an Allen wrench to make a space for the ligament material during assembly. Size 0 silk suture material (shown in Figure 1.5.34) was braided using 6 strands and inserted into the set screws (Figure 1.5.35). The resulting cross-sectional geometry of the braided suture material was: width= 0.08in, thickness= 0.025in.

Figure 1.5.34: Silk suture used for stifle model ligaments.

Figure 1.5.35: Custom set screws and braided suture ligament comprised of 6 strands.

A single suture strand was found, via tensile test (Figure 1.5.36a), to have an Ultimate Tensile Load of 7.3 lbs. Braiding six strands increased the UTL to 30.94 lbs and changed the shape of the stress-strain curve to include a slight toe region which is more representative of an actual ligament (Figure 1.5.36b).

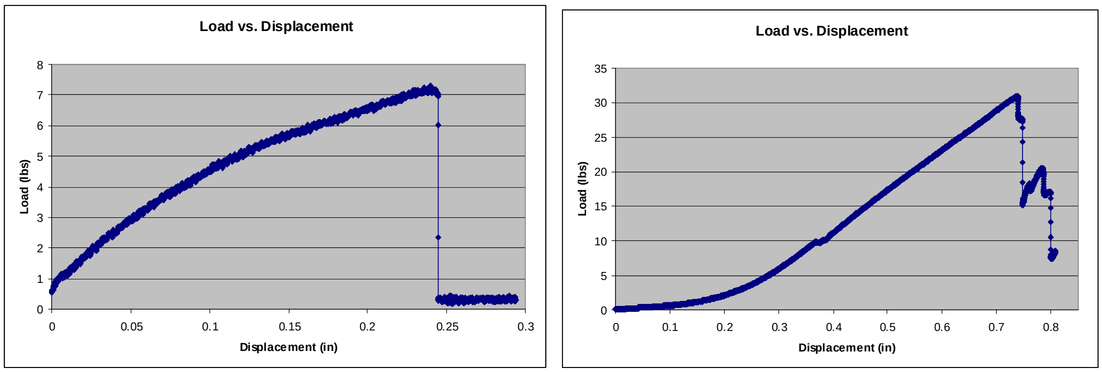

(a) (b)

Figure 1.5.36: Tensile test results for silk suture. (a) one strand (b) six braided strands

The length of each ligament was chosen so that no cranial or caudal drawer occurred in the intact model, and so that the collateral ligaments were taught in the full extension of 148º. The ligament lengths are shown below in Table 1.5.1. The length of the patellar ligament was determined by the method described previously in Section 1.5.8. In order to stabilize the patella during articulation, a hole was drilled mediolaterally through the center of each, and a thin elastic band passed through and attached to the origins of the gastrocnemius to mimic the naturally present parapatellar fibrocartilage.

Table 1.5.1: Ligament lengths measured as "knot-to-knot" plus two set screw lengths.

Cranial Cruciate	1.270"
Caudal Cruciate	1.495"
Lateral Collateral	1.512"
Medial Collateral	2.083"
Patellar Ligament	2.508"

After assembly, the joints were inspected to ensure that no cranial or caudal drawer existed and that the range of motion was identical in each. Figure 1.5.37 shows various views of the identical leg models, temporarily held with rubber bands.

Figure 1.5.37: Collage of identical, assembled leg models.

1.5.15 Quadriceps and Gastrocnemius Muscles

In order for the leg models to resist a load applied to the femoral head and translate that load to the ligaments without flexion in the stifle and talocrural joints, a series of wires and turnbuckles were used to constrain the models as seen in similar studies [2,121]. The purpose of these components was not to mimic the physiologic function of the quadriceps and gastrocnemius, but to represent the muscle-tendon units when they are loaded and opposed further elongation [60, 121]. The quadriceps muscle group includes the rectus femoris (RF), vastus intermedius (VI), vastus medialis longus (VML), vastus medialis obliquus (VMO), vastus laterialis longus (VLL), and vastus lateralis obliquus (VLO). For our study we assumed that the entire quadriceps force will be applied through the RF component as we are primarily interested in patellofemoral interaction and proximodistal subluxation of the patella with respect to the trochlear groove [39]. Putting too much tension on the quadriceps can produce inaccurate results pertaining to patellofemoral articulation [53]. This is likely due to the simplification of the quadriceps muscle group. For this reason, the leg models in the testing fixture were only loaded to 1.5lbs – the minimum load that was required to achieve cranial drawer in the CCL deficient stifle model at all five loading angles.

1.5.16 Testing Fixture

The purpose of the testing fixture is to hold the completed leg models securely at the five angles of interest. A small load was applied at the top to ensure the femur was seated snugly within the meniscus on top of the tibial plateau. The frame of the testing fixture was assembled from 1” 80/20 aluminum. The overall dimensions of the frame are 17”x17”x34”. Two nylon sliding brackets were used to hold the 3” load applicator. Attached to the base of the load applicator lies the femoral head attachment pin which was allows femoral rotation about two axes. A counterbalance mechanism was finally attached (shown in Figure 1.5.38) to the top of the fixture.

Figure 1.5.38: Testing fixture with assembled leg fixed for testing.

1.5.17 Testing Procedure

Both an intact and CCL deficient leg model were tested at each of five angles representative of maximum and minimal angles during walking and trotting [34]. After assembly, the models were attached to the fixture via the femoral head attachment pin. The hock rests on the support structure on the base plate (shown in Figure 1.5.38). The turnbuckles representing the quadriceps muscle group and gastrocnemius were rotated in turn to position the leg in one of the five stifle angles. Stifle joint angles were measured according to literature [52] and to ensure accuracy and consistency were measured using three different instruments shown in Figure 1.5.39: a universal plastic goniometer, an electrogoniometer and rigid wires bent to the five angles. A load of 1.5lbs (the minimum necessary to cause cranial drawer in the CCL deficient model at all five angles) was applied to the models. Photographs were taken and observations regarding drawer, subluxation, and stability were recorded. Patellar location within the trochlear groove was randomly recorded from the resulting pictures for each model and angle according to methods found in literature [34].

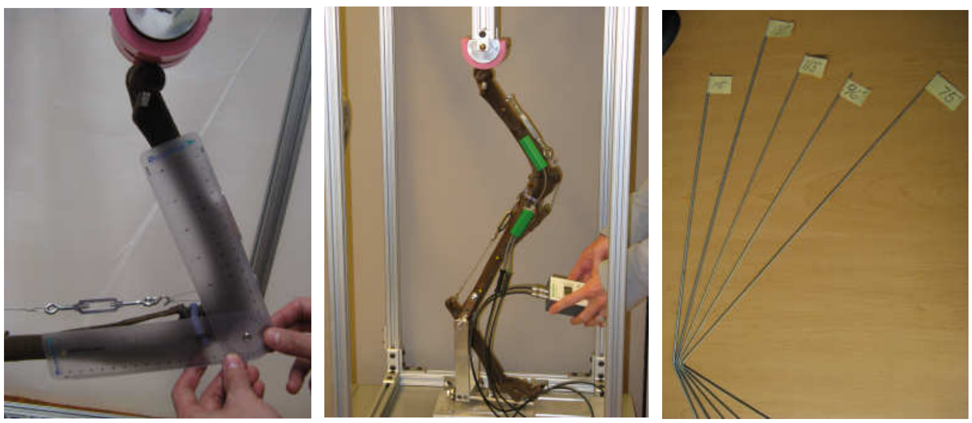

(a) (b) (c)

Figure 1.5.39: Instruments used to measure stifle angle. (a) universal plastic goniometer (b) electrogoniometer (c) rigid wires bent to the angles of interest

1.6 RESULTS

Table A.1 containing the sample data and Table A.2 containing the consolidated average data graphed in Figure 1.6.1 and Figure 1.6.2 can be found in the Appendix A.

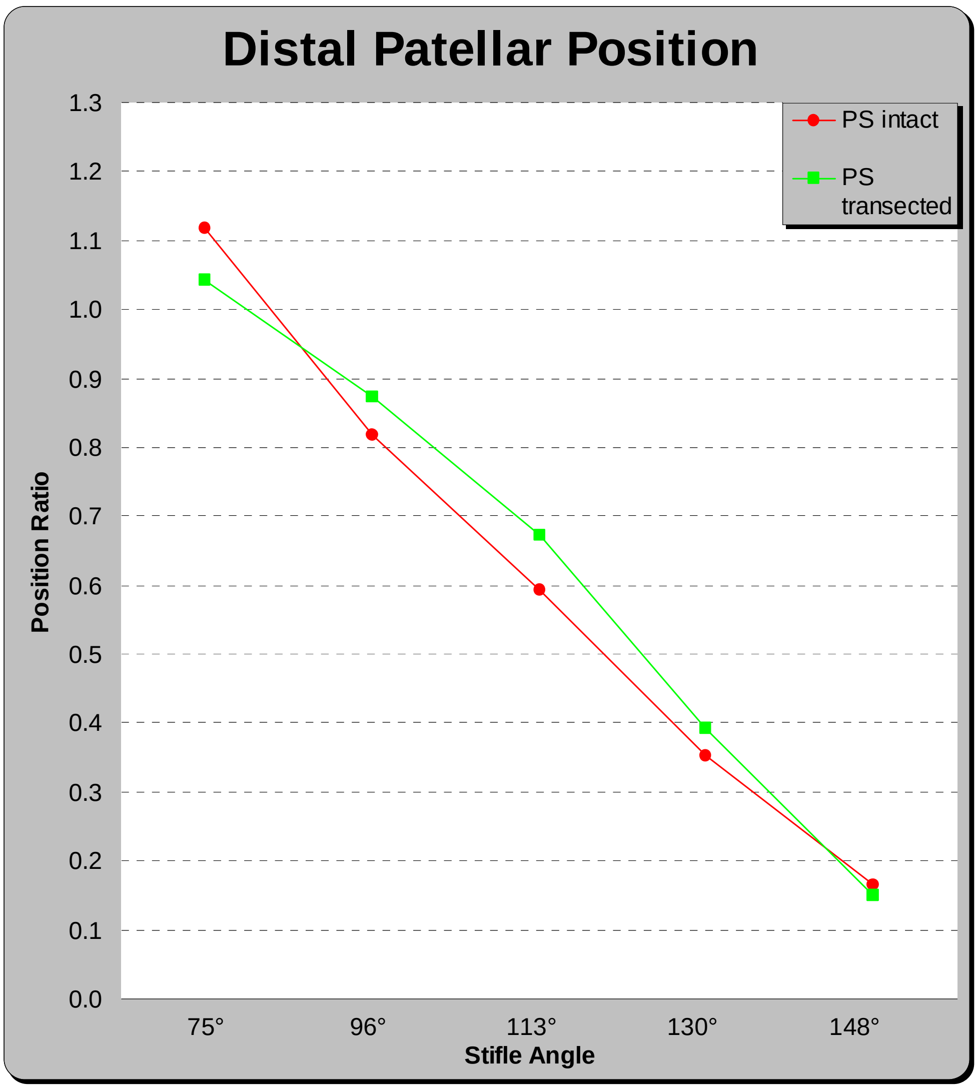

Figure 1.6.1: Graph of the distal patellar location with respect to the trochlear groove.

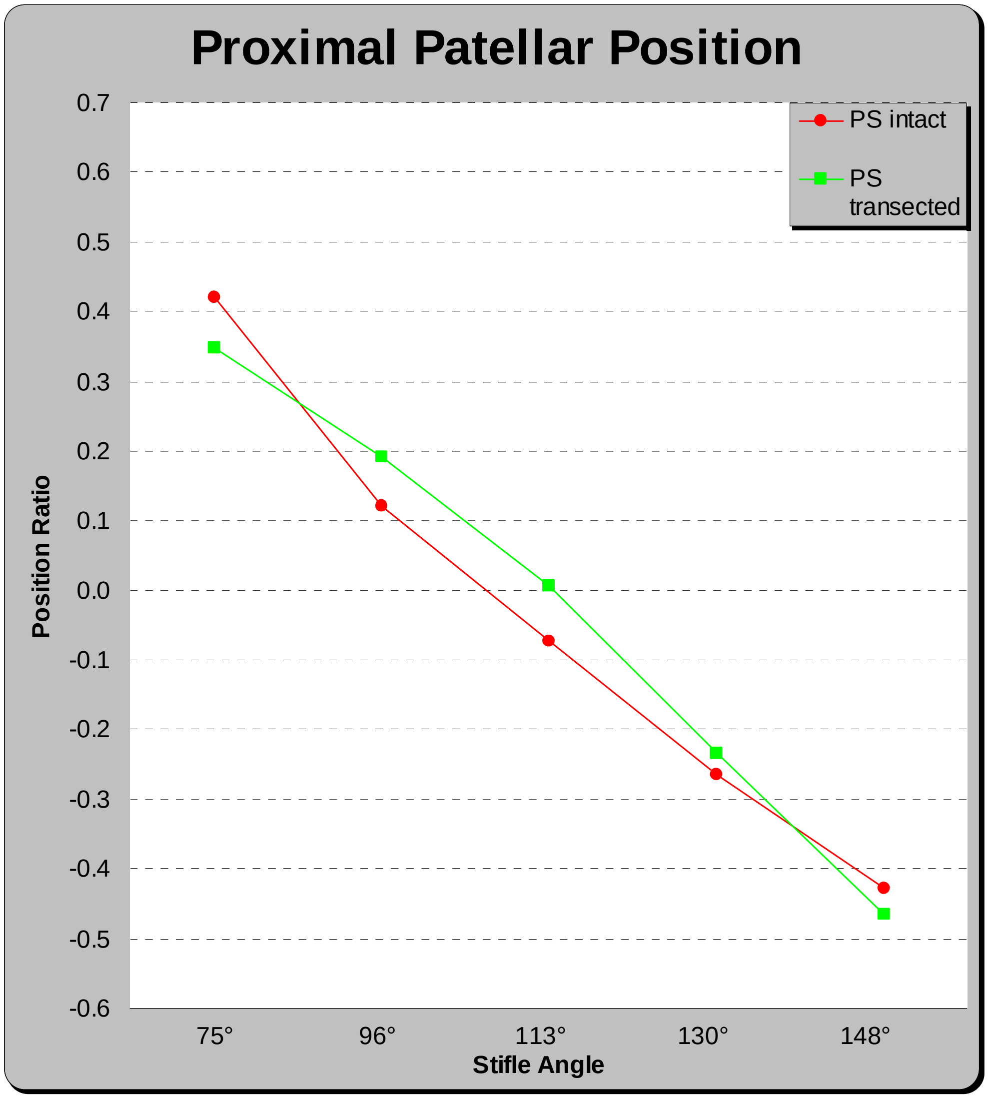

Figure 1.6.2: Graph of the proximal patellar location with respect to the trochlear groove.

Table 1.6.1: Patellar displacement from PS intact stifle as a percentage of trochlear length.

		Location Difference	
		PS Intact	PS Transected
75°	PPP = X / TL	0.4210	-7.45%
	DPP = Y / TL	1.1175	-7.42%
96°	PPP = X / TL	0.1215	6.91%
	DPP = Y / TL	0.8177	5.53%
113°	PPP = X / TL	-0.0739	8.07%
	DPP = Y / TL	0.5936	7.78%
130°	PPP = X / TL	-0.2649	3.10%
	DPP = Y / TL	0.3536	3.84%
148°	PPP = X / TL	-0.4278	-3.85%
	DPP = Y / TL	0.1662	-1.74%

Additional pictures of patellar position at 96°, 113°, and 130° can be found in Appendix A.

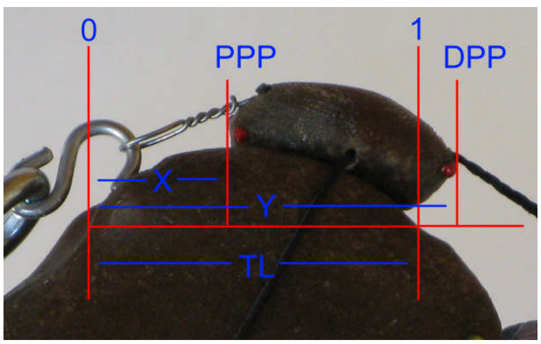

Figure 1.6.3: Patellar position measurements for the PS intact model at 75°.

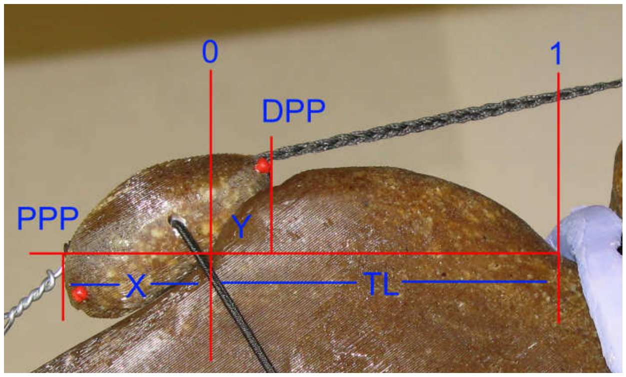

Figure 1.6.4: Patellar position measurements for the PS intact model at 148°.

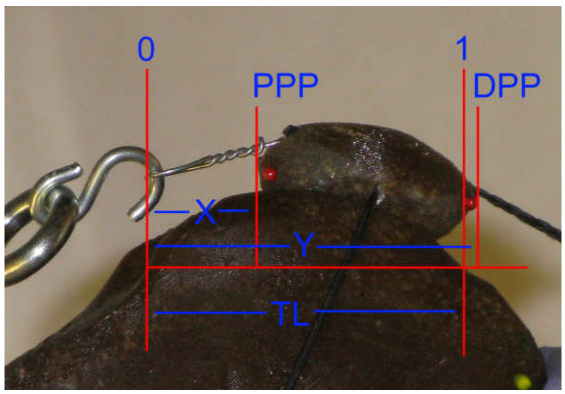

Figure 1.6.5: Patellar position measurements for the PS transected model at 75°.

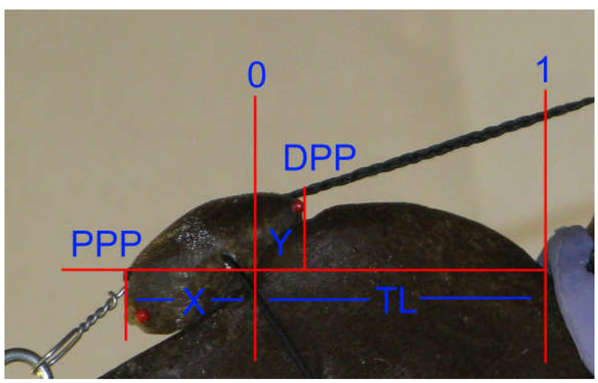

Figure 1.6.6: Patellar position measurements for the PS transected model at 148°.

1.7 DISCUSSION

The tibial plateau slope angle for the intact model of this study (28º) was within ranges for large-breed dogs reported in literature. The age of the subject, 5.5 years, was also similar to the average age of subjects used in clinical and experimental studies for the investigation of CCL deficiency.

It has been confirmed in literature [92] that transection of the CCL causes a cranial tibial translation. An apparent cranial subluxation existed after axial loading in the CCL deficient physical model at all stifle angles, with the most subluxation occurring at angles of extension. The maximum tibial translation for the CCL deficient model was present at 113º followed by 130º (shown in Table A.4). These stifle angles are most representative of the stance phase of the canine gait, where this cranial translation is most often noted. It was noted that the collateral ligaments were fully taut in full extension while the LCL was completely lax and the MCL partially lax in flexion. This is consistent with literature [120] and although the suture material used to represent the ligaments in the physical model do not have the identical properties of actual ligaments, this tightening and loosening behavior of the collaterals are indicative of normal stifle function throughout the canine range of motion and helped to validate the function and performance of the model and testing setup. Studies have shown that in the healthy intact stifle, a “cross-over flexion point” occurs at a patellar tendon angle (TPA) of 90º flexion [99]. Thus, in a healthy stifle, there should be no shear at a stifle angle of 90º of flexion and the cruciates should be unloaded. At angles less than 90° of flexion the shear force should change to be directed caudally, thereby increasing the load on the CaCL as it becomes the primary restraint to craniocaudal motion. At angles greater than this crossover point, the load should be taken up by the CCL and the shear force should be cranially directed. The results from the physical testing showed that during flexion (at angles less than 90º) the CaCL appeared to take up a large amount of the load, biting into the meniscus in most cases. In the transected model at extension, the MCL seemed to be the primary restraint. Therefore, the models and testing fixture were deemed to be functioning appropriately and limb behavior was in good agreement with literature over the entire range of motion for both the intact and transected models.

The patellar position within the trochlear groove for the intact models and CCL deficient models at 75º, 96º, 113º, 130º and 148º were recorded, measured using methods outlined in literature [34]. The results for the intact model showed a relatively linear relationship between patellar position and stifle flexion (shown in Figures 1.6.1 and 1.6.2). This is in agreement with previous research [34]. However, the exact values of the DPP and PPP for this study are slightly higher than those recorded by Johnson *et al.* This could be attributable to the subject-specific nature of this study as well as the fact that slight differences in the definition of the trochlear groove's proximal and distal extents could skew the ratio.

For the CCL deficient stifle, a slightly parabolic curve for patellar position was realized. At a stifle angle of 75º the DPP ratio for the transected model was less than that of the intact model. This signifies a more proximally located patella. For stifles angles of 96º, 113º, and

130º, the DPP ratio of the transected model was greater than that of the intact model, signifying a more distally located patella. This is thought to be caused by the cranial tibial translation present due to CCL insufficiency. At these three angles, the cranial tibial translation was largest. Specifics of this can be found in Appendix A. At 148º, despite the stifle being above the cross-over point where cranial tibial thrust is the primary shear force, and despite evidence of some cranial subluxation, the DPP ratio of the transected model was again less than that of the intact model. It has been shown in literature that the collateral ligaments serve to stabilize the CCL deficient stifle at full extension [120]. Having shown above that the collateral ligaments were fully taut in extension, it is believed that their role as a stabilizing mechanism for the CCL deficient limb is the cause for the more normalized patellar position seen here. At 148°, the distal patellar position (DPP) of the PS transected model only differed from the PS intact model by 1.74% of the length of the trochlea. In order to ensure that these two values are statistically different, an independent two sample t-test was performed at $\alpha = .05$. Given that each measurement was performed three times (Table A.1), the tabled value was $t_{.05,2} = 2.110$.

The hypothesis is stated as follows:

$$\begin{aligned} &H_o : \overline{X}_1 = \overline{\mathrm{X}}_2 \\ &\mathrm{H}_{\mathrm{a:}}\ \overline{X}_1 \neq \overline{\mathrm{X}}_2 \end{aligned} \tag{1}$$

The pooled variance is calculated as:

$$S_{X_1X_2} = \sqrt{\frac{S_{X_1}^2 + S_{X_2}^2}{2}} = 0.0015816 \tag{2}$$

The resulting statistic is much larger than the tabled value and so we reject the null hypothesis and conclude that the values in Table 1.6.1 are significantly different.

$$t_o = \frac{\overline{X}_1 - \overline{X}_2}{S_{X_1 X_2} * \sqrt{\frac{2}{n}}} = 13.439 \qquad (3)$$

The magnitude of the difference between DPP and PPP data points for a specific model were not always equal between the angles of interest. This is due to the fact that as the patella travels over the radial-shaped surface of the trochlear groove, its rotation with respect to the trochlear axis causes its distal and proximal aspects to undergo a slight tilt.

Several simplifying assumptions were made in the development of the physical models used in this study. The quadriceps muscle group was assumed to be directed along a single line of action, corresponding to the rectus femoris, since only proximodistal patellofemoral articulation was of interest. This has been done is several other in vitro and 3D modeling studies [53]. This assumption was also deemed acceptable in a parallel FEA study [30] using the same limb CT data. Although, it has been found that putting too much tension on the quadriceps can produce inaccurate results pertaining to patellofemoral articulation [53].

1.8 CONCLUSION

In summary, physical models were created to simulate the canine stifle with and without a cranial cruciate ligament at five angles throughout the normal range of motion of large-breed dogs. The models showed good agreement with literature, replicating the effects of cranial tibial translation in CCL deficient stifles as well as exhibiting a relatively linear relationship for patellar position in intact joints.

The transected model at 75º resulted in a slight distal shift of the patella. At stifle angles of 96º, 113º and 130º, cranial tibial translation caused the patellar to be more proximally located with respect to the trochlear groove in the CCL transected model. At full extension, 148º, the difference between the DPP measurements of the intact and transected was very small, but still statistically significant. It is believed this is the result of the collateral ligaments being taut and fully engaged in extension, thus somewhat stabilizing the CCL deficient stifle joint.

2. SURGICAL PROCEDURES AND TESTING

2.1 INTRODUCTION

The admission of geometry altering procedures has had a profound effect on the treatment options for cranial cruciate ligament deficient stifles. Unlike humans, CCL deficiency has been found to be better treated with the use of procedures that alter the geometry and eliminate the tibial shear force rather than trying to replace the lost ligament. Although there remains a great need for an understanding of causes and effects of CCL rupture, investigation into the available surgical procedures used to correct this condition is a valuable endeavor. With the advent of the TPLO procedure [110] several other similar techniques, such as the TTA and TTO, have since been introduced. One of the most imperative questions for veterinary surgeons and clients today is which surgical option will best restore joint function and minimize the risk of serious complications. While there have been several clinical tests performed, in vivo experiments are difficult to conduct and nearly impossible to keep devoid of bias [106]. In vitro studies are also widely used but they are most often inconclusive. A large percentage of surgeons continue to select a technique based on cadaveric analysis, case studies, and personal preferences [3].

It has been hypothesized that changing the geometry of the proximal tibia through tibial osteotomy procedures may have a negative impact on the patellar tendon. Patellar desmitis has been shown to occur after treatment with TPLO [26,70] and the TTA has shown slight inflammation of the patellar ligament in clinical observation. Patellar luxation has also been identified as a possible postoperative complication of the TPLO [9]. Patella alta has been considered a significant cause of recurrent luxation of the patella [50,56,62,82]. However, there is an apparent lack of both experimental and clinical information regarding patellar luxation and patella alta diagnosis in the canine. Furthermore, no studies to date have evaluated postoperative patellar location after either a TPLO, TTA or TTO procedure. As three of the most widely used tibial osteotomy procedures today, there is a need for investigation into the effect of these procedures on stifle mechanics.

The intent of this project was to utilize previously constructed three-dimensional, anatomically accurate physical models created using a combination of rapid prototyping technologies and casting techniques and investigate postoperative stifle joint mechanics and patellar position with respect to the trochlear groove resulting from each of the three aforementioned procedures: TPLO, TTA and TTO. A study into the post-operative effects on patellar location does not currently exist. Physical testing of these models at 75°, 96°, 113°, 130°, and 148° will provide data regarding postoperative stifle geometry, patellar position, and possible threats to patellofemoral stabiliy that are at this time unavailable to veterinary orthopaedic surgeons and researchers.

2.2 BACKGROUND INFORMATION

2.2.1 Intra-Articular and Extra-Articular Techniques

Mimicking the surgical answer for anterior (cranial) cruciate ligament deficiency in humans, the first applied treatments in the canine stifle were intra-articular and extra-articular procedures. These are still used in practice today although their popularity is declining with the advent of newer, more advanced procedures. Extra-articular techniques rely on non-absorbable, heavy gauge suture materials, wires, or transposition of periarticular tissues to provide joint stability over time. Consequences of this technique include limited tibial rotation, increased compression of the joint surfaces and possible cartilage and meniscal wear [121]. Intra-articular techniques utilize a more biomechanical approach and implement allografts, autogeneous tissues or synthetic materials to anatomically reconstruct the ruptured ligament and mimic its function and orientation. This allows for normal stifle range of motion and no limitation to tibial internal rotation. Most studies have cited good to excellent limb function in dogs that have had intra-articular procedures. However, intra-articular techniques have been found to be susceptible to early failure, even more so than extra-articular procedures. Grafting tissues undergo early avascular necrosis and encounter a considerable loss of structural and material properties after implantation. Fixing these complications is a slow and complicated process and the resulting ligament is often times left with a maximal strength that does not exceed 30% of the intact ligament [121].

If the true test of treatment for CCL rupture is the procedure's ability to restore normal joint function and prevent progression of secondary joint disease, then intra- and extra-articular techniques have failed as a treatment option. Neither extra- nor intra-articular techniques consistently preserve long-term stifle stability or prevent progression of arthritis and secondary meniscal damage.

2.2.2 Tibial Osteotomy Procedures: A Novel Approach to CCL Deficiency

The Tibial Wedge Osteotomy (TWO), proposed by Slocum and Devine, was the first of a series of new approaches for the treatment of CCL rupture. This was then improved upon by Slocum and Slocum [110] to create the Tibial Plateau Leveling Osteotomy (TPLO). Unlike intra- and extra-articular techniques, the TPLO aims to eliminate the tibial shear forces that occur in the stifle during weight bearing by reducing what they coined as cranial tibial thrust. This was a novel approach to the problem of CCL deficiency. There have been several studies on the complications after TPLO with several intra-operative and postoperative complications reported clinically. These include under- and over-rotation of the tibial plateau, incorrectly centered osteotomies, infections, implant failure, tibial crest fractures, and patellar tendinosis. Other studies have found that the procedure does not consistently prevent the progression of osteoarthritis [88,91,113]. Patellar tendon thickening is another complication that has been reviewed and confirmed in literature [9]. A caudal tibial thrust has been shown to exist accompanied by a caudal tibial translation that increases with increasing axial tibial load [92]. This has been thought to increase the load seen on the caudal cruciate ligament and potentially predispose it to failure. It has been identified that imprecise placement of the osteotomy results in inaccurate tibial plateau leveling and if under-rotated may lead to persisting cranial subluxation. If over-rotated, an excessive caudal tibial thrust may further increase the load seen on the caudal cruciate [121].

Montavon *et al.* proposed that there are actually two possibilities for neutralizing the cranial tibial thrust in the CCL deficient stifle [115]. They stated that one option is to make the tibial plateau perpendicular to the Achilles' tendon and essentially the tibial long axis as proposed by Slocum and the TPLO. The other possibility for stabilization is to make the tibial plateau perpendicular to the patellar ligament. This second option was implemented in a new technique they called the Tibial Tuberosity Advancement technique (TTA). The TTA procedure was based upon a biomechanical model of the joint forces of the human knee. Correcting the angle of the patellar ligament is well known in human orthopedics, but had not been used to treat CCL deficiency in dogs. The TTA positions the patellar ligament perpendicularly to the tibial plateau by advancing the tibial tuberosity and eliminates the tibiofemoral shear force, stabilizing the stifle during weight bearing. The developers claim it to be a less invasive technique and clinical results have been shown to be satisfactory. However, complications have been found to occur such as failure to maintain patellar ligament advancement, implant failure, tibial tuberosity fracture, medial patellar luxation, CaCL injury because of excessive advancement, and meniscal injury [61,58]. The TTA preserves the natural tibiofemoral articulation because no rotation of the tibial plateau is induced. Natural load transmission across the stifle and menisci will also be more likely to remain unaltered. The technique is still relatively new and in depth experimental studies have yet to be done to fully define the effects and benefits.

The Triple Tibial Osteotomy (TTO) procedure is a recently developed treatment option for CCL rupture. It can be thought of as a hybrid of a Tibial Wedge Osteotomy (TWO) and TTA procedure. Similar to the intent of the TTA, this procedure aims to reposition the patellar ligament so that it is perpendicular to the tibial plateau in extension. This is achieved, however with a series of proximal tibial osteotomies that rotate the tibial plateau and subsequently advance the tibial crest cranially. Very little study based on clinical cases has been reported thus far [20]. Complications encountered included tibial tuberosity fractures, infection and meniscal injury. Advantages of the TTO procedure include the minimal change to the orientation of the tibiofemoral articulating surfaces, no loss of limb length, and low technical difficulty [58].

2.3 REVIEW OF LITERATURE AND RESEARCH

With cranial cruciate disease remaining one of the largest threats to rear limb function and a growing concern for both pet owners and orthopedic surgeons, research related to joint motion, joint function and surgical treatment for CCL disease continue to be a greatly valued area of research. Several considerations must be made when it comes to diagnosis of CCL disease, treatment selection and procedure performance. A fundamental prerequisite, however, is a thorough understanding of knee anatomy, possible complications and both existing and novel approaches to correcting a ruptured ligament. There is a vast wealth of knowledge on each of these subjects. This section aims to inform the reader of issues concerning cruciate disease, joint degeneration and corrective surgeries by providing a selection of prominent research related to the contents and purpose of the project.

2.3.1 The Cruciate Ligaments

The canine stifle is an intricate joint whose function and stability relies entirely upon the cooperation of five major ligaments, a few large muscle groups, supporting cartilaginous tissue and bony structures such as the tibia, femur and patella. There have been several who deem the cranial cruciate among the most important components in this system [4,23]. Kinematic studies in dogs were able to confirm that transection of the CCL results in substantial cranial tibial subluxation during the stance phase of the gait [59,114]. These studies demonstrated that forces from the surrounding muscle groups are unable to compensate for the loss of stability provided by the CCL. Complications concerning the

CCL are frequent and in most cases detrimental to the dog. The understanding of the role both cruciate ligaments play to the overall function of the joint is an important and valued task. De Rooster *et al.* presented a thorough investigation into the makeup, function and clinical relevance of the cruciate ligaments [33]. Their paper is a compilation of previous research and literature regarding the cruciate ligaments in order to present a concise and complete description of their attributes and roles and establish their significance in stifle joint stability. They proposed that little may actually be known about the canine cruciate ligaments because existing information is sometimes not delineated between species and they also argue that an understanding of CCL geometry and function is essential for the understanding, diagnosis and treatment of CCL rupture. Among the most important comments in this paper are that the CCL is the most important ligament in cranio-caudal stifle joint stability because it is the primary restraint against cranial drawer movement, that the importance of the Caudal Cruciate is much less understood but is known to stabilize the knee against caudal drawer motion, and that the behavior of the cruciates is largely due to their biomechanical makeup, most noteworthy being the crimped pattern of their fibril bundles which others have also attributed as a significant determinant of their structural properties [45].

Many other sources agree that the primary significance of the CCL is its restraint against cranial tibial thrust, the component of tibiofemoral reaction force that causes the tibia to translate cranially relative to the femur [106,109,110,121,125]. Mechanical tests have been done to determine the restraining action of each stifle ligament and findings also support this assertion. One study in the 1970's, selectively cut each ligament and determined after force application the amount of increased tibial translation [23]. Researchers such as Butler found this method to be imprecise and developed a methodology that uncoupled the applied force and measure of ligament significance [23]. Using this method, they were able to identify the contribution of each ligament. Their research established the ACL as the primary ligament to knee function and contested the findings of others at that time by stating that that ACL restrains anterior movement.

2.3.2 CCL Rupture

Due to its significance to the stability of the stifle joint, as mentioned in the previous section, the causes for distress and rupture as well as the effects of cranial cruciate insufficiency have been studied in numerous papers and through various methods. Hayashi *et al.* studied morphologic features in the cranial cruciate ligament in order to identify the changes that ultimately lead to its structural failure [45]. The authors focused on identifying histologic changes in ruptured cranial cruciate ligaments. Their study was sound and they were able to quantify the alterations in ruptured canine CCL and show a correlation between rupture and changes in ligament fibroblasts, ECM, "epiligamentous reparative response", loss of normal ligament crimp, and loss of birefringence. They agreed with the other studies they sited that these changes, which may be largely due to age, could be the reason for changes in mechanical properties and ultimate failure of the ligament. This, as mentioned in the next section, is one argument against growing speculation that other characteristics such as steep tibial plateau slope could lead to CCL rupture.

Understanding the effects of CCL rupture on the other components of the stifle as well as the overall function of joint and limb is necessary in treatment and prevention of cranial cruciate disease. DeCamp *et al.* [35] provided a gait analysis showing the changes in flexion and extension due to the loss of the CCL in the stifle in order provide a basis for diagnosis of the treatment of cranial cruciate disease. Their results were based on experimental induction of CCL rupture in test subjects and the analysis of change in movement of the hind limb after removal of the CCL. As the authors stated, the differences in motion are likely an adaptive response to pain and the unstable joint as well as the altered biomechanics of the joint but they did find that the flexion/extension capabilities of the major joints of the hind limb changed following transection of the CCL as well as the stride length of the gait. Although this paper was titled a "noninvasive" approach, the method for procuring their results was direct manipulation of live test subjects. This method may also have lead to misleading results. For example, all dogs in the study also developed meniscal injury which could have further impaired joint movement by increasing discomfort in the dog and therefore changed the dogs' motion. The authors even assert that there has been no correlation found between CCL rupture and eminent meniscal injury so this occurrence may not be representative of the larger population but a result of testing procedure and unnatural stresses put on the animal subjects.

Some speculation has been made regarding the effect that CCL rupture has on the caudal cruciate ligament [33,44,125]. Zachos *et al.* presented an experimental study on the morphologic effects of CCL insufficiency on the CaCL [125]. One possible effect is an increase in stress in the caudal cruciate after the loss of its cranial counterpart. Although there are always uncertainties associated with in vivo studies such as differences in specimen makeup, the researchers identified differences in the fibril diameter of the CaCL in the intact and CCL deficient stifles that show a possibility of compromised material properties in the caudal cruciate ligament after repeated cranial thrust in a CCL deficient stifle. Their research does not show enough evidence or quantification of the morphologic changes on the CaCL and the authors support further research related to this endeavor. Other research has shown that the caudal cruciate ligament undergoes a substantial increase in tensile load during weight bearing due to its change in role to prime stabilizer of craniocaudal joint motion [121]. This, as several research papers have suggested, is reason to believe that a stress increase in the caudal cruciate ligament accompanies cranial cruciate ligament insufficiency [121]. This increase in stress and tensile load may cause the CaCL to be more prone to rupture. Also mentioned is the concern that surgical procedures for correcting CCL rupture may further injure the potentially compromised caudal cruciate ligament by further increasing the post-operative tensile load and stress [106,121].

Work has also been done on the mechanical response of articular cartilage to joint instability caused from rupture or transection of the cranial cruciate ligament [102]. Osteoarthritis has been found both clinically and experimentally to follow the loss of function of the CCL [91, 102]. Setton *et al.* stated that damage to the solid matrix of the cartilage may be the most contributing factor to cartilage degeneration and conditions such as osteoarthritis [102]. The findings of their research, based on measurements of material properties as well as cartilage hydration, showed significant changes in structural properties following transection of the CCL, linking loss of this ligament and the resulting instability of the joint to the damage of the surrounding articular cartilage. Most notable of these structural changes was a decrease in the stiffness and shear as early as six weeks after removal of the ligament and which continued to decrease over time. The authors stated other studies done in a similar fashion but resulted in slightly different findings with regards to certain aspects such as changes in compression stiffness. These differences are likely due to variations in testing methods and specimens but the authors were objective in stating contrasting research and not insisting that theirs was superior or more accurate. There remains, however, an area of uncertainty regarding the correct trend in material property changes of the stifle articular cartilage and may need further investigation.

2.3.3 Tibial Plateau

The tibial plateau is defined as the bony surface of the lateral or medial condyle of the tibia that articulates against the analogous condyles of the femur [74]. The lateral and medial condyles of the tibia are separated from the corresponding femoral condyles by the lateral and medial menisci. The angle that the tibial plateau makes with a line perpendicular to the long axis of the tibia is often designated the tibial plateau angle (TPA) or tibia plateau slope (TPS). The tibial long axis is a line from the midpoint of the intercondylar eminence to the center of the talus and the plateau is measured from the cranial aspect of the medial tibial articular surface to its caudal aspect [41,52].

2.3.3.1 Steep tibial plateaus

There are several instances in literature which state that cranial tibial thrust is directly proportional to the tibial plateau angle and would thus significantly increase, along with more severe joint instability, with CCL injury [83,88]. However, some researchers offer that increased TPA is not a common risk factor for CCL rupture and many dogs with a steep tibial plateau do not experience cruciate disease [44,45]. Through experimental testing, Havig *et al.* found no correlation between TPA and clinical outcome for dogs treated with lateral suture technique (LST), suggesting that, at least for this case, tibial plateau angle is not a means for predicting CCL injury [44]. Research by Osmond, Marcellin-Little, Harrysson *et al.* assessed the morphology of proximal tibial abnormalities that could result in a steep TPS and suggest that the abnormalities themselves could be the cause for ligament failure and the steeper slope [83]. The influence of the biomechanical properties of the stifle ligaments themselves on CCL failure has also been investigated [33,45]. De Rooster *et al.* mentioned that recent investigations discovered infiltration of the CCL by synovial fluid is possible and could lead to inflammation of the synovial membrane and CCL epiligament similar to those that typically accompany joints with CCL rupture [33]. It is unknown, as the authors stated, whether this inflammation occurs prior to rupture and they suggest this is a worthwhile research topic. Ultimately, though a correlation between cranial thrust and tibial slope has been reported clinically, no relationship between a steep TPS and eminent CCL failure has been proven to date [83].

2.3.3.2 Tibial Plateau Measurement Concerns

Regardless of its connection to CCL failure, the tibial plateau slope remains an important element for both research and pre-surgical planning. Measurement of this slope, however, is often times subject to position and observer variability [44]. Caylor, Zumpano *et al.* [28] assessed the intra-observer and inter-observer variability in the tibial plateau slope measurement from lateral radiographs measured by three different observers of varying experience levels. Their results showed no statistical variation between intra-observer measurements, a significant difference in the inter-observer variability of the novice observer and no difference in inter-observer variability between the experienced and intermediate observers. Since their research study, others have investigated similar facets of the tibial plateau measurement concerns. Fettig *et al.* [41] used a larger sample size (40 dogs of various breeds and a mix of both right and left hind limbs) and more observers (11 observers of varied experience with measuring TPA) and investigated the correlation between observer variability and characteristics of the dog such as age and degree of joint degeneration. They found evidence of both intra- and inter-observer variability but found no correlation between the variability and dog characteristics or angle of plateau itself. Their results showed that at least one pair of points needed to measure the TPS showed significant variation and this also showed correlation to the degree of degenerative joint disease.

The variability in TPA measurements has encouraged a better description and methodology for measuring this value. Baroni, Mathias, Marcellin-Little *et al.* researched two possible methods for measuring this important reference angle [12]. They contend that known significant observer variability, supported through research such as those previously mentioned, necessitates a re-thinking of the conventional TPS measurement method. Their proposed method relies more on the articulating surface and could more accurately measure the TPS and result in less variability. The researchers also investigated the use of digitized radiographs and their effect on TPS measurement. Figure 2.3.1 below shows a diagram from their paper illustrating the two different measurement techniques.

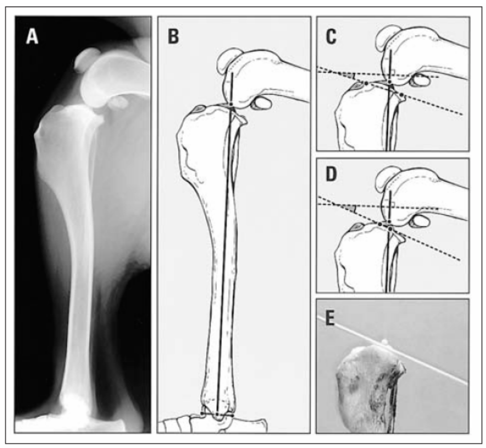

Figure 1—Mediolateral radiographic view (A), illustrations (B, C, D), and photograph (E) of a tibia and stifle joint in a dog. Femoral condyles are superimposed. Tibial plateau slope (TPS) is conventionally measured by comparing orientation of the functional axis of the tibia defined as the line joining the intercondylar eminence and a point equidistant to the cranial and caudal aspects of the trochlea of the talus (B) and the axis of the medial tibial condyle defined as the line joining the small, discreet cranial margin of the tibial plateau and the point of insertion of the caudal cruciate ligament (C). Alternatively, the axis of the medial tibial condyle may be defined as a line tangential to the cranial linear portion of the medial tibial condyle at the femorotibial contact point (D). The latter measurement more closely approximates the anatomic slope of the medial tibial condyle (E).

Figure 2.3.1: Illustrations of the conventional TPS measurement method and that proposed by Baroni, Marcellin-Little *et al.* [12]. Used with permission from the publisher.

The setup of their experiment kept very good control over all variables, especially observer experience with each measurement method. Those observers who measured using the alternative method were not trained in using the conventional technique and vice versa.

Thus, the authors could ensure that no outside influence to measurement techniques would be included. The TPS measurements using the alternative method were not significantly different from the anatomic TPS measurements. Results for measurements taken using the conventional method were considerably lower than the anatomic measurements. For both alternative and conventional methods, the mean ± SD for the TPS measured using digitized radiographs was closer to the actual anatomic values than those from printed radiographs. The duration for measurements using printed radiographs versus digitized was not significantly different but the inter-observer variability and mean absolute deviation decreased significantly for the measurements resulting from digitized radiographs, with the measurements using a combination of alternative TPS measuring technique and digitized radiographs giving the smallest mean absolute deviation to the anatomic TPS measurements. This research suggest that if variability and accuracy are a concern, there are alternatives to the measurement approach, such as the alternative technique proposed in their paper or use of digitized radiographs in place of conventional printed ones, that could lead to more precise and repeatable results.

2.3.6 Tibial Osteotomies

There are many currently available techniques for correcting a ruptured CCL in dogs. While surgical methods vary, the main objective of most is to eliminate cranial tibial subluxation resulting from the loss of the ligament and limit tibial internal rotation throughout the range of motion. Extra-articular techniques rely on nonabsorbable suture materials and while joint stability may be restored, the tibia is fixed in external rotation and stifle rotation is limited to a single transverse axis whereby disrupting normal joint kinematics [7,121]. Intra-articular techniques use grafting or similar means to create a replacement ligament which can mimic the function of the CCL and allow for normal stifle range of motion [96,112,121]. Many studies have been done on the effects of intra-articular and extra-articular procedures, which have been shown to be susceptible to early failure and result in a ligament whose maximal strength is only a fraction of the normal CCL [1,5,6,22,29,36,96,107,112]. Due to the limitations offered by these methods, a new branch of preventative measure was accepted with the development of tibial plateau osteotomies. Several osteotomy procedures are available but a review of only those methods to be used in this research is outlined below.

2.3.6.1 TPLO

The Tibial Plateau Leveling Osteotomy (TPLO) was the first procedure based on an elimination of cranial tibial thrust by altering the proximal tibial geometry and remains one of the most popular surgical techniques, especially in large breed dogs, for the treatment of CCL rupture or injury [12,106,110]. The idea behind this procedure is not to replace the injured ligament, but to rearrange the loads and stresses and essentially make the absent ligament unnecessary while eliminating consequences of the rupture such as increased cranial tibial thrust or cranial tibial translation [41].

Several clinical studies and cadaver experiments have been done to determine the post-operative results of the TPLO procedure and also to contest the assertions of its proponents that it is superior to all other surgical techniques [106]. The transformation of cranial thrust to caudal thrust is one of the aspects that have been investigated [92]. Following the techniques outlined by Slocum and Slocum and using cadaver canine hind limbs, Reif *et al*. loaded the dog leg in a custom testing fixture to evaluate changes in joint stability before and after a TPLO procedure. They did not include the patella or patellar ligament in the study. Joint behavior for a CCL deficient stifle was mimicked in that the cranial tibial thrust resulted in a cranial tibial translation after severance of the CCL. Measurements confirmed that caudal tibial thrust resulted after the TPLO was performed and the authors assumed, but did not investigate further, that the forces within the CaCL also increase after the procedure. They mention that the caudal tibial thrust may be correlated to the axial load just as they showed that cranial tibial thrust was dependent upon the axial load. Though they make several predications and assumptions on the post-operative stresses of the ligaments, there was no such measurement of these variables and no quantification or validation of these assumptions. Jandi and Shulman investigated the post-operative effects of the TPLO procedure on the flexion and extension capabilities of the joint in a clinical case experiment of 412 cases [54]. The procedure performed on the stifles in their experiment was a modification to that proposed by Slocum but was performed by a board certified surgeon. The modification was not mentioned. The dogs were evaluated at two separate occurrences after surgery and lameness, flexion, and extension were recorded. The conclusion of their study reported no significant motion loss due to the TPLO but a positive correlation between clinical lameness and extreme motion loss (>10%). Those dogs with slight motion loss (<10%) did not experience any signs of clinical lameness. The authors suggest that motion loss after knee injury and treatment is most likely related to developments such as the formation of fibrous tissue, adherence of the patella to the trochlear groove due to fibrous tissue accumulation and progression of conditions such as osteoarthritis. Complications other than motion loss due to TPLO have also been reported [88,113]. In a study from Stauffer *et al.* [113] the majority of complications found resulting from surgery (9.5%) were short-term such as swelling and tibial fracture, though long-term complications were found in nearly just as many patients (8.3%). The authors concluded that the TPLO had good overall clinical results and that the complications resulting from the TPLO procedure are not greater than any other similarly invasive orthopedic procedure. However, they do not state the complication rates or procedures to which they are referring. The overall complication rate stated in their report (18.8%) was less than a similar study by Priddy *et al.* [88], which reported a complication rate of 25%, but their sample size was considerably larger. In the latter study, the complications that did occur responded well to treatment but the authors overall were borderline disapproving of the procedure, stating that the complication rate found was higher than other surgical techniques used to treat a ruptured CCL. This was a contradictory assertion to a previous statement they made that few complication rates have been documented for other techniques and "direct comparisons of complication rates for the various surgical techniques are not possible because of differences in study designs and reporting of data." Without adequate comparison or quantification of complication rates, the conclusions for clinical studies such as these are more of an opinion than fact.

In a study by Warzee *et al.*, a significant caudal tibial translation and associated increase in strain experienced by the CaCL following the TPLO procedure was confirmed [121]. Their findings showed that the resultant force through the weight bearing stifle was directed 6.5º more cranially than the tibial long axis. For this reason, the authors recommended an optimal plateau rotation angle of 6.5º and cautioned against over-rotation of the tibial plateau to avoid excessive increase in post-operative stress in the CaCL. They do not quantify or verify an increase in stress following the procedure. Tibial internal rotation was also investigated and a correlation was determined and illustrated below in Figure 2.3.2. As shown, tibial internal rotation was not completely eliminated after the procedure. The effect or relationship of this rotation to the CaCL was not investigated and the clinical significance of this rotation remains unknown. Testing for this study was done using a custom testing fixture and the specimens were positioned and tested at only one stifle angle. This study also failed to fully duplicate all of the muscle forces acting on the canine stifle.

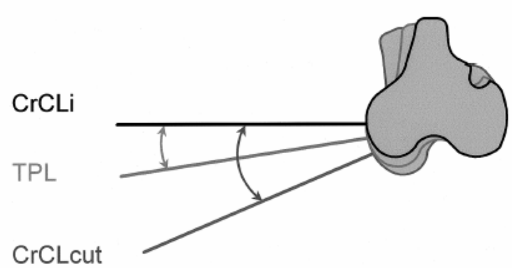

Fig 7. Schematic representation of the dorso-ventral projections of the tibial transcondylar pin used to determine tibial axial rotation. Tibial axial rotation angles were measured with respect to the pin projection in the intact specimens after: 1) CrCL transection, and 2) TPL.

Figure 2.3.2: Schematic showing tibial axial rotation [Warzee *et al.*, 121]. Used with permission from the publisher.

A 3-dimensional, theoretical model of the canine stifle was examined by Shahar and Milgram in order to determine similar biomechanical effects due to altering the tibial plateau angle [106]. They were particularly interested in the forces experienced by the various stifle ligaments. Comparison of the intact stifle and the same stifle rotated through two different TPLO angles showed that the force in the CCL was greatly reduced for a TPA of 0º but only partially decreased for a 5º TPA. In order to keep the CaCL remaining unloaded the authors recommended a tibial plateau rotation to a TPA of no less than 5º. This study showed congruence with the study done by Warzee *et al.* in that the caudal cruciate ligament in the CCL deficient stifle experienced a considerable increase in tensile load as a result to a change in the TPA. The authors did mention that mathematical models such as they presented have several disadvantages and limitations. Their model included simplifying assumptions such as ignoring the effect of the menisci, limiting the movement of the patella to only rotation in the sagittal plane and material property simplifications such as modeling the ligaments as nonlinear springs. Lessening or limiting these assumptions would improve upon the theoretical model and provide a more accurate picture of joint motion in a CCL deficient stifle before and after a TPLO procedure or newer procedures such as those mentioned in the following sections.

Expanding on the effects of tibial plateau rotation on the function of the stifle and success of the TPLO procedure, a study was done to evaluate whether the center of this rotation also has an adverse effect on the clinical outcome [60]. Only one stifle angle and one loading condition was tested. The angles were readjusted after loading to assure their original positions. The analysis was organized and the results were clear and meaningful. The study found that positioning the osteotomy too far distal resulted is an incomplete neutralization of cranial tibial thrust and when centered appropriately the osteotomy resulted in the correct and expected biomechanical effect. Another benefit this paper yields is a rethinking of the method in which tibial subluxation is measured. They offer a sound argument for using a corrected subluxation value and found, for this experimental circumstance, that the correctly centered osteotomy resulted in a subluxation value that was not significantly different from the intact stifle but the distally centered osteotomy had considerably higher tibial subluxation, similar to the value of the untreated CCL deficient stifle. There was also a positive correlation between the distal osteotomy and a shift in the tibial long axis. It may be useful to expand this research to more stifle angles.

Mattern *et al*. did a study confirming patellar ligament desmitis following TPLO and mentioned the possibility of increased stresses on the patellar ligament following the procedure [70]. They did not directly measure the stresses nor compare them with pre-operative conditions but compared the change in cross-sectional area. Confirmation of a significant change in stresses would be notable since it has been said that stress changes is suspected to be an "important factor in the development of patellar ligament desmitis" [70]. Expanding on this research to include an investigation into the occurrence of patellar tendinosis as a complication of TPLO, Carey *et al.* confirmed this patellar ligament inflammation and discovered that patellar tendinosis only occurred in dogs with severe patellar tendon thickening [26]. Also, the pre-surgical state of the CCL was linked to the PTS in that dogs with a partial rupture were more likely to develop the condition.

The notion that TPLO prevents progression of osteoarthritis and degenerative joint disease has also been challenged [49,63,91,106]. Rayward *et al.* studied this in a clinical experiment [91]. After two post-operative reviews of the subjects' radiographs and evaluating progression of osteoarthritis based on osteophyte score, the authors discovered that while the majority of cases resulted in relatively no change in osteophyte score, nearly half of them resulted in a significant increase. This is shown below in a chart from their paper.

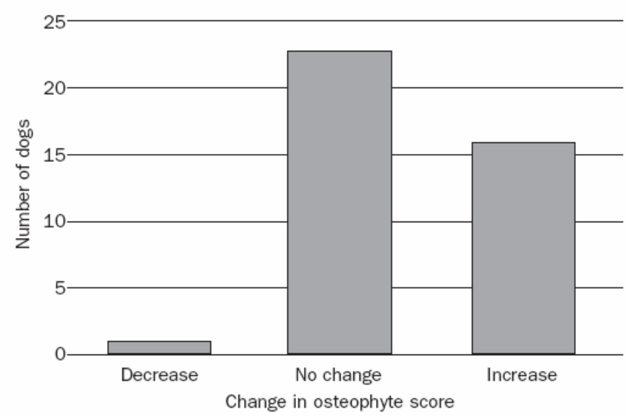

FIG 4. Change in osteophyte score from entry to six months

Figure 2.3.3: Chart showing change in osteophyte score over six months [Rayward *et al.*, 91]. Used with permission from the publisher.

The authors mention the possibility that the majority of unchanged osteophyte score could be attributed to the success of the procedure or could also have been merely due to intrinsic variation in the individual patients. There were several uncertainties in their study. The procedures varied from case to case depending on the dog's condition. Due to the fact that some of the subjects were treated differently, other variables could have been introduced that could account for different osteophyte scores. These variables should be removed in order to present a clearer picture of the post-operative effects. A longer study would also help elucidate the long-term results of a TPLO concerning osteoarthritis progression since it has been found that osteophyte score is highly correlated with the duration of the disease. Hurley *et al.* also investigated the progression of osteoarthritis and managed to eliminate some of the variation from which the previously mentioned study suffered [49]. Their study was also much shorter, reporting after only 8 weeks as compared to 6 months. A slight but measurable increase in degenerative joint disease (measured by progression of osteophytes) after the 8 week radiographic review was found. A higher number of patients resulted from a decrease in osteophytes than in the study done by Rayward *et al*. The study also investigated the change in tibial slope angle (TSA) and found that there was a considerable increase in TSA after 8 weeks for those dogs who received the smallest TPLO plate. This was also confirmed in a study by Moeller et al. [76]. This relationship or possible connection to DJD progression was not investigated.

As several issues concerning the TPLO procedure remain unanswered other procedures have since been developed. Information regarding one of these, the tibial tuberosity advancement technique, follows in the next section.

2.3.6.2 TTA

The Tibial Tuberosity Advancement (TTA) is a more recently developed technique for treating cranial cruciate ligament deficiency. Developed at the University of Zürich, it is based off a mechanical model of the human knee with assumptions pertaining to the canine stifle [61]. The approach maintains biomechanical considerations similar to the TPLO but rather than eliminating cranial thrust by rotating the tibial plateau, it aims to do so by positioning the patellar ligament perpendicularly to the tibial plateau [61,79,80,81,115,116]. Montavon, Damur and Tepic praise the TPLO procedure for “[reinvigorating] small animal veterinary orthopedics in an unparalleled way” but justify advancement of the tibial tuberosity as being the less invasive counterpart approach that gives greater attention to the global muscular function and takes into account the functional use of the limb instead of false loading conditions [31,81,115]. The authors and developers of the procedure rationalize that the total joint force is not, as Slocum has maintained, parallel to the functional axis of the tibia but rather approximately parallel to the patellar ligament [116]. In one of their preliminary publications of the TTA method the results from a clinical study were presented [80]. The results of 200 procedures showed mainly good outcomes with nearly all of the complications being related to poor placement of the pronged plate and a couple concerning the location of the osteotomy. All complications were successfully treated and healed normally. There also appeared to be a positive learning curve in that the last 40 patients treated with the TTA showed no complications. In an accompanying article they mention that surgeons throughout Europe, USA and Japan performing the procedure under the controlled clinical release reported reproducibility, as well as reduced complexity and morbidity in comparison to the TPLO [116]. Also referenced in this publication were some preliminary findings such as evidence of a general reduction of all reaction forces due to increasing the lever arm of the active stifle force. They also asserted that while there is an increase in loading of the caudal cruciate, it is to a lesser extent than the TPLO. The means for acquiring this information was not stated and no quantitative evidence was reported. Several other comparisons between the TTA and TPLO were mentioned which could have been based on post-operative evaluation and not require any particular experimental testing to discover. The authors mention that TPLO often causes patellar ligament inflammation and that the TTA results in no apparent inflammation. Although they refer to experimental models which have found meniscal injury or degradation associated with TPLO, they do not mention beyond the statement of maintained joint congruency any reported findings on the effect of the TTA on the meniscus.

Since these early publications and preliminary conclusions, outside research studies have been done to evaluate the clinical outcome and effect of the TTA procedure. Lafaver *et al*. reported complications and clinical outcome from a study of 101 dogs [61]. Approximately 40% of the patients had a partial meniscal tear at time of surgery which was removed by a partial menisectomy. For 22 dogs, later in the study, a meniscal release was performed on intact menisci but the reasons for this were not mentioned and is not in the guidelines of the procedure [79,80,115,116]. Of the complications which required additional surgical intervention (12.3%) only one joint needed re-stabilization (lateral retinacular stabilization). Minor complications (i.e. chip fractures, implant failures, infection, etc) did not require treatment in most cases. An adequate estimation of healing time was not available due to inconsistent radiographic assessments. Overall, their complication rates (~31%) were similar to findings for TPLO. They attribute many of these complications to inexperience and poor pre-surgical planning. Their findings contradict the proposal that the TTA might obviate the need for a meniscal release, as nearly 21% of the joints suffered from meniscal tears and needed debridement through meniscal release and was notably the most frequently occurring complication.

Though limited experimental results are available for this relatively new method, in vitro studies have been done [2,73]. In an experimental study by Apelt, Kowaleski *et al.* the effects of TTA on tibiofemoral shear force and cranial tibial subluxation was investigated [2]. Their study was done for one loading case and an average stifle and talocrural joint angles of $136.1^{\circ} \pm 2.01^{\circ}$ and $144.5^{\circ} \pm 2.51^{\circ}$, respectively. Results from their physical tests confirmed a cranially directed thrust at patellar tendon angles (PTA) greater than 90º, neutrality at angles around 90º and a caudally directed tibiofemoral thrust at angles less than the desired PTA of 90º. No comparisons were made directly to other methods such as TPLO but the authors mentioned that similar to TPLO, the TTA appeared to neutralize the cranial tibial thrust in the CCL deficient stifle. Miller *et al.* also confirmed a reduction in cranial tibial thrust with an in vitro cadaveric study [73]. Their study simulated only one loading case at only one stifle angle and used only the 9mm cage when performing the surgery. Their model also only included the effects of the quadriceps muscle group. They confirmed that the quadriceps force is not in itself enough to resist and neutralize the cranial tibial thrust from a CCL deficient stifle. The TTA resulted in less CTT though it did not fully eliminate the translation in all specimens.

A study by Schwandt *et al.* focused on the determination of the ‘cross-over point’ (defined as the angle in which the PTA is 90º and no tibiofemoral shear force exists) for a canine stifle [99]. Their study agreed with previous reporting that this point occurs at a flexion angle of 90º for a healthy, intact stifle. For a stifle with a partial rupture of the CCL, the crossover point was found to be 100º and the dogs with this condition carried their limb more flexed in order to neutralize the shear force present. For angles less than this cross-over point, the force changed to a caudally directed shear force.

The expansion on techniques such as the TPLO and TTA has been seen in other recent surgical developments for the treatment of CCL deficiency. Each of the previously mentioned techniques has its benefits and limitations and one new procedure aims to combine the positive aspects of both. Literature on this procedure, the Triple Tibial Osteotomy, is outlined in the following section.

2.3.6.3 TTO

The Triple Tibial Osteotomy (TTO) developed by Dr. Warrick Bruce, combines features of both the tibial tuberosity advancement and tibial wedge osteotomy (predecessor to the TPLO) for treatment of cranial cruciate rupture in dogs. Similar to the basis of the TTA (discussed in the previous section), the TTO aims to make the angle between the tibial plateau and patellar ligament 90º [20]. Instead of moving the patellar ligament, however, the tibial plateau is rotated following a series of proximal tibial osteotomies. In a prospective clinical study of TTO in 64 dogs with post-operative reassessment at both six-weeks and eleven months, no lameness was observed in most dogs at final examination [20]. Complications were encountered in 36% of cases, including tibial tuberosity fractures, infection, and subsequent meniscal injury. The most frequently encountered complication was intraoperative tibial tuberosity fracture while advancing the tibial crest which necessitated tension- band wire fixation. Significant increases in thigh circumference and stifle range of motion were also noted. All owners assessed their dog as being normal or near normal for all physical activities except sitting (2% mildly abnormal) and standing (4% mildly abnormal). Cranial drawer was still present in most patients after long-term follow-up. The researchers attribute this to a mean post-operative PTA that was larger than the intended 90º which may have been due to an underestimation of wedge angle, incorrectly positioned wedge ostectomy, and difficulties in measuring the TPA and patellar ligament angle. No significant increase in osteoarthritis score was presented and good clinical outcome, on the whole, was determined. As a relatively new surgical procedure more work needs to be done to fully evaluate its effect on the joint biomechanics and its comparison to other surgical techniques.

2.3.7 Summary

The admission of biomechanical considerations has had a profound effect on the treatment options for cranial cruciate deficient stifles. There remains a great need for a thorough understanding of the precise effect of CCL rupture on the function of the joint and its surrounding counterparts, but investigation into the different surgical procedures used to correct this condition would be most valuable. Unlike humans, CCL deficiency is better treated with the use of procedures that alter the geometry and eliminate the tibial shear force rather than trying to replace the lost ligament. Among the currently available treatment options are the widely accepted and researched TPLO, and the newer TTA and TTO procedures. While there have been several clinical tests done, especially on the TPLO, in vivo experiments are difficult to conduct and nearly impossible to keep devoid of bias [106]. In vitro studies have been done but they are most often inconclusive. Because of a lack of information regarding several aspects of these procedures, a large percentage of surgeons still select a technique based on these cadaveric studies, case series and personal preferences [3]. Certainly one of the most pressing questions for veterinary surgeons and clients today is deciding which surgical option will restore joint function and which procedure is superior to others. While in vivo and in vitro experiments, clinical cases as well as mathematical models have helped identify material properties, biomechanical and histological changes after CCL transection and complications for a select few treatment options, a combination of finite element modeling with physical testing would be useful for evaluating a variety of procedures such as the TPLO, TTA and TTO. This mean of investigation would allow for joint positions to show the effects over a greater range of motion and prediction of characteristics that currently remain pure speculation. In particular, there has been no research to this date to quantify the change in stresses in the caudal cruciate ligament after CCL rupture, let alone after corrective surgery. Also, the condition of patella alta has been associated with patellar luxation, but a study into the post-operative effects on patellar location does not currently exist. All in all, CCL rupture is the primary cause for rear limb lameness and one of the most frequently occurring injuries in dogs. Continued research into the cause and treatment of this condition is both influential and necessary to the veterinary community and pet owners alike.

2.4 STATEMENT OF THE PROBLEM

Cranial cruciate ligament disease is the primary cause for rear limb lameness and one of the most frequently occurring injuries in dogs. Because of the importance the CCL has on the stability and function of the stifle and its link to degenerative joint problems, the treatment and prevention of CCL rupture remain vital research topics in both veterinary medicine and biomedical related engineering. Several techniques exist which alter the geometry of the proximal tibia in order to eliminate the harmful and destabilizing cranial tibial shear force that affects a cranial cruciate ligament deficient stifle. These procedures have been found to be more successful in canines than intra- and extra-articular surgeries that attempt to replace or repair the ruptured ligament [1,5,6,22,36,107]. However, several of these osteotomy procedures have been found, through clinical, mathematical and experimental testing, to cause complications such as osteoarthritis progression [88,91,113] and patellar luxation [9]. Additionally, an increased load on the caudal cruciate [121] and patellar inflammation has been noted [26,70]. It is believed that these surgical procedures may also alter the position of the patella, and consequently lead to possible patellar dislocations or further degenerative problems. It would be extremely beneficial to gain insight into the true effects of the surgical procedures used to treat CCL disease. This research aims to use modern technology and reliable, recognized engineering tools to determine the post-operative effects of several tibial osteotomy procedures on patellar location.

2.5 MATERIALS AND METHODS

The models created previously, as outlined in Chapter 1, were utilized to determine the effects of three different tibial osteotomy procedures. The procedures were performed by board certifies orthopedic surgeons on the intact model at each stifle angle (75º, 96º, 113º, 130º, 148º). Specifics of each procedure are discussed in the following sections. These physical surgeries were used as guides for a parallel FEA study from the same CT data [Crimi CM, 30].

2.5.1 Tibial Plateau Leveling Osteotomy

The tibial plateau leveling osteotomy (TPLO) was performed at The Hope Center in Vienna, VA by Dr. Anke Langenbach according to the method developed by Slocum and Slocum [110]. Mediolateral radiographic projections of the intact model were used to determine preoperative tibial plateau angle (TPA) as shown in Figure 2.5.1. The stifle and talocrural joints were included and positioned to achieve superimposition of the femoral condyles. The preoperative TPA was determined according to conventional methods [12,41,92] to be 28º. In order to center the radial osteotomy on the intercondylar eminence and achieve the correct amount of rotation of the proximal tibia, a 30mm bi-radial saw (Slocum Enterprises, Inc., Eugene, OR, USA) was used for this model. Based on rotation guides (shown in Table 2.5.1), the amount of ventral rotation for this procedure for a 30mm saw and preoperative TPA of 28º would be approximately 12mm.

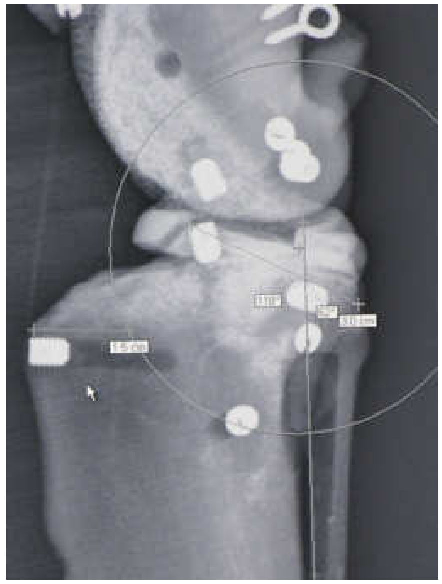

Figure 2.5.1: Mediolateral stifle radiograph for pre-surgical planning of the TPLO procedure.

Table 2.5.1: Excerpt of TPLO ventral rotation guide for TPA of 25º to 30º.

Tibial Angle	12mm	15mm	18mm (2.7pk)	20mm	24mm (3.5pk)	27mm	30mm
25.00	4.25	5.50	6.00	6.98	8.25	9.25	10.40
26.00	4.40	6.00	6.25	7.33	8.75	9.70	11.00
27.00	4.60	6.25	6.75	7.68	9.00	10.15	11.50
28.00	4.85	6.50	7.00	8.02	9.50	10.60	12.00
29.00	5.00	6.75	7.25	8.37	10.00	11.05	12.50
30.00	5.25	7.00	7.50	8.72	10.25	11.60	13.00

The use of a cutting jig was not employed as they have been found to have no effect on the accuracy of the TPLO procedure [15,97]. Water was used to flush chips from the cut and keep the temperature of the work material cool. As can be seen in Figure 2.5.1, the radial line of the cut passes directly through the insertion of the medial collateral ligament. For this reason, the ligament was temporarily removed for the procedure and reinserted afterwards.

The 30mm bi-radial saw blade was positioned on the medial side of the tibia so that the cut originated at the intercondylar eminence and was perpendicular to the caudal aspect of the shaft distally and caudally. This is shown below in Figure 2.5.2.

Figure 2.5.2: Performing radial osteotomy on proximal tibia with 30mm bi-radial saw.

The tibial fragment was initially held in place with a 2mm diameter Kirschner wire and then rotated ventrally by 12mm as shown in Figure 2.5.3 below.

Figure 2.5.3: Ventral rotation of the proximal tibia by 12mm.

After plateau rotation, a pre-contoured 3.5mm Broad TPLO plate (Synthes, Inc., West Chester, PA, USA) was secured to the medial aspect of the proximal tibia. This large plate is used for dogs ≥ 35 kg [20]. Figure 2.5.4 (a-b) shows the two step process of drilling the holes and fixing the plate with conventional screws.

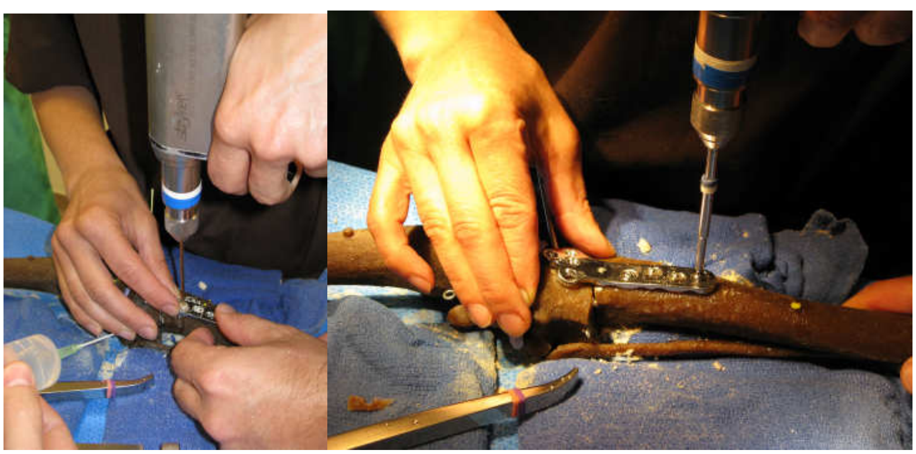

(a) (b)

Figure 2.5.4: Attachment of the 3.5mm Broad TPLO plate (Synthes, Inc.). (a) drilling the holes using the plate as guide (b) securing the plate with conventional screws

Post-surgical and pre-surgical radiographs of the stifle were compared postoperatively in Figure 2.5.5 to demonstrate that the bi-radial cut and subsequent ventral rotation of the tibial fragment were executed as planned. Figure 2.5.6 shows an assembly of the TPLO model.

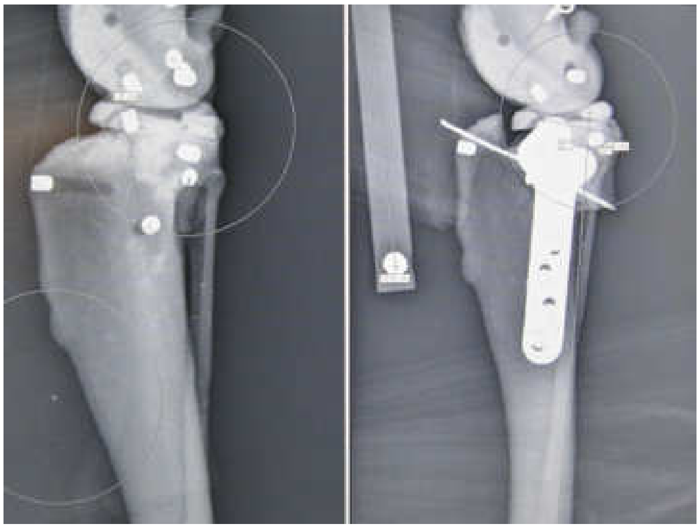

Figure 2.5.5: Comparison of preoperative and postoperative mediolateral radiographs.

Figure 2.5.6: Final outcome of the TPLO procedure, pictured here with stifle angle of 113º.

2.5.2 Tibial Tuberosity Advancement

The tibial tuberosity advancement (TTA) was performed at The Hope Center in Vienna, VA by Dr. Tibor Lazar according to methods outlined by Montavon, Damur and Tepic [79,80,115,116]. Preoperative planning included examination of mediolateral radiographs of the extended stifle and use of existing transparent templates (Kyon, Zürich, Switzerland) to determine the amount of advancement required to position the patellar ligament perpendicular to the tibial plateau in a standing position of roughly 135º. The template also helps determine the size of the plate necessary to stabilize the osteotomized tibial tuberosity. Figure 2.5.7 shows the application of said template on the mediolateral projection centered on the stifle joint with perfect positioning confirmed by superimposition of both femoral condyles.

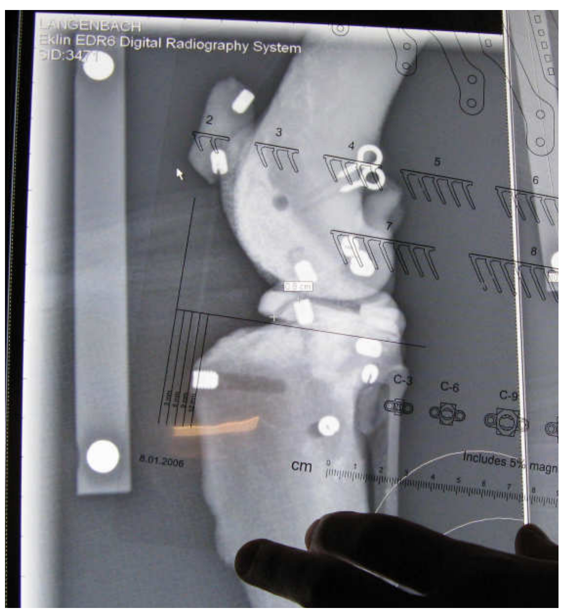

Figure 2.5.7: Mediolateral radiograph of extended stifle and TTA plate template (Kyon).

Plate sizes vary from 2-hole to 8-hole, which correspond to the size of the tibial crest. Cage widths are 3, 6, 9, or 12mm depending on degree of tuberosity advancement required for optimal results. Based on the preoperative mediolateral radiograph shown in Figure 2.5.7, a seven-hole plate was decided upon. An 8-hole drill guide (Kyon, Zürich, Switzerland) was placed parallel to the cranial margin of the tibial crest such that the first hole was placed at the level of and just medial to the tibial insertion of the patellar ligament and the distal end of the plate was slightly forward of the central tibial axis to ensure that after subsequent advancement, the distal screw-holes in the plate would overlay the central tibia. The desired number of holes (7) for placement of the plate with its prongs was drilled with a special drill guide and a 2.0mm drill bit. The most proximal and distal holes were drilled first and secured with alignment pins (shown in Figure 2.5.8), followed by the remaining holes. A bicortical osteotomy of the tibial tuberosity was then performed distally, but only extended through the medial cortex proximally.

Figure 2.5.8: Alignment pins placed in proximal and distal holes to stabilize drill guide.

After the appropriate sized plate and fork were assembled, a small mallet was used to seat the plate/fork combination into the tibial crest. This is shown in Figure 2.5.9. The osteotomy of the tibia crest was then completed, the crest was opened via a 9mm spreader (Kyon) and a 9mm cage was inserted 2-3mm below the proximal extent of the tibia and secured with 2.4mm screw directed caudodistally. The titanium plate (Kyon) was then secured at its distal end as shown in Figure 2.5.10. The end result of the procedure is shown in Figure 2.5.11 and postoperative radiographs are shown in Figure 2.5.12 (a-b).

Figure 2.5.9: Mallet used to seat the plate/fork combination into the tibial crest.

Figure 2.5.10: Distal attachment of titanium plate in line with tibial central axis.

Figure 2.5.11: Final tibial crest position and hardware placement after TTA procedure.

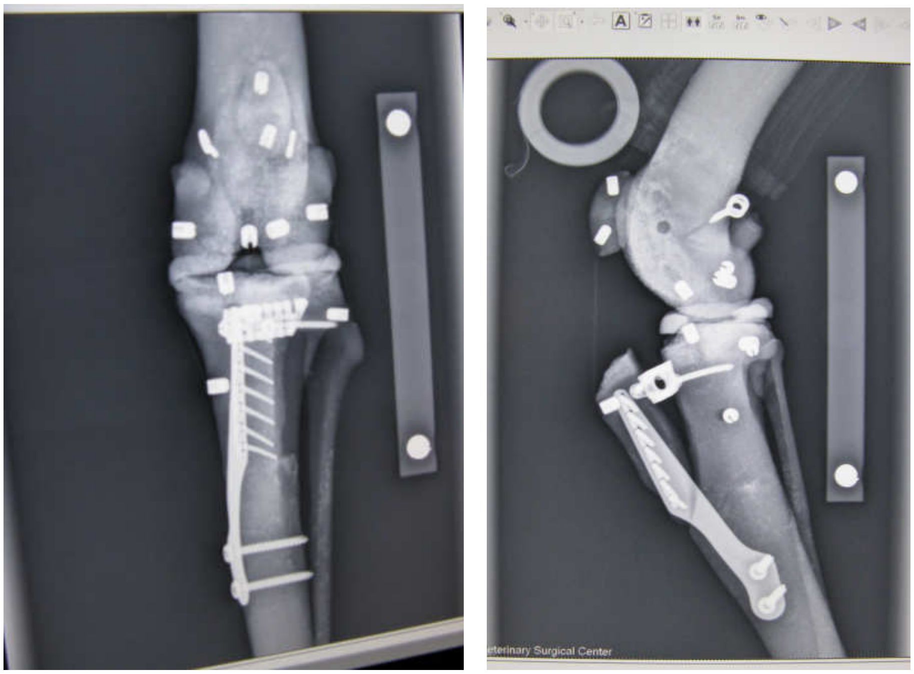

(a) (b)

Figure 2.5.12: Postoperative radiographs after TTA. (a) craniocaudal view (b) lateral view

2.5.3 Triple Tibial Osteotomy

The triple tibial osteotomy (TTO) was performed by Dr. Denis Marcellin-Little at North Carolina State University's College of Veterinary Medicine according to the methods outlined by Bruce [20,118]. The preoperative tibial plateau slope angle (TPA) was found from a mediolateral radiograph of the stifle positioned at full extension and such that the femoral condyles were superimposed and measured using conventional methods [12,41,92] and found to be 28º. The correction angle was defined as the angle between the straight patellar ligament and a line perpendicular to the TPA. The wedge angle (WA) was calculated as being two thirds of the correction angle and outlined by Bruce [20,118]. The wedge angle was calculated to be 19º. Due to the location of the osteotomies to be performed, it was necessary to temporarily remove the medial collateral and patellar ligaments. Before beginning the first cut, a transverse 2.0mm hole was drilled on the medial side, caudal to the cranial cortex of the tibia and distal to the patellar ligament insertion by a distance equal to the length of the patellar ligament (~51.21mm). A cutting jig was pinned in place, parallel to the cranial aspect of the tibial crest. The 60mm osteotomy was performed so that the tibial crest was attached to the tibia only by its most distal aspect. This is shown in Figure 2.5.13.

Figure 2.5.13: TTO cutting jig used to perform the tibial crest osteotomy.

Half the distance of the tibial crest cut was measured and a line perpendicular to the cut was drawn back to the caudal aspect of the tibia (Figure 2.5.14). A transverse osteotomy was then made from this point of the caudal aspect of the tibia and extending to the pre-drilled 2.0mm hole. A wedge osteotomy was subsequently performed with the apex of the wedge at the pre-drilled 2mm hole. The 19º wedge is bisected by the line perpendicular to the tibial crest cut. Therefore, the cutting jig was angled 9.5º above and below the zero mark (transverse osteotomy line) for each cut as shown in Figure 2.5.15.

Figure 2.5.14: Marking the caudal aspect of the tibia at half the distance of the tibial crest osteotomy.

Figure 2.5.15: Osteotomy performed 9.5º above and below a previous transverse osteotomy, resulting in a 19º removable wedge.

After retraction of the osteotomized wedge, the tibial plateau was tilted ventrally causing the area where the wedge had been to collapse without displacement of its caudal aspect. This causes a cranial displacement of the tibial crest while still being attached to the tibial body at its distal aspect. A pre-contoured 3.5mm Broad TPLO plate (Synthes, Inc., West Chester, PA, USA) was then secured to the medial aspect of the proximal tibia. Plate selection was based, as in the case of the TPLO, on body weight. The final outcome of the TTO procedure is shown below in Figure 2.5.16.

Figure 2.5.16: Resulting TTO, secured with 3.5mm broad TPLO plate (Synthes, Inc.)

2.5.3 Testing Procedure

All three tibial osteotomy procedures, on CCL deficient models, were tested at each of five angles representative of maximum and minimal angles during walking and trotting [34]. After assembly, the models were attached to the fixture via the femoral head attachment pin. The hock rests on the support structure on the base plate (specifics of testing fixture found in section 1.5.17). The turnbuckles representing the quadriceps muscle group and gastrocnemius were rotated in turn to position the leg in one of the five stifle angles. Stifle joint angles were measured according to literature [52] and to ensure accuracy and consistency were measured using three different methods: a universal plastic goniometer, an electrogoniometer and rigid wires bent in the five angles (measured by the universal plastic goniometer). A load of 1.5lbs was applied to the top of the fixture mechanism. Photographs were taken and observations regarding drawer, subluxation, and stability were recorded. Measurements of patellar location within the trochlear groove were later recorded for each model and each angle according to methods found in literature [34].

2.6 RESULTS

Table A.1 containing the sample data and Table A.2 containing the consolidated average data graphed in Figure 2.6.1 and Figure 2.6.2 can be found in Appendix A.

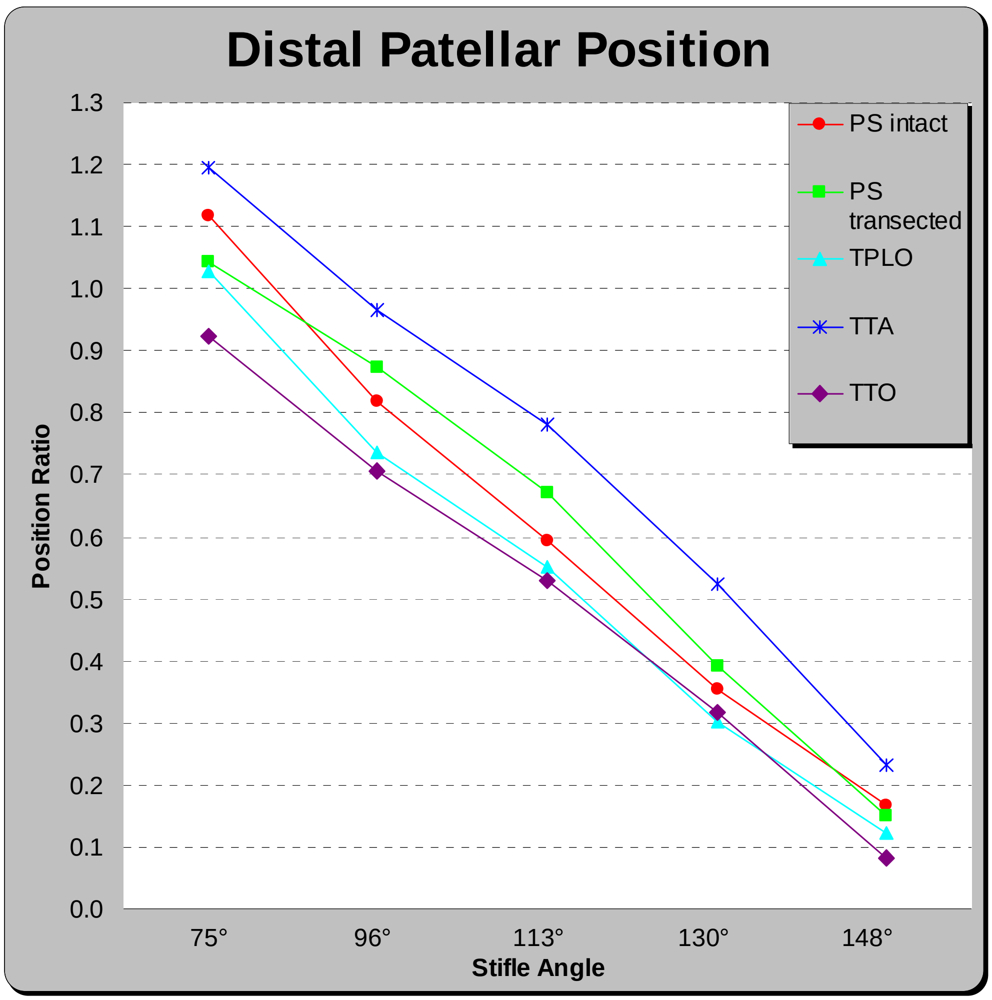

Figure 2.6.1: Graph of the distal patellar location with respect to the trochlear groove.

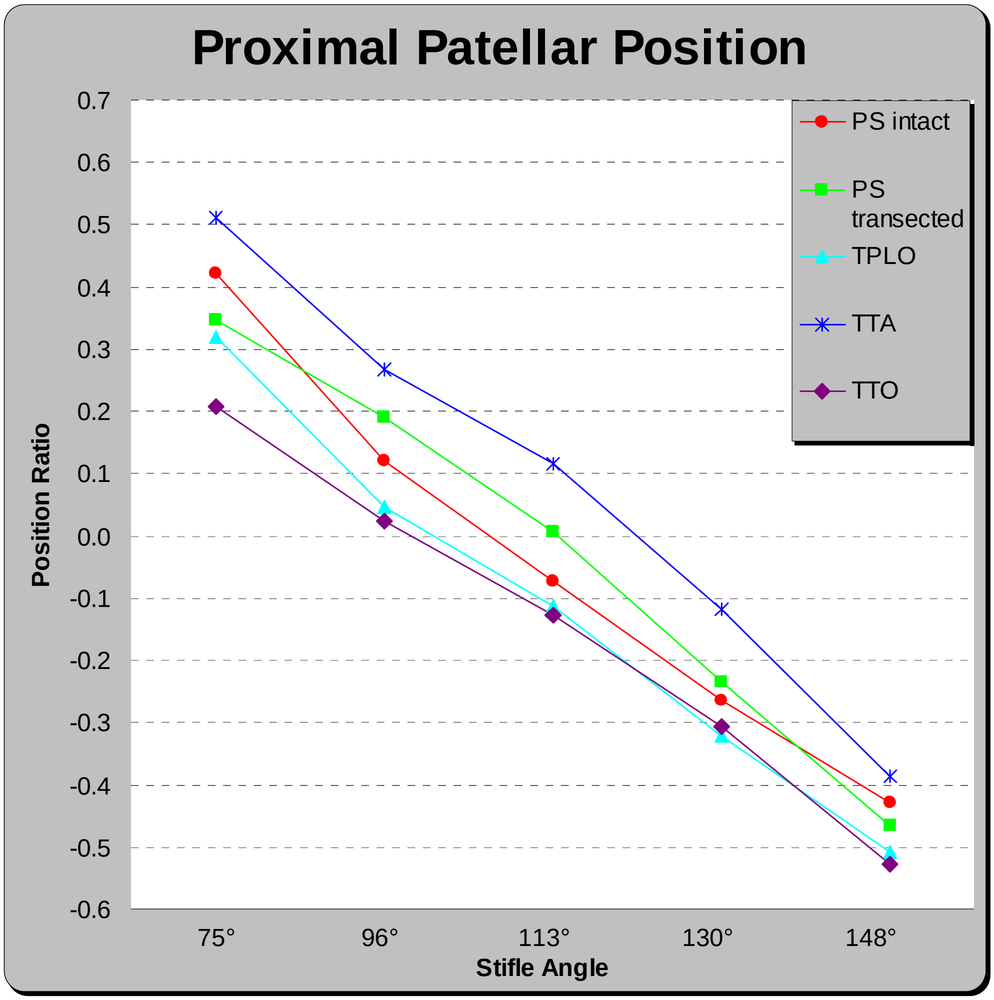

Figure 2.6.2: Graph of the proximal patellar location with respect to the trochlear groove.

Table 2.6.1: Patellar displacement from PS intact stifle as a percentage of trochlear length.

		Location Difference				
		PS Intact	PS Transected	TPLO	TTA	TTO
75°	PPP = X / TL	*0.4210*	-7.45%	-10.14%	9.13%	-21.29%
	DPP = Y / TL	*1.1175*	-7.42%	-9.00%	7.78%	-19.49%
96°	PPP = X / TL	*0.1215*	6.91%	-7.50%	14.57%	-9.88%
	DPP = Y / TL	*0.8177*	5.53%	-8.28%	14.90%	-11.17%
113°	PPP = X / TL	*-0.0739*	8.07%	-4.00%	19.02%	-5.36%
	DPP = Y / TL	*0.5936*	7.78%	-4.15%	18.80%	-6.56%
130°	PPP = X / TL	*-0.2649*	3.10%	-5.56%	14.79%	-4.12%
	DPP = Y / TL	*0.3536*	3.84%	-5.26%	17.13%	-3.56%
148°	PPP = X / TL	*-0.4278*	-3.85%	-8.06%	4.24%	-10.08%
	DPP = Y / TL	*0.1662*	-1.74%	-4.50%	6.56%	-8.34%

Additional pictures of patellar position at 96°, 113°, and 130° can be found in Appendix A.

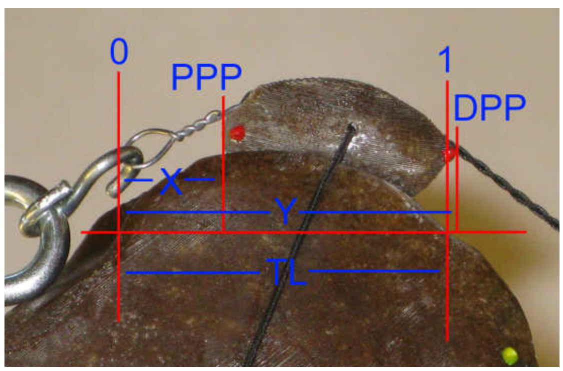

Figure 2.6.3: Patellar position measurements for the TPLO model at 75°.

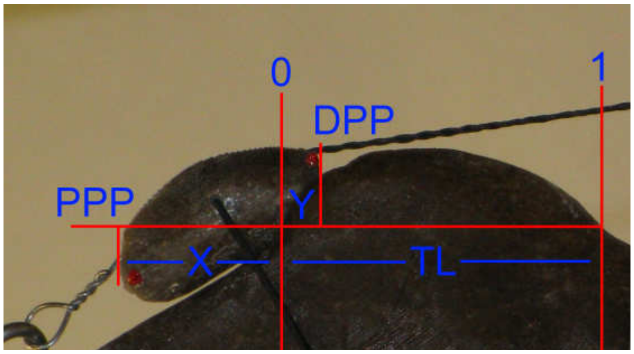

Figure 2.6.4: Patellar position measurements for the TPLO model at 148°.

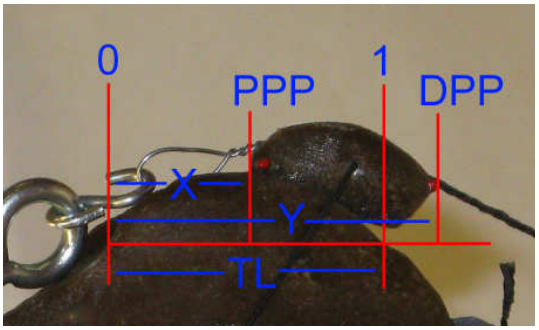

Figure 2.6.5: Patellar position measurements for the TTA model at 75°.

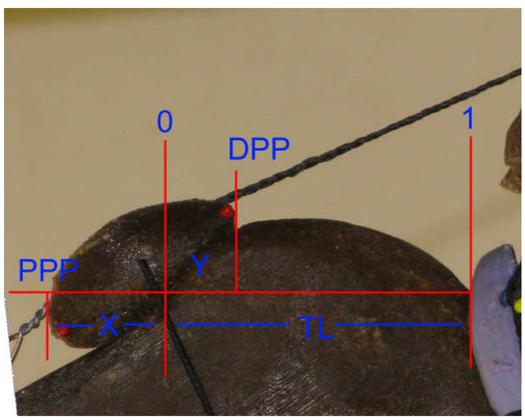

Figure 2.6.6: Patellar position measurements for the TTA model at 148°.

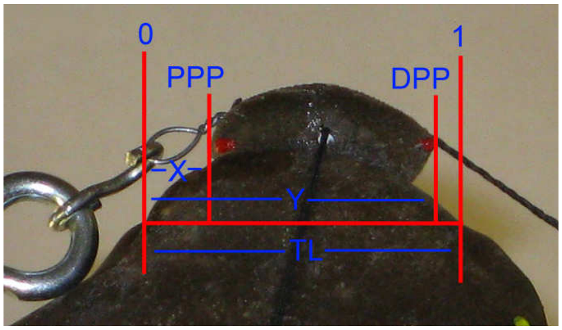

Figure 2.6.7: Patellar position measurements for the TTO model at 75°.

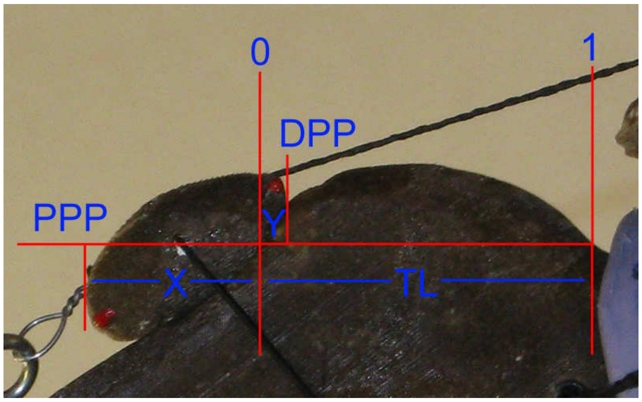

Figure 2.6.8: Patellar position measurements for the TTO model at 148°.

2.7 DISCUSSION

Postoperative tibial plateau angles (TPA) for this study were approximately 6.2º for the TPLO and 11.3º for the TTO using established methods [12,41,92]. The TTA resulted, as expected, in no change to TPA since no rotation of the tibial plateau occurred. These values are in good agreement with previous studies investigating the effects of these surgeries [20].

The tibial tuberosity advancement (TTA) technique was based a procedure developed for the human knee and has recently been extended to canine anatomy [116]. The theory behind this procedure that by advancing the patellar ligament so that it lies perpendicular to the tibial plateau when the stifle is in extension, the destabilizing shear forces resulting from a CCL deficient stifle will be eliminated during weight bearing. Studies have shown that in the healthy intact stifle, this 90º "cross-over flexion point" of the patellar tendon angle (TPA) occurs at 90º of flexion [99]. A TTA aims to move this cross over point to naturally occur at full extension. Thus in a stifle treated with TTA, the point of neutrality among the cruciate ligaments should shift to occur at full extension. The same theory applies to both the TPLO and TTO as they all aim, by different osteotomy techniques, to eliminate the cranial shear forces by causing the point of zero shear (cross over point) to occur at extension rather than 90º. Thus, there should be no remaining thrust or a thrust that is now caudally directed. The results of this study showed that the TPLO caused a caudal tibial translation for all angles except for 130º, at which there was nearly no translation. The TTO likewise caused caudal tibial translation for all angles except for one. At 148º there was cranial translation of the tibia. When testing the TTA, a slight persisting cranial tibial thrust was noted for the stifle angles of 113º and 130º. This was confirmed by the subluxation measurements recorded and shown in Table A.4. The measurements show that there was slight cranial drawer at the other angles as well.

From Figure 2.6.1 it can be seen that the TTA procedure causes a significant distal displacement of the patella at all angles tested. Comparing the shape of the plot of the TTA to that of the pre-surgical transected model shows a similarity in curvature. The fact that it matches the PS transected line more closely than the PS intact line is supported by the existence of cranial tibial drawer that was verified through measurement (Table A.4).

The DPP data points for the TTO and TPLO are within 5% of the trochlear length of each other for all stifle angles except for 75º. At this angle, the patellar position of the TTO model is located slightly more proximally with respect to the trochlear groove as compared with the patellar position resulting from the TPLO. The patellar ligament lengths were verified to ensure no material stretch could account for this behavior. It is hypothesized that the wedge osteotomy of the TTO procedure lowered the intercondylar eminence, thus bringing the trochlear groove within closer proximity of the tibial tuberosity. This may also account for the resulting proximal shift in patellar position. Other differences in osteotomy geometries may also have contributed to the differences in patellar position between the two models at this stifle angle.

Several simplifying assumptions were made in the design of the models and testing procedures stated in this study. This was an entirely subject-specific study. The subject was a large-breed dog of an average weight and initial tibial plateau slope similar to subjects used in comparable studies found in literature. Extrapolating the data to other scenarios should be done with caution. An additional limitation is that the modeled collateral ligaments are essentially thin lines and thus do not accurately portray the three dimensional geometry found in live subjects. The effect that this may have on the pre-and postoperative patellar position is unknown, but it can be hypothesized that these oversimplified ligamentous representations may allow for more craniocaudal tibial translation than would otherwise be permitted in the actual CCL deficient canine stifle.

2.8 CONCLUSION

It was found that the physical models used in this study could be used to accurately simulate real proximal tibial osteotomy procedures and to determine the postoperative effects on patellar location at five specific angles throughout the normal range of motion of large-breed dogs. Despite the limitations and assumptions, these models exhibited postoperative behaviors similar to those reported in literature and found through analysis of FE models in a parallel study [Crimi CM, 30].

It was found that the TTA procedure resulted in a more distally located patella at all stifle angles tested. The TPLO and TTO shared similar results at all stifle angles except for 75º, in which case the TTO resulted in a more proximally located patella with respect to the trochlear groove.

Abnormal patellar position has been associated with degenerative joint disease including chondromalacia as well as medial patellar luxation. CCL rupture is one of the most prominent and debilitating conditions in dogs. It is not only important to effectively treat this condition, but it is essential to understand the effect that the various corrective surgeries have on patellar position in order to prevent further degenerative complications.

3. FUTURE RESEARCH

The need to acquire greater insight into the effects of proximal tibial osteotomies on the canine stifle and the resulting geometries from these procedures is ever prevalent. By more clearly understanding the effects they have on patellar position, post-operative complications ranging from patellar subluxation to degenerative joint disease can be avoided.

The models created for this study could be used in future research to develop new tibial osteotomies and make modifications to current ones. Using the methods presented in this study and the custom testing fixture, different plateau angles and patellar tendon angles can be tested to determine the optimum combination that leads to joint stabilization as well as a natural patellar position throughout a range of motion.

Additionally, there is need for a less subjective method of measuring patellar position with respect to the trochlear groove so that post-operative, between-subject comparisons can be made. This and additional experiments regarding ligament shape and resulting post-operative craniocaudal drawer from physical testing would be exceptionally useful to understanding the change in stifle joint kinematics after CCL surgical intervention.

4. REFERENCES

1. Amiel D, Kleiner JB, Roux RD: The phenomenon of ligamentization: Anterior cruciate ligament reconstruction with autogenous patellar tendon. J Orthop Res 4:162-172, 1986.
2. Apelt D, Kowaleski MP, Boudrieau RJ. Effect of tibial tuberosity advancement on cranial tibial subluxation in canine cruciate-deficient stifle joints. Veterinary Surgery 2007;36:170-177.
3. Aragon CL, Budsberg SC. Applications of evidence-based medicine: cranial cruciate ligament injury repair in the dog. Veterinary Surgery 34:93-98, 2005.
4. Arnoczky SP, Marshall JL: The cruciate ligaments of the canine stifle: an anatomical and functional analysis. Am J Vet Res 38:1807–1814, 1977.
5. Arnoczky SP, Tarvin GB, Marshall JL: Anterior cruciate ligament replacement using patellar tendons. J Bone Joint Surg 64:217-224, 1982.
6. Arnoczky SP, Tarvin GB, Marshall JL: The “over-the-top” procedure: A technique for anterior cruciate ligament substitution in the dog. J Am Anim Hosp Assoc 15:283-290, 1979.
7. Arnoczky SP, Torzilli PA, Marshall JL: Biomechanical evaluation of anterior cruciate ligament repair in the dog: An analysis of the instant center of motion. J Am Anim Hosp Assoc 13:553-558, 1977.
8. Arnoczky, SP. Cruciate Ligament Rupture and Associated Injuries. Textbook of Small Animal Orthopaedics. Ithaca: International Veterinary Information Service, 1985.

9. Arthurs GI, Langley-Hobbs SJ. Patellar luxation as a complication of surgical intervention for the management of cranial cruciate ligament rupture in dogs. Vet Comp Orthop Traumatol 2007;20:204-210.

10. Bach JM, Hull ML, Patterson HA. Direct measurement f strain in the posterolateral bundle of the anterior cruciate ligament. J. Biomechanics 1997;30:281-283.

11. Barink M, van Kampen A, et al. A three-dimensional dynamic finite element model of the prosthetic knee joint: simulation of joint laxity and kinematics. J Engineering in Medicine 2005;219:415-424.

12. Baroni E, Matthias RR, Marcellin-Little DJ, et al. Comparison of radiographic assessments of the tibial plateau slope in dogs. AJVR 2003;64:586-589.

13. Barry, D., Ahmed, A.M., 1986. Design and performance of a modified buckle transducer for measurement of ligament tension. Journal of Biomechanical Engineering 108, 149–152.

14. Beillas P, Papaioannou G, et al. A new method to investigate in vivo knee behavior using a finite element model of the lower limb. Journal of biomechanics 2004;37:1019-1030.

15. Bell JC, Ness MG. Does use of a jig influence the precision of the tibial plateau leveling osteotomy surgery? Veterinary Surgery 2007;36:228-233.

16. Berg EE, Mason SL, Lucas MJ. Patellar height ratios: a comparison of four measurement methods. The American journal of sports medicine 1996;24:217-221.

17. Blackburne JS, Peel TE. A new method of measuring patellar height. The journal of bone and joint surgery 1977;59:241-242.

18. Blankevoort L, Huiskes R. Ligament-bone interaction in a three-dimensional model of the knee. Journal of Biomechanical Engineering 1991;113:263-269.

19. Blankevoort L, Huiskes R. Validation of a three-dimensional model of the knee. J Biomechanics 1996;29:955-961.

20. Bruce WJ, Rose A, et al. Evaluation of the triple tibial osteotomy. A new technique for the management of the canine cruciate-deficient stifle. Vet Comp Orthop Traumatol 2007;3:159-168.

21. Burks RT, Haut RC, Lancaster RL: Biomechanical and histological observations of the dog patellar tendon after removal of its central one-third. Am J Sports Med 18: 146-153, 1990.

22. Butler DL, Hulse DA, Matthew DK, et al: Biomechanics of cranial cruciate ligament reconstruction in the dog: II. Mechanical properties. Vet Surg 12:113-118, 1983.

23. Butler DL. Anterior Cruciate Ligament: Its Normal Response and Replacement. Journal of Orthopaedic Research 1989;7:910-921.

24. Cabaud HE, Feagin JA, Rodkey WB: Acute anterior cruciate ligament injury and augmented repair. Am J Sports Med 8: 395-401, 1980.

25. Canapp SO. The canine stifle. Clin Tech Small Anim Pract 2007;22:195-295.

26. Carey K, Aiken SW, DiResta GR, et al. Radiographic and clinical changes of the patellar tendon after tibial plateau leveling osteotomy. Vet Comp Orthop Traumatol 2005;18:235-242.

27. Carpenter DH, Cooper RC. Mini review of canine stifle joint anatomy. Anat Histol Embryol 2000;29:321-329.

28. Caylor KB, Zumpano CA, et al. Intra- and interobserver measurement variability of tibial plateau slope from lateral radiographs in dogs. Journal of the American animal hospital assoc. 2001;37:263-268.

29. Christel P. Prosthetic replacement of the anterior cruciate ligament: a challenge. Clinical Materials 1994;15:3-13.

30. Crimi CM. Stresses in the Cranial Cruciate Ligament Deficient Canine Stifle Following Three Tibial Osteotomy Procedures: A Finite Element Analysis. (Thesis), 2008.

31. Damur DM: Tibial tuberosity advancement (TTA): Clinical results. Proceedings of the 2005 ACVS Veterinary Symposium. October, 2005, pp 441–442.

32. Daniel, W.J.T., 2001. Three-dimensional orthotropic viscoelastic finite element model of a human ligament. Computer Methods in Biomechanics and Biomedical Engineering 4 (3), 265–279.

33. De Rooster H, De Bruin T, Van Bree H. "Morphologic and Functional Features of the Canine Cruciate Ligaments." Veterinary Surgery 2006;35:769-780.

34. DeCamp CE, Johnson AL, Probst CW, et al. Vertical position of the patella in the stifle joint of clinically normal large-breed dogs. AJVR 2002;63:42-46.

35. DeCamp CE, Riggs CM, Olivier NB, et al. Kinematic evaluation of gait in dogs with cranial cruciate ligament rupture. AJVR 1996;57:120-126.

36. Dickinson CR, Nunamaker DM: Repair of ruptured anterior cruciate ligament in the dog: Experience of 101 cases using a modified fascia lata strip technique. J Am Vet Med Assoc 170:827-830, 1977.

37. Donahue TLH, Hull ML, et al. How the stiffness of meniscal attachments and meniscal material properties affect tibio-femoral contact pressure computed using a validated finite element model of the human knee joint. Journal of biomechanics 2003;36:19-34.

38. Donahue TLH, Hull ML, Rashid MM, et al. A Finite Element Model of the Human Knee Joint for the Study of Tibio-Femoral Contact. Journal of Biomechanical Engineering 2002;124:273-280.

39. Elias JJ, Bratton DR, et al. Comparing two estimations of the quadriceps force distribution for use during patellofemoral simulation. J Biomechanics 2006;39:865-872,

40. Feeney LC, Lin CF, Marcellin-Little DJ, et al. Validation of two-dimensional kinematic analysis of walk and sit-to-stand motions in dogs. AJVR 2007;68:277-282.

41. Fettig AA, Rand WM, et al. Observer variability of tibial plateau slope measurement in 40 dogs with cranial cruciate ligament-deficient stifle joints. Veterinary Surgery 2003;32:471-478.

42. Harner CD, Livesay GA, Kashiwaguchi S, et al. Comparative study of the size and shape of human anterior and posterior cruciate ligaments. Journal of Orthopaedic Research 1995;13:429-434.

43. Harrysson OLA, Hildreth BE, Marcellin-Little DJ, et al. In Vitro Evaluation of Five Canine Tibial Plateau Leveling Methods. AJVR 2006;67;693-700.

44. Havig ME, Dyce J, Kowaleski MP, et al. Relationship of tibial plateau slope to limb function in dogs treated with a lateral suture technique for stabilization of cranial cruciate ligament deficient stifles. Veterinary surgery 2007;36:245-251.

45. Hayashi K, Frank JD, et al. Histologic changes in ruptured canine cranial cruciate ligament. Veterinary Surgery 2003;32:269-277.

46. Hayashi K, Manley PA, Muir P. Cranial cruciate ligament pathophysiology in dogs with cruciate disease: a review. Journal of the American Animal Hospital Assoc. 40:385-390, 2004.

47. Henning, C.E., Lynch, M.A., Glick, K.R., 1985. An in-vivo strain gauge study of elongation of the naterior cruciayte ligament. Americal Journal of Sports in Medicine 13, 22–26.

48. Hottinger HA, DeCamp CE, Olivier NB, et al. Noninvasive kinematic analysis of the walk in healthy large-breed dogs. Am J Vet Res 1996;57:381–388.

49. Hurley CR, Hammer DL, Shott S. Progression of radiographic evidence of osteoarthritis following tibial plateau leveling osteotomy in dogs with cranial cruciate ligament rupture: 295 cases (2001-2005). JAVMA 2007;230:1674-1679.

50. Hvid I, Andersen LI, Schmidt H. Patellar height and femoral trochlear development. Acta orthop scand 1983;54:91-93.

51. Insall J, Salvati E. Patella position in the normal knee joint. Radiology 1971;101(1):101-104.

52. Jaegger G, Marcellin-Little DJ , Levine D. Reliability of goniometry in Labrador Retrievers. AJVR 2002;63:979-986.

53. Jafari A, Faramand F, Meghdari A. The effects of trochlear groove geometry on patellofemoral joint stability - a computer model study. J Engineering in Medicine 2008;222:75-88.

54. Jandi AS, Schulman AJ. Incidence of Motion Loss of the Stifle Joint in Dogs with Naturally Occurring Cranial Cruciate Ligament Rupture Surgically Treated with Tibial Plateau Leveling Osteotomy: Longitudinal Clinical Study of 412 Cases. Veterinary Surgery 2006;36:114-121.

55. Jerram RM, Walker AM. Cranial cruciate ligament injury in the dog: pathophysiology, diagnosis and treatment. New Zealand Veterinary Journal 51(4):149-158, 2003.

56. Johnson AL, Broaddus KD, Hauptman JG, et al. Vertical Patellar Position in Large-Breed Dogs with Clinically Normal Stifles and Large-Breed Dogs with Medial Patellar Luxation. The American College of Veterinary Surgeons 2006;35:78-81.

57. Jurvelin JS, Arokoski JPA, et al. Topographical variation of the elastic properties of articular cartilage in the canine knee. Journal of Biomechanics 2000;33:669-675.

58. Kim SE, Pozzi A, Kowaleski MP, et al. Tibial osteotomies for cranial cruciate ligament insufficiency in dogs. Veterinary Surgery 2008;37:111-125.

59. Korvick DL, Pijanowski GJ, Schaeffer DJ: Three-dimensional kinematics of the intact and cranial cruciate ligament deficient stifle of dogs. J Biomech 27:77–87, 1994.

60. Kowaleski MP, Apelt D, Mattoon JS, et al. The Effect of Tibial Plateau Leveling Osteotomy Position on Cranial Tibial Subluxation: An In Vitro Study. Veterinary Surgery 2005;34:332-336.

61. Lafaver S, Miller NA, Stubbs WP, et al. Tibial tuberosity advancement for stabilization of the canine cranial cruciate ligament-deficient stifle joint: surgical technique, early results, and complications in 101 dogs. Veterinary Surgery 2007;36:573-586.

62. Lancourt JE, Cristini JA. Patella alta and patella infera. Their etiological role in patellar dislocation, chondromalacia, and apophysitis of the tibial tubercle. J Bone Joint Surg Am. 1975;57:1112-1115.

63. Lazar TP, Berry CR, et al. Long-term radiographic comparison of tibial plateau leveling osteotomy versus extracapsular stabilization for cranial cruciate ligament rupture in the dog. Veterinary Surgery 2005;34:133-141.

64. Li G, Gil J, et al. A validated three-dimensional computational model of a human knee joint. Journal of biomechanical engineering 1999;121:657-662.

65. Limbert G, Taylor M, Middleton J. Three-dimensional finite element modelling of the human ACL: simulation of passive knee flexion with a stressed and stress-free ACL. Journal of biomechanics 2004;37:1723-1731.

66. Limbert, G., Taylor, M., 2001b. Three-dimensional finite element modelling of the human anterior cruciate ligament. Influence of the initial stress field. In: Middleton, J., Jones, M.L., Pande, G.N. (Eds.), Computer Methods in Biomechanics and Biomedical Engineering. Vol. 3. Gordon and Breach Science Publishers, London, pp. 355–360.

67. Linder LH, Sukin DL, Burks RT, et al. Biomechanical and histologic properties of the canine patellar tendon after removal of its medial third. American Journal of Sports Medicine 1994;22:136-142.

68. Markolf, K.L., Gorek, J.F., Kabo, J.M., Shapiro, M.S., 1990. Direct measurement of resultant forces in the anterior cruciate ligament. An in vitro study performed with a new experimental technique. Journal of Bone and Joint Surgery 72A (4), 557–567.

69. Marsolais GS, McLean S, Derrick T, et al. Kinematic analysis of the hind limb during swimming and walking in healthy dogs and dogs with surgically corrected cranial cruciate ligament rupture. JAVMA 2003;222:739-743.

70. Mattern KL, Berry CR, Peck JN, et al. Radiographic and ultrasonographic evaluation of the patellar ligament following tibial plateau leveling osteotomy. Veterinary Radiology & Ultrasound 2006;47:185-191.

71. Meijer, R.C.M.B., Huiskes, R., Kauer, J.M.G., 1989. A stereophotogrammetric method for measurements of ligamenyt structure. Journal of Biomechanics 22, 177–184.

72. Meister BR, Michael SP, Moyer RA, et al. Anatomy and kinematics of the lateral collateral ligament of the knee. Am J Sports Med 2000;28:869-878.

73. Miller JM, Shires PK, et al. Effect of 9 mm tibial tuberosity advancement on cranial tibial translation in the canine cranial cruciate ligament-deficient stifle. Veterinary Surgery 2007;36:335-340.

74. Miller ME, Evans HE, Christensen GC. Miller's Anatomy of the Dog (2nd edition). Philadelphia: W.B Saunders Company, 1979.

75. Miller TT, Staron RB, Feldman F. Patellar height on sagittal MR imaging of the knee. AJR 1996;167:339-341.

76. Moeller EM, Cross AR, Rapoff AJ. Change in tibial plateau angle after tibial plateau leveling osteotomy in dogs. Veterinary Surgery 2006;35:460-464.

77. Moeller TB, Emil Reif, and T.C. Telger. Pocket Atlas of Sectional Anatomy CT and MRI (2 ed.). New York: Thieme, 2000.

78. Monahan JJ, Grigg P, et al. In vivo strain patterns in the four major canine knee ligaments. Journal of Orthopaedic Research 1984;2:408-418.

79. Montavon PM, Damur DM, Tepic S: Advancement of the tibial tuberosity for the treatment of cranial cruciate deficient canine stifle. Proceedings of the 1st World Orthopaedic Veterinary Congress; Munich Germany, September 2002, p. 152.

80. Montavon PM, Damur DM, Tepic S: Tibial tuberosity advancement (TTA) for the treatment of cranial cruciate disease in dogs: evidences, technique and initial clinical results. Proceedings of the 12th ESVOT Congress, Munich Germany, September 2004, pp 254-255.

81. Montavon PM, Tepic S. Joint surgery in canine hind limb - recent contributions from the university of zurich. European Companion Animal Health 2006;25-28.

82. Mostafa AA, Griffon DJ, Thomas MW, et al. Proximodistal Alignment of the Canine Patella: Radiographic Evaluation and Association with Medial and Lateral Patellar Luxation. Veterinary Surgery 2008;31:201-211.

83. Osmond CS, Marcellin-Little DJ, Harrysson OLA, et al. Morphometric assessment of the proximal portion of the tibia in dogs with and without cranial cruciate ligament rupture. Veterinary Radiology & Ultrasound 2006;47:136-141.

84. Peña E, Calvo B, Martínez MA, et al. A three-dimensional finite element analysis of the combined behavior of ligaments and menisci in the healthy human knee joint. Journal of Biomechanics 2006;39:1686-1701.

85. Phatak NS, Sun Q, et al. Noninvasive determination of ligament strain with deformable image registration. Annals of biomedical engineering 2007;35:1175-1187.

86. Pioletti, D.P., 1997. Viscoelastic properties of soft tissues: Application to knee ligaments and tendons. Departement de Physique. Lausanne, Switzerland, Ecole Polytechnique F!ed!erale de Lausanne.

87. Policy Implications of the Computed Tomography (CT) Scanner: An Update. Washington DC, U.S. Government Printing Office, 1981.

88. Priddy II NH, Tomlinson JL, et al. Complications with and owner assessment of the outcome of tibial plateau leveling osteotomy for treatment of cranial cruciate ligament rupture in dogs: 193 cases (1997-2001). JAVMA 2003;222:1726-1732.

89. Prokop Mathias, Michael Galanski, Aart Van Der Molen, et al. Spiral and Multislice Computed Tomography of the Body. New York: Thieme, 2000.

90. Ralphs SC, Whitney WO. Arthroscopic evaluation of menisci in dogs with cranial cruciate ligament injuries: 100 cases (1999-2000). JAVMA 2002;221:1601-1604.

91. Rayward RM, Thomson DG, Davies JV, et al. Progression of Osteoarthritis Following TPLO Surgery: a Prospective Radiographic Study of 40 Dogs. Journal of Small Animal Practice 2004;45:92-97.

92. Reif U OLA, Hulse DA, Hauptman JG. Effect of Tibial Plateau Leveling on Stability of the Canine Cranial Cruciate-Deficient Stifle Joint: An In Vitro Study. Veterinary Surgery 2002;31:147-154.

93. Reiser M, Banno T, Takahashi M, et al. Multislice CT. New York: Springer, 2004.

94. Renstrom, P., Arms, S.W., Stanwyck, T.S., Johnson, R.J., Pope, M.H., 1986. Strain within the naterior cruciate ligament during hamstring and quadriceps activity. American Journal of Sports in Medicine.

95. Rivière, Patrick. Medical Imaging Systems Technology: Analysis and Computational Methods (Chapter 1). Singapore: World Scientific Publishing Co., 2005.

96. Rooster H, Vangheluwe L, Van Bree H, et al. Biomechanical Properties of Braided Polyester Tapes Intended for use as Intra-articular Cranial Cruciate Ligament Prostheses in Dogs. AJVR 2001;62:48-53.

97. Schmerbach KI, Boeltzig CKM, Reif U, et al. In vitro comparison of tibial plateau leveling osteotomy with and without use of a tibial plateau leveling jig. Veterinary Surgery 2007;36:156-163.

98. Schoepf UJ, Aldrich JE, Becker CR. Multidetector-Row CT of the Thorax. New York: Springer, 2003.

99. Schwandt CS, Bohorquez-Vanelli A, Tepic S, et al. Angle between the patellar ligament and tibial plateau in dogs with partial rupture of the cranial cruciate ligament. AJVR 2006;67:1855-1860.

100. Schwandt CS, Bohorquez-Vanelli A, Tepic S, et al. Angle between the patellar ligament and tibial plateau in dogs with partial rupture of the cranial cruciate ligament. AJVR 2006;67:1855-1860.

101. Seil R, Müller B, et al. Reliability and interobserver variability in radiological patellar height ratios. Knee Surg, Sports Traumatol, Arthrosc 2000;8:231-236.

102. Setton LA, Mow VC, et al. Mechanical properties of canine articular cartilage are significantly altered following transection of the anterior cruciate ligament. Journal of orthopaedic research 1994;12:451-463.

103. Shahar R, Banks-Sills L, Eliasy R. Mechanics of the canine femur with two types of hip replacement stems. Vet Comp Orthop Traumatol 2003;3:145-152.

104. Shahar R, Banks-Sills L, Eliasy R. Stress and strain distibution in the intact canine femur: finite element analysis. Medical Engineering & Physics 2003;25:387-395.

105. Shahar R, Banks-Sills L.A Quasi-Static Three-Dimensional, Mathematical, Three-Body Segment Model of the Canine Knee. Journal of Biomechanics 2004;37:1849-1859.

106. Shahar R, Milgram J. Biomechanics of Tibial Plateau Leveling of the Canine Cruciate-Deficient Stifle Joint: A Theoretical Model. Veterinary Surgery 2006;35;144-149.

107. Shires PK, Hulse DA, Liu W: The under-and-over fascial replacement technique for anterior cruciate ligament rupture in the dog: A retrospective study. J Am Anim Hosp Assoc 20:69-77, 1984.

108. Silverman, Paul M. Multislice Computed Tomography: A Practical Approach to Clinical Protocols. Philadelphia: Lippincott Williams & Wilkins, 2002.

109. Slocum B, Devine T: Cranial tibial thrust: a primary force in the canine stifle. J Am Vet Med Assoc 183:456–459, 1983

110. Slocum B, Slocum TD. Tibial plateau leveling osteotomy for repair of cranial cruciate ligament rupture in the canine. Vet Clin North Am Small Anim Pract 1993; 23: 777–95.

111. Song Y, Debski RE, et al. A three-dimensional finite element model of the human anterior cruciate ligament: a computational analysis with experimental validation. Journal of biomechanics 2004;37:383-390.

112. Spindler KP, Murray MM, et al. The central ACL defect as a model for failure of intra-articular healing. Journal of orthopaedic research 2006;401-406.

113. Stauffer KD, Tuttle TA, Elkins AD, et al. Complications Associated With 696 Tibial Plateau Leveling Osteotomies (2001-2003). Journal of the American Animal Hospital Association 2006;42:44-50.

114. Tashman S, Anderst W, Kolowich P, et al: Kinematics of the ACL-deficient canine knee during gait: serial changes over two years. J Orthop Res 22:931–941, 2004.

115. Tepic S, Damur DM, Montavon PM: Biomechanics of the stifle joint. Proceedings of the 1st Word Orthopaedic Veterinary Congress, Munich Germany, September 2002, pp 189–190.

116. Tepic S, Montavon PM: Is cranial tibial advancement relevant in the cruciate deficient stifle? Proceedings of the 12th ESVOT Congress, Munich Germany, September 2004, pp 132–133.

117. Thomas TM, Marcellin-Little DJ, Roe SC, et al. Comparison of measurements obtained by use of an electrogoniometer and a universal plastic goniometer for the assessment of joint motion in dogs. AJVR 2006;67:1974-1979.

118. Triple Tibial Osteotomy (TTO). <www.vetinst.com>

119. van Dijk, R., Huiskes, R., Selvik, G., 1979. Roentgen stereophotogrammetric methods for the evaluation of the three-dimensional kinematic behavior and cruciate ligament length patterns of the human knee joint. Journal of Biomechanics 12, 727–731.

120. Vasseur PB, Arnoczky SP. Collateral Ligaments of the Canine Stifle Joint: Anatomic and Functional Analysis. Am J Vet Res 1981;42:1133-1137.

121. Warzee CC, Dejardin LM, Arnoczky SP, et al. Effect of Tibial Plateau Leveling on Cranial and Caudal Tibial Thrusts in Canine Cranial Cruciate-Deficient Stifles: An In Vitro Experimental Study. Veterinary Surgery 2001;30:278-286.

122. Weiss JA, Gardiner JC, Ellis BJ, et al. Three-dimensional finite element modeling of ligaments: Technical aspects. Medical Engineering & Physics 2005;27;845-861.

123. Woo SLY, Debski RE, Withrow JD, et al. Biomechanics of knee ligaments. Am J Sports Med 1999;27:533-543.

124. Yao J, Snibbe J. Stresses and strains in the medial meniscus of an ACL deficient knee under anterior loading: a finite element analysis with image-based experimental validation. Journal of biomechanical engineering 2006;128:135-141.

125. Zachos TA, Arnoczky SP, Lavagnino M, et al. The Effect of Cranial Cruciate Ligament Insufficiency on Caudal Cruciate Ligament Morphology: An Experimental Study in Dogs. Veterinary Surgery 2002;31:596-603.

126. Zielinska B, Donahue TLH. 3D finite element model of meniscectomy: changes in joint contact behavior. Journal of biomechanical engineering 2006;128:115-123.

APPENDICES

APPENDIX A

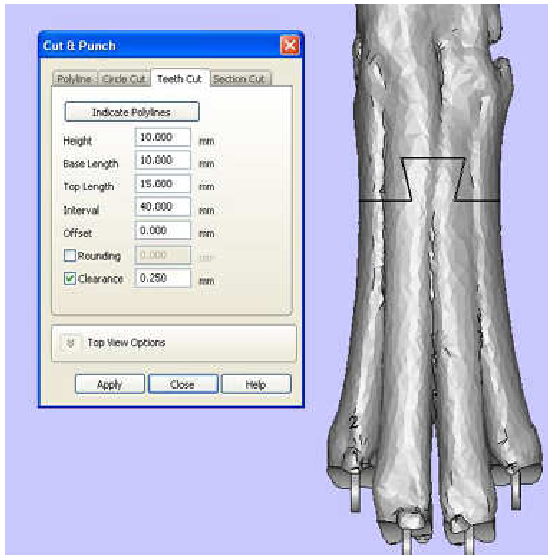

Figure A.1: Parameters used to section the leg component due to build platform limitations.

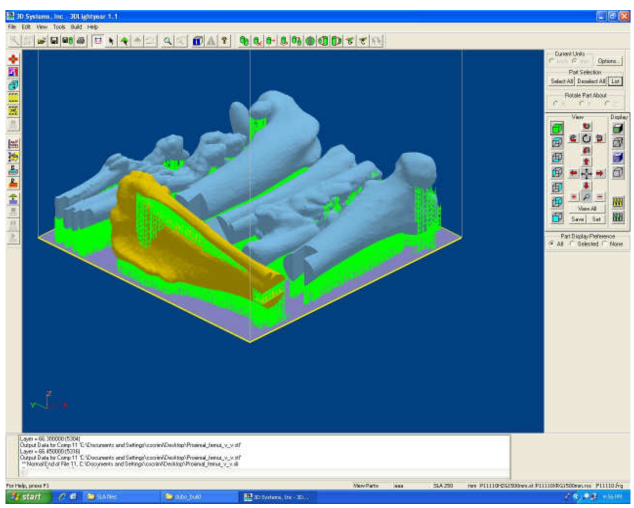

Figure A.2: Build platform arrangement with support structure [3D Lightyear 1.1, 3D Systems Corporation].

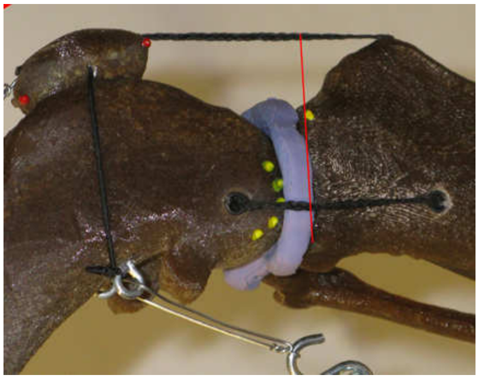

Figure A.3: PS intact model at a stifle angle of 96° displaying a PTA of 94°.

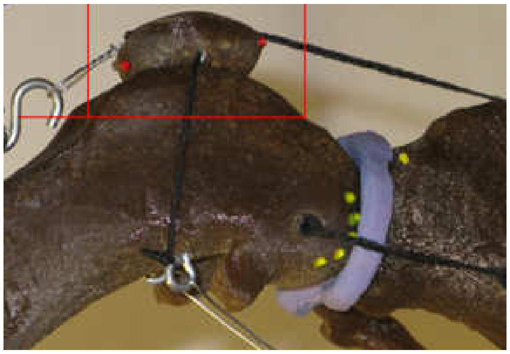

Figure A.4: PS intact model at a stifle angle of 96° with trochlear axis.

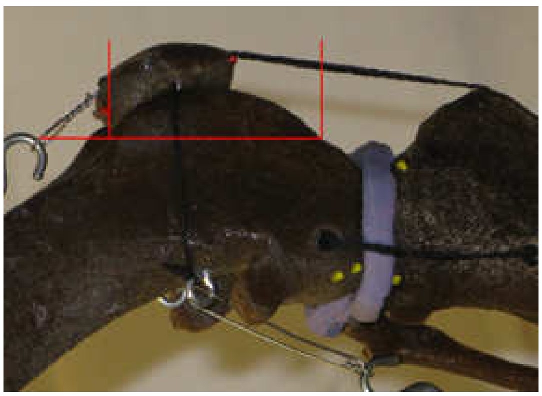

Figure A.5: PS intact model at a stifle angle of 113° with trochlear axis.

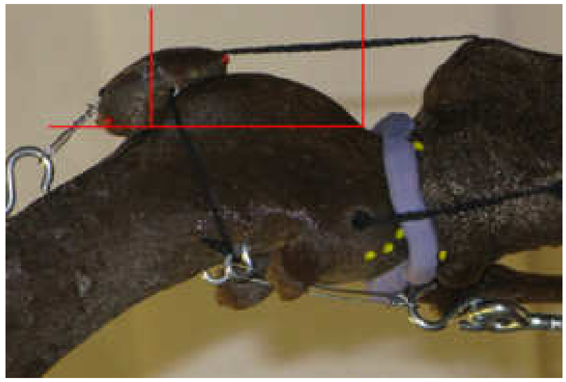

Figure A.6: PS intact model at a stifle angle of 130° with trochlear axis.

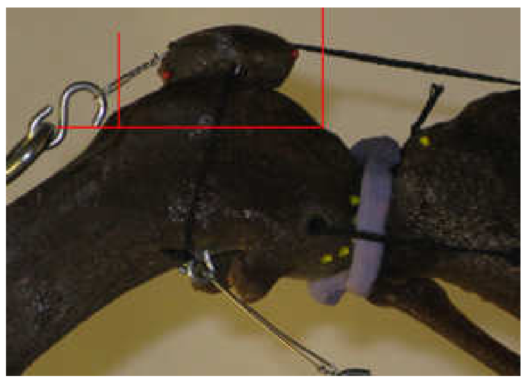

Figure A.7: PS transected model at a stifle angle of 96° with trochlear axis.

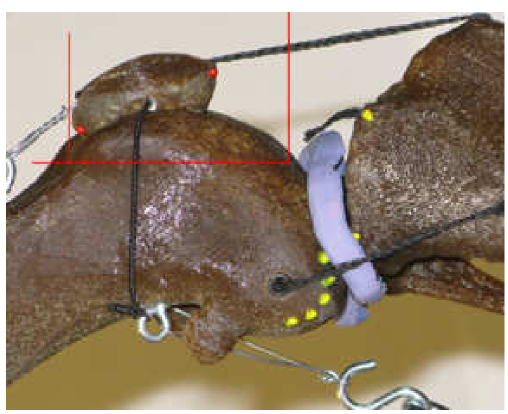

Figure A.8: PS transected model at a stifle angle of 113° with trochlear axis.

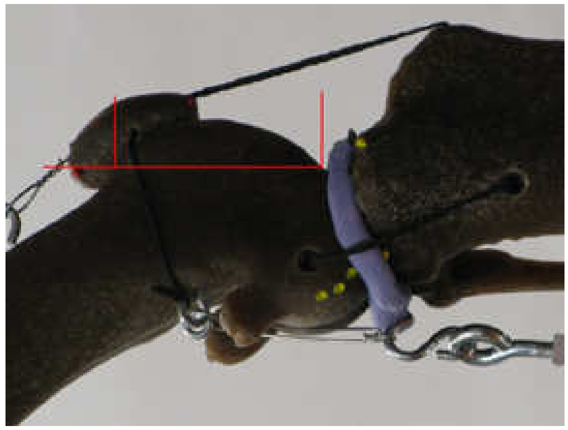

Figure A.9: PS transected model at a stifle angle of 130° with trochlear axis.

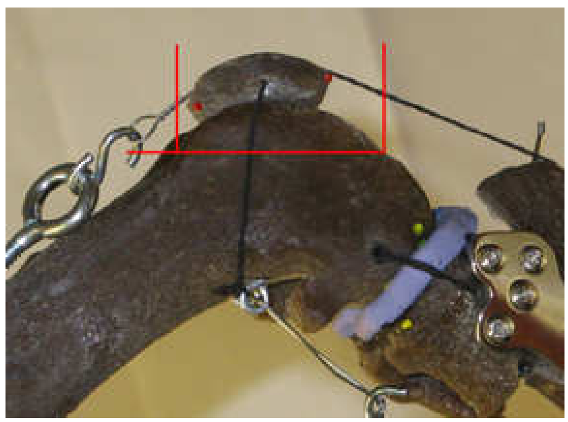

Figure A.10: TPLO model at a stifle angle of 96° with trochlear axis.

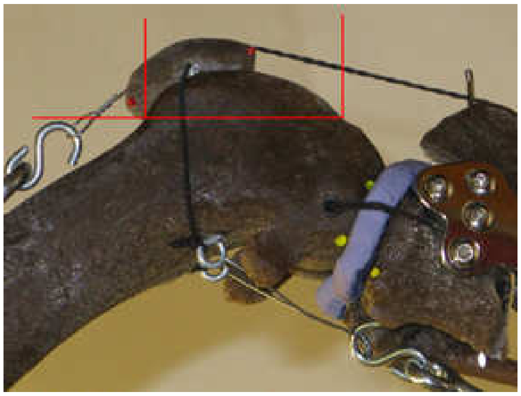

Figure A.11: TPLO model at a stifle angle of 113° with trochlear axis.

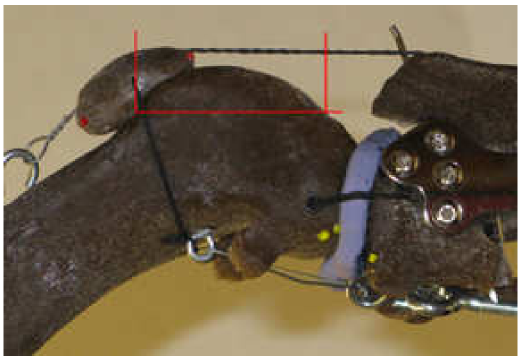

Figure A.12: TPLO model at a stifle angle of 130° with trochlear axis.

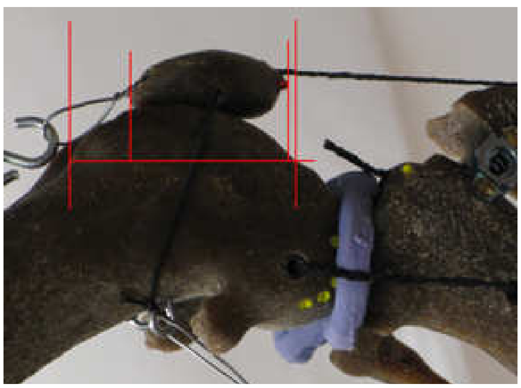

Figure A.13: TTA model at a stifle angle of 96° with trochlear axis.

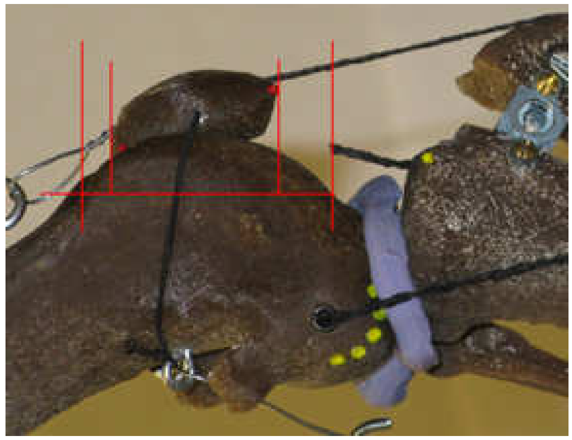

Figure A.14: TTA model at a stifle angle of 113° with trochlear axis.

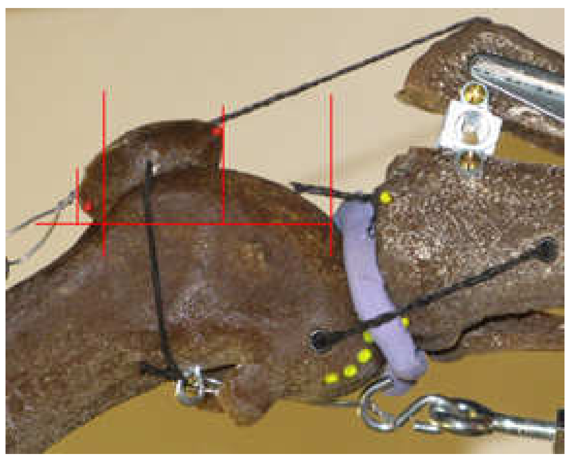

Figure A.15: TTA model at a stifle angle of 130° with trochlear axis.

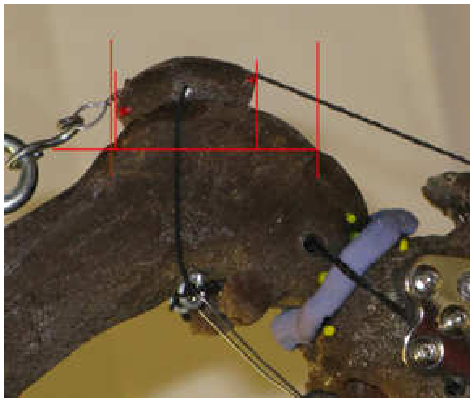

Figure A.16: TTO model at a stifle angle of 96° with trochlear axis.

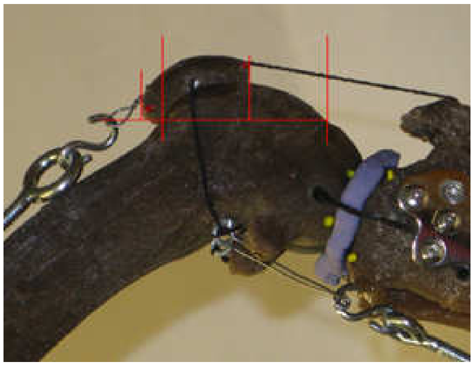

Figure A.17: TTO model at a stifle angle of 113° with trochlear axis.

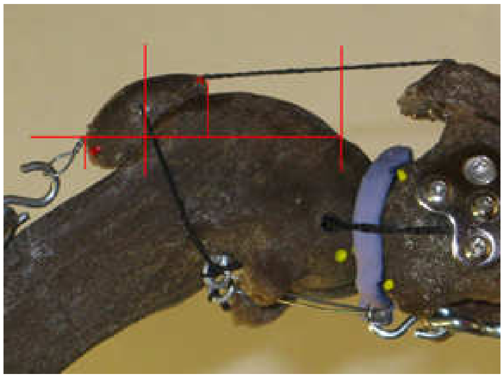

Figure A.18: TTO model at a stifle angle of 130° with trochlear axis.

Table A.1: Sample values for each measurement including their average and range.

Measurement	Data Type	Sample 1	Sample 2	Sample 3	Average	Range
PS intact 75	Trochlear Length	10.467	10.597	10.346		
	X	4.448	4.441	4.334		
	Y	11.772	11.799	11.529		
	PPP	0.425	0.419	0.419	0.4210	0.006049
	DPP	1.125	1.113	1.114	1.1175	0.011249
PS intact 96	Trochlear Length	10.867	10.837	10.789		
	X	1.221	1.313	1.414		
	Y	8.855	8.849	8.864		
	PPP	0.112	0.121	0.131	0.1215	0.018701
	DPP	0.815	0.817	0.822	0.8177	0.006725
PS intact 113	Trochlear Length	8.803	8.721	8.597		
	X	-0.641	-0.644	-0.644		
	Y	5.169	5.161	5.174		
	PPP	-0.073	-0.074	-0.075	-0.0739	0.002094
	DPP	0.587	0.592	0.602	0.5936	0.014652
PS intact 130	Trochlear Length	7.809	7.882	7.961		
	X	-2.087	-2.095	-2.082		
	Y	2.775	2.785	2.804		
	PPP	-0.267	-0.266	-0.262	-0.2649	0.005731
	DPP	0.355	0.353	0.352	0.3536	0.003142
PS intact 148	Trochlear Length	10.870	10.914	10.940		
	X	-4.666	-4.680	-4.652		
	Y	1.812	1.822	1.805		
	PPP	-0.429	-0.429	-0.425	-0.4278	0.004026
	DPP	0.167	0.167	0.165	0.1662	0.001951
PS transected 75	Trochlear Length	9.392	9.362	9.380		
	X	3.251	3.252	3.244		
	Y	9.783	9.786	9.783		
	PPP	0.346	0.347	0.346	0.3464	0.001519
	DPP	1.042	1.045	1.043	1.0433	0.003658
PS transected 96	Trochlear Length	7.682	7.701	7.732		
	X	1.418	1.474	1.515		
	Y	6.725	6.715	6.738		
	PPP	0.185	0.191	0.196	0.1906	0.011352
	DPP	0.875	0.872	0.871	0.8729	0.003980
PS transected 113	Trochlear Length	11.700	11.732	11.767		
	X	0.072	0.096	0.072		
	Y	7.878	7.871	7.885		
	PPP	0.006	0.008	0.006	0.0068	0.002064
	DPP	0.673	0.671	0.670	0.6714	0.003239
PS transected 130	Trochlear Length	9.180	9.168	9.145		
	X	-2.108	-2.140	-2.181		
	Y	3.585	3.593	3.601		
	PPP	-0.230	-0.233	-0.238	-0.2338	0.008861
	DPP	0.391	0.392	0.394	0.3921	0.003244
PS transected 148	Trochlear Length	11.102	11.050	11.022		
	X	-5.148	-5.144	-5.176		
	Y	1.634	1.646	1.658		
	PPP	-0.464	-0.466	-0.470	-0.4663	0.005906
	DPP	0.147	0.149	0.150	0.1489	0.003246

Table A.1 continued.

TPLO 75	Trochlear Length	9.078	9.038	9.043		
	X	2.984	2.888	2.808		
	Y	9.287	9.322	9.297		
	PPP	0.329	0.320	0.311	0.3196	0.018190
	DPP	1.023	1.031	1.028	1.0275	0.008400
TPLO 96	Trochlear Length	5.910	5.910	5.901		
	X	0.272	0.272	0.281		
	Y	4.331	4.343	4.349		
	PPP	0.046	0.046	0.048	0.0466	0.001595
	DPP	0.733	0.735	0.737	0.7349	0.004168
TPLO 113	Trochlear Length	7.358	7.449	7.534		
	X	-0.810	-0.843	-0.891		
	Y	4.111	4.112	4.110		
	PPP	-0.110	-0.113	-0.118	-0.1138	0.008180
	DPP	0.559	0.552	0.546	0.5521	0.013185
TPLO 130	Trochlear Length	8.483	8.432	8.378		
	X	-2.695	-2.702	-2.709		
	Y	2.529	2.542	2.543		
	PPP	-0.318	-0.320	-0.323	-0.3205	0.005653
	DPP	0.298	0.301	0.304	0.3010	0.005407
TPLO 148	Trochlear Length	7.912	7.943	7.998		
	X	-4.038	-4.039	-4.049		
	Y	0.957	0.963	0.972		
	PPP	-0.510	-0.508	-0.506	-0.5084	0.004112
	DPP	0.121	0.121	0.122	0.1212	0.000575
TTA 75	Trochlear Length	6.501	6.536	6.583		
	X	3.349	3.361	3.340		
	Y	7.814	7.826	7.811		
	PPP	0.515	0.514	0.507	0.5122	0.007784
	DPP	1.202	1.197	1.187	1.1953	0.015428
TTA 96	Trochlear Length	10.593	10.509	10.431		
	X	2.810	2.809	2.808		
	Y	10.157	10.149	10.174		
	PPP	0.265	0.267	0.269	0.2673	0.003928
	DPP	0.959	0.966	0.975	0.9666	0.016521
TTA 113	Trochlear Length	10.685	10.772	10.715		
	X	1.292	1.198	1.254		
	Y	8.383	8.395	8.368		
	PPP	0.121	0.111	0.117	0.1164	0.009703
	DPP	0.785	0.779	0.781	0.7816	0.005222
TTA 130	Trochlear Length	9.748	9.792	9.809		
	X	-1.146	-1.150	-1.136		
	Y	5.160	5.138	5.107		
	PPP	-0.118	-0.117	-0.116	-0.1169	0.001751
	DPP	0.529	0.525	0.521	0.5249	0.008695
TTA 148	Trochlear Length	9.907	9.919	9.958		
	X	-3.722	-3.819	-3.937		
	Y	2.318	2.302	2.283		
	PPP	-0.376	-0.385	-0.395	-0.3854	0.019667
	DPP	0.234	0.232	0.229	0.2318	0.004713

Table A.1 continued.

TTO 75	Trochlear Length	5.256	5.361	5.451		
	X	1.115	1.111	1.116		
	Y	4.948	4.940	4.932		
	PPP	0.212	0.207	0.205	0.2080	0.007405
	DPP	0.941	0.921	0.905	0.9226	0.036612
TTO 96	Trochlear Length	9.305	9.464	9.467		
	X	0.274	0.152	0.216		
	Y	6.644	6.639	6.648		
	PPP	0.029	0.016	0.023	0.0228	0.013386
	DPP	0.714	0.702	0.702	0.7059	0.012524
TTO 113	Trochlear Length	6.052	6.084	6.131		
	X	-0.785	-0.786	-0.757		
	Y	3.221	3.202	3.222		
	PPP	-0.130	-0.129	-0.123	-0.1275	0.006238
	DPP	0.532	0.526	0.526	0.5280	0.006695
TTO 130	Trochlear Length	6.704	6.924	6.805		
	X	-2.087	-2.092	-2.073		
	Y	2.162	2.162	2.174		
	PPP	-0.311	-0.302	-0.305	-0.3060	0.009169
	DPP	0.322	0.312	0.319	0.3181	0.010247
TTO 148	Trochlear Length	5.928	5.749	5.777		
	X	-3.086	-3.073	-3.066		
	Y	0.482	0.476	0.488		
	PPP	-0.521	-0.535	-0.531	-0.5286	0.013947
	DPP	0.081	0.083	0.084	0.0829	0.003164

Table A.2: Consolidated table of averages for each measurement.

		PS Intact	PS Transected	TPLO	TTA	TTO
75°	**PPP = X / TL**	0.4210	0.3464	0.3196	0.5122	0.2080
	DPP = Y / TL	1.1175	1.0433	1.0275	1.1953	0.9226
96°	**PPP = X / TL**	0.1215	0.1906	0.0466	0.2673	0.0228
	DPP = Y / TL	0.8177	0.8729	0.7349	0.9666	0.7059
113°	**PPP = X / TL**	-0.0739	0.0068	-0.1138	0.1164	-0.1275
	DPP = Y / TL	0.5936	0.6714	0.5521	0.7816	0.5280
130°	**PPP = X / TL**	-0.2649	-0.2338	-0.3205	-0.1169	-0.3060
	DPP = Y / TL	0.3536	0.3921	0.3010	0.5249	0.3181
148°	**PPP = X / TL**	-0.4278	-0.4663	-0.5084	-0.3854	-0.5286
	DPP = Y / TL	0.1662	0.1489	0.1212	0.2318	0.0829

Table A.3: Table displaying patellar tendon angle (PTA) between stifle angles and procedures.

	PS intact 96°	PS intact 130°	TTA 130°	TTO 130°
PTA	94°	104.9°	84.5°	87.7°

In order to quantify the tibial subluxation, if any occurred, the methods described in literature by Warzee *et al*. [121] were used and the resulting measurements are shown below in Table A.4. It should be noted that the subluxation value is always with respect to the PS Intact model; a positive subluxation value corresponds to cranial tibial subluxation while a negative subluxation value denotes caudal tibial subluxation. The values were normalized using the length of the trochlear axis in each image and converted to millimeters by multiplying by the actual value of the trochlear length (41.07 mm).

Table A.4: Measurements of tibial subluxation in millimeters.

Stifle Angle	PS Intact	PS transected	TPLO	TTA	TTO
75°	3.35	2.78	7.17	3.30	8.70
Subluxation		0.57	-3.81	0.05	-5.35
96°	4.57	-2.57	7.72	-2.56	10.42
Subluxation		7.15	-3.14	7.13	-5.84
113°	6.96	-10.15	8.02	-6.21	10.74
Subluxation		17.12	-1.06	13.17	-3.78
130°	10.18	2.04	10.04	-0.92	11.03
Subluxation		8.14	0.14	11.10	-0.84
148°	14.15	7.05	14.84	10.21	7.93
Subluxation		7.10	-0.69	3.94	6.22

APPENDIX B

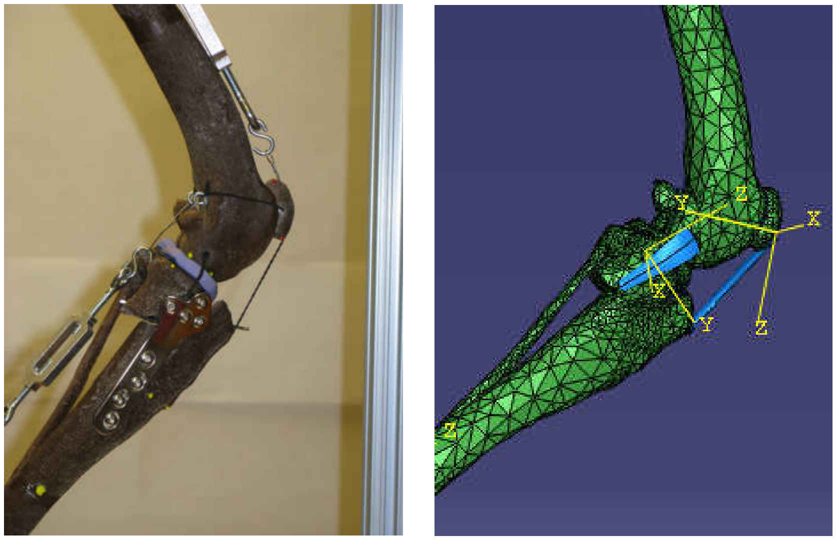

(a) (b)

Figure B.1: Medial view of TPLO procedures for comparison. (a) physical RP model (b) FEA model [30]

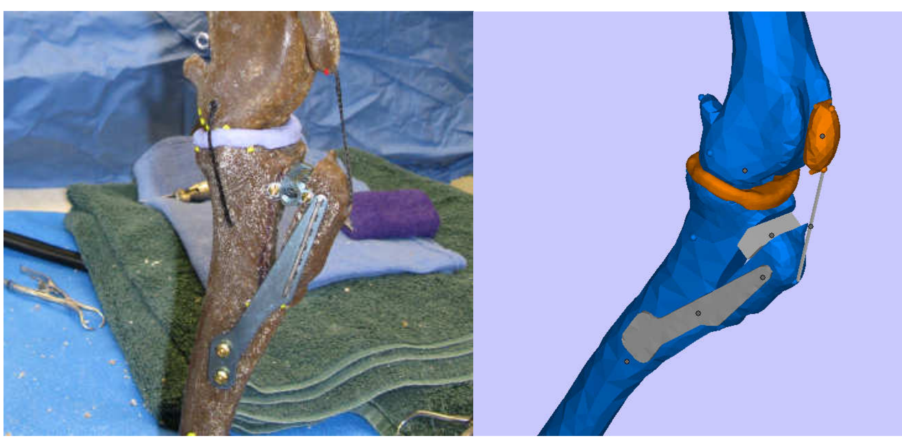

(a) (b)

Figure B.2: TTA procedure and hardware. (a) physical RP model (b) FE model [30]

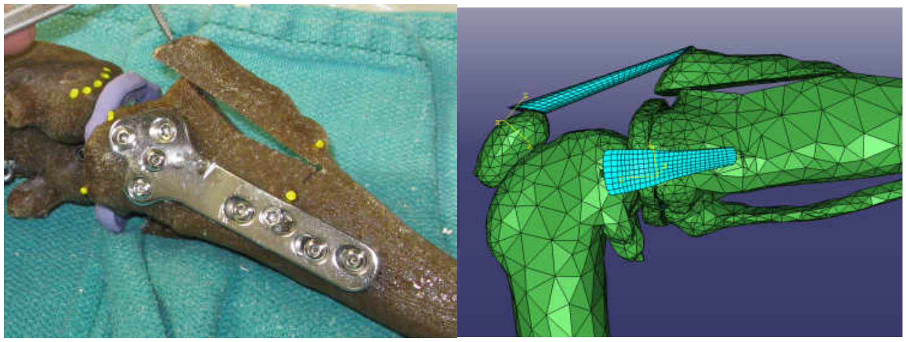

(a) (b)

Figure B.3: TTO performed on two different models. (a) RP model (b) FE model [30]